OPTIMAL DIGITAL MECHANIZATIONS OF STOCHASTIC FILTERING ALGORITHMS

By

VIJAYENDRA MOHAN GUPTA

Bachelor of Engineering (Honours)
Birla Institute of Technology and Science
Pilani, Rajasthan, India
1971

Master of Science
Oklahoma State University
Stillwater, Oklahoma
1973

Submitted to the Faculty of the Graduate College
of the Oklahoma State University
in partial fulfillment of the requirements
for the Degree of
DOCTOR OF PHILOSOPHY
July, 1976

OPTIMAL DIGITAL MECHANIZATIONS OF

STOCHASTIC FILTERING ALGORITHMS

Thesis Approved:

James R. Rowland
Thesis Adviser

Bennett Basore

Robert J. Mulholland

Donald M. Grace

Norman D. Durham
Dean of the Graduate College

ACKNOWLEDGMENT

I wish to express my sincere appreciation to my thesis adviser and committee chairman, Dr. James R. Rowland, for suggesting the problem and for spending many hours in valuable guidance to enable me to carry out this research. His constant encouragement and great insight into the problem made this thesis possible. I wish to acknowledge the other members of my committee, Dr. Bennett L. Basore, Dr. Robert J. Mulholland, and Dr. Donald W. Grace, for suggestions and teaching excellence.

Gratitude is expressed to the Rama Watumull Foundation for the scholarship grant during the summer of 1975.

This research was made possible by the graduate research and teaching assistance provided by the School of Electrical Engineering during the entire study.

Sincere appreciation is also expressed to Mr. Sunil Jhobalia for making drafting equipment available.

I would like to thank my wife, Neeru, for helping me during the preparation of the figures in this thesis. Also, I would like to thank her for her patience and encouragement during this study.

A loving thanks is expressed to my brother, sister-in-law, and parents-in-law for their encouragement and faith.

Finally, I would like to dedicate this thesis to my parents for their constant encouragement and unwavering confidence in my ability to successfully complete this dissertation.

TABLE OF CONTENTS

LIST OF FIGURES

Figure Page

CHAPTER I

INTRODUCTION

The digital mechanization of stochastic filtering algorithms for nonlinear system applications has received an increasing amount of attention in recent years. Due in part to the availability of ultra-fast digital computers and to the sophistication called for in a broad range of applications, the digital mechanization problem has taken on a renewed importance in research and development circles. A major research emphasis has evolved on the discrete representation of continuous stochastic algorithms and equations. Often the resulting digital mechanization is to be performed on-line in real time for continuous nonlinear system applications. Such cases require suitable tradeoffs between computational speed and algorithm accuracy.

Previously, estimation algorithms were usually developed on the basis of achieving the best accuracy possible. It was assumed that any equipment needed for mechanization would be not only available but also capable of operating fast enough for use in realtime applications. Therefore, the physical realizability of the developed algorithm was the primary design consideration. Computer operations were counted and cataloged for existing filtering algorithms, and a particular digital mechanization corresponding to one of the developed algorithms was selected over the other candidates on the basis of accuracy and computer operation counts. It is apparent that this separate development of the

estimation algorithm and the selection of the mechanization procedure may result in an overall non-optimal solution. Moreover, digital mechanizations were often performed under the assumption that only discrete formulations of filtering algorithms should be used. On the contrary, efficient utilization of numerical integration formulas for discretizing continuous algorithms, involving computational speed-versus-accuracy considerations, can provide a useful alternative to discrete algorithms for nonlinear systems.

In this thesis research optimal digital mechanizations of stochastic filtering algorithms were investigated. A systematic procedure for simultaneously optimizing the realtime digital mechanization with the filtering algorithm for nonlinear systems was developed. The imbedding of established filtering algorithms as well as standard numerical formulas into a generalized format provided an appropriate framework for optimization. Trajectory optimization was utilized within this framework to further improve the optimal discrete representations for stochastic algorithms. The background information needed to develop these optimization results is given in the next section.

History of the Problem

The basic problem of estimating the state of a noise-corrupted physical process leads to the stochastic filtering problem. It was approximately two centuries ago when Gauss developed the least-squares method while trying to determine planet orbits from many observations. The first explicit solutions for least-squares estimates of stochastic processes were given by Wiener in 1942 (1) under the assumptions of a scalar observation process, a semi-infinite observation

interval ($t_0 = -\infty$) and jointly stationary signal and noise processes. Wiener used a variational argument to determine the optimum estimate and showed that it satisfied the Wiener-Hopf equation (1). The similar discrete-time filtering problem was solved by Kolmogorov (2). In 1961 Kalman and Bucy (3) developed new techniques based on the state-space approach. They presented a nonlinear differential equation of the Riccati type for the optimal filtering error. The estimate of the state obtained by the Kalman-Bucy theory was optimal for linear systems with Gaussian noise. This theory has been very useful in space activities such as the Gemini and Apollo missions.

For either linear or nonlinear systems with non-Gaussian inputs the optimal mean-square filter is nonlinear. The search for improved methods of state estimation has resulted in exact nonlinear filtering algorithms based on Bayesian estimation theory and approximate nonlinear recursive filtering.

Several approximate algorithms for implementing exact nonlinear filters have been developed in recent years. Kushner (4) derived exact, infinite-dimensional dynamical equations for the conditional mode and developed finite-dimensional approximations involving moment sequences for their solution. Ho and Lee (5) formulated the discrete nonlinear filtering problem in terms of Bayesian estimation theory, and Bucy (6) and Mortensen (7) applied Bayesian results in function space to continuous systems. Kuo and Rowland (8,9) demonstrated that density storage and Bayesian solutions can be achieved effectively by using moments of the measurement data. Bucy and Senne (10) considered a point-mass representation on a floating grid of indices for implementing the indicated Bayesian computations. Sorenson and Alspach (11) and Lo (12)

approximated conditional density functions by a sum of Gaussians for nonlinear Bayesian estimation, and Jan and de Figueiredo (13) performed Bayesian calculations by using a multivariate B-spline for approximating density functions.

Probably the most common approximate method for nonlinear filtering is to expand the system message model in a Taylor series which is truncated after the first few terms. The series may then be substituted into the equations for the conditional mean and covariance of the state derived from the Fokker-Planck equation (14,15). Depending upon how many terms are retained, either a first, second, or higher order approximate filter is obtained. If the nonlinear system equations are expanded about a deterministic nominal trajectory, a linearized variational Kalman filter is obtained by using the linear perturbation equations. The extended Kalman filter is the approximate nonlinear filter obtained by expanding the message model about the current state estimate. Other approximate nonlinear filters include the truncated second-order filter (16,17) and the Gaussian second-order filter (18,19).

Schwartz and Stear (20) compared several filtering algorithms on the basis of their estimation error history. They observed that no particular approximate filter is consistently better than any other. They concluded that the nonlinear filters examined are better than a strictly linear one (Kalman Filter). Wishner et al. (21) examined three distinct methods for the recursive estimation of the state variables of a continuous-time nonlinear plant on the basis of measuring the discrete-time outputs of the plant in the presence of noise. They concluded that the single-stage iteration filter has superior mean-

squared error performance under all conditions, followed by the second-order filter. Square-root filtering (22,23) has been developed as a means of controlling the divergence problem encountered during filtering.

Realtime applications of the recursive filtering algorithms for on-line state estimation depends upon acceptable tradeoffs between accuracy and computational speed. The practicality of the Kalman filter for on-line operations is answered in part by Mendel (24) by providing computational requirements, such as computing time per iteration and storage, for a discrete Kalman filter. Kaminski et al. (22) presented four efficient square-root implementations and compared them with three common conventional implementations in terms of computational complexity and precision. Bierman (23) continued these comparisons and developed several improvements in the digital mechanization of the filters. While the computational time per iteration has been determined in these papers, meaningful comparisons between filtering algorithms for realtime applications must utilize data rates compatible with the speed of a particular filtering mechanization. Moreover, the choice between discrete and continuous filtering algorithms must be examined for given classes of problems. Much of the previous work has been based on the assumption that discrete filters should be used if the implementation is to be digital. However, this approach requires that discrete transition matrices are determined a priori, which is difficult to realize for extended Kalman filters. This problem is circumvented when continuous filters are utilized, even if implemented digitally. Gaston and Rowland (25) obtained realtime digital integration results for mechanizing continuous Kalman filters for nonlinear systems by making comparisons between variational and extended Kalman filtering algorithms as

functions of input noise levels and system nonlinearity characteristics. Specific operating conditions were identified in typical cases for which certain combinations of numerical formulas, step sizes, and filtering algorithms should be used for improved performance.

In addition to realtime applications of mechanizing filtering algorithms digitally, the use of the hybrid computer as a realtime simulation tool has also provided a motivation for improvements on a speed-versus-accuracy basis. Bucy, Merritt, and Miller (26) demonstrated the enormous computational advantage in using hybrid computers for a particular nonlinear estimation problem. Holmes and Rowland (27,28) investigated the sampling and hybridization errors inherent in the mechanization of Kalman filtering algorithms on the hybrid computer. Reduced errors were achieved by re-partitioning of the dynamical system model between the analog and digital computers and by performing an on-line modification of the Kalman gains.

The discrete representations of continuous systems and signals, in the present context of filtering mechanizations, depends on the efficient numerical integration of dynamic system equations based on both speed and accuracy. Reporting the results of seven years of simulation experience, Benyon (29) showed that in particular aerospace simulations, second-order numerical formulas were over 30 percent faster with comparable accuracy than the commonly used fourth-order Runge-Kutta formula. These results were used by Gaston and Rowland (25) in their selection of numerical integration formulas for comparing different Kalman filtering algorithms with respect to nonlinear characteristics of a typical system. A variational technique was developed by Rowland and Holmes (30) to yield improved results over Runge-Kutta formulas for

mildly nonlinear applications. Instead of developing new, highly efficient, numerical integration formulas, the alternate approach of developing computer-aided analysis and design programs was used by Nigro et al. (31) and Rowland and Holmes (32). The program by Nigro et al. (31) considered consistency requirements, stability, truncation error, roundoff error, propagated error, and required computing time in the derivation of optimum methods as well as in the evaluation of user-supplied methods for realtime digital flight simulation. Rowland and Holmes (32) developed a computer-aided design tool for optimally allocating digital execution time for the numerical integration of several selected subsystems in a hybrid simulation. The precise objective was to minimize the sum-squared error of the given subsystems under the constraint that the total time allowed for executing all subsystem integrations is specified in advance. This problem definition permitted the use of different integration formulas within the complete system. Most significantly, the utilization of this computer-aided design approach makes it possible to uniquely tailor the solution technique to the given problem.

The problem of modeling continuous noise inputs for dynamic systems on the digital computer has been investigated by Rowland and Gupta (33) with particular emphasis on the reduction in accuracy due to discretizing approximations. The use of a single random variable within each discretization interval was shown to produce the same power spectral density as the use of a time function of several uncorrelated random variables. The variance of the resulting random number sequence is the variance of the continuous white noise process divided by the discretization interval. Results obtained by using

time-domain techniques for matching autocorrelation functions showed that the variance of the input random number sequence should be modified according to the parameters of the shaping filter. Rowland (34) developed a generalized approach for modifying discrete input signal variances. The concepts from optimization theory were used to realize optimal digital simulations for linear, time-varying, continuous dynamical systems having random inputs. The cost functional based on the state covariance matrices of the continuous system and its discrete model led to a two-point boundary value problem which then was solved by known numerical techniques. The result was a systematic procedure for determining optimal digital simulations under the constraints that the numerical integration formula and integration step size have been specified in advance. Previously, Brown and Rowland (35,36) had demonstrated that with specific nonlinear examples considerable improvement over the commonly used method of linearizing the system equations about the deterministic optimal trajectory can be realized by trajectory optimization. They concluded that, for a particular combined estimation and control example being considered, the system performance was much more sensitive to the choice of the nominal trajectory than to the selection of a nonlinear filter producing greater estimation accuracy. The contribution of this research is the utilization in a single optimization format of techniques for optimal digital simulations and trajectory optimization to yield optimal digital mechanizations based on speed and accuracy for stochastic filtering algorithms.

Basic Approach

The thesis research objectives were to (1) develop an optimization

procedure based on accuracy considerations to yield a two-point boundary value problem whose solution gives the optimal discrete representation for given continuous stochastic estimation algorithms, (2) extend this optimization procedure to obtain optimal digital mechanizations based on computational speed and accuracy tradeoffs, and (3) apply trajectory optimization concepts as a means of further improving the overall optimization procedure for linearized incremental variations about deterministic trajectories in nonlinear cases. These objectives are described in more detail in the following paragraphs.

Optimal Discrete Representations on an Accuracy Basis

A major contribution of this thesis research is the formulation and development of an optimization format for the discretization of continuous stochastic filtering algorithms. This optimization is based on achieving the best possible accuracy for the resulting discrete filter under the configuration constraints imposed in the problem. The optimization procedure initially was developed for the linear system, and the resulting two-point boundary value problem was solved for typical cases. Later, several nonlinear cases were handled by considering linearized incremental variations about given nominal trajectories. Optimal discrete results were obtained as a function of the nonlinear system characteristics and the system noise inputs. Comparisons with available techniques were made to demonstrate the accuracy improvements obtained by using the optimization results.

Optimization on an Accuracy-Versus-Speed Basis

The basic optimization procedure described above was expanded to include algorithm accuracy and computational speed tradeoffs. The optimal discrete representations of continuous stochastic algorithms was developed to operate in real time. The resulting optimal digital mechanizations are suitable for use in on-line data processing applications. Acceptable performance criteria for optimization have been determined. These criteria indicate appropriate tradeoffs between computational speed and accuracy in specific examples under consideration. One approach was the use of constraints on computational speed in which some positive, monotonically decreasing function of the discretization interval T is incorporated directly into the cost functonal J for optimization. An alternate approach, which is more appropriate in other cases, was to treat computational speed as a hard constraint, e.g., a definite lower bound on computational speed is specified as part of the problem formulation. The mathematical development in both of these approaches follows traditional optimization techniques found in the literature, and the selection of appropriate cost functionals and/or optimization constraints yields significant new results for the discrete representation problem.

Trajectory Optimization

In the first two parts of this research, optimal discrete representations of continuous stochastic algorithms were developed for linearized variations about noise-free nominal trajectories for nonlinear systems. It was assumed in those cases that message and

measurement noises cause small perturbations about nominal operating conditions. Deterministic nominal trajectories were obtained by replacing noise inputs by their mean values. The resulting continuous equations for incremental variations about these trajectories were then linearized and discrete representations found as described above. However, excessive errors could be expected to occur when the system equations are highly nonlinear. A trajectory optimization technique could be applied in such cases to determine the best deterministic nominal trajectory about which the linearized variations should be formed. Numerical results have been presented in earlier papers (35,36) indicating that for a particular example the system performance appeared to be much more sensitive to the choice of this nominal trajectory than to the selection of a nonlinear filter of greater accuracy. The approach used here involved the simultaneous optimization of the nominal trajectory, the incremental filtering algorithm parameters, and the discrete representation itself on a speed-versus-accuracy basis. Specific characteristics were identified for those nonlinear system applications where trajectory optimization provided a significant improvement for the discrete representation problem under consideration.

Optimal Digital Simulations

In digital simulations it is always the objective to obtain the best possible discrete representation of a continuous system. The modeling of continuous noise inputs for dynamical systems on the digital computer was investigated by Rowland and Gupta (33). An accurate digital representation of the given continuous stationary correlated noise process was obtained by selecting both the digital shaping filter

and the variance Q_d of the discrete white noise representation as a function of the variance Q_c of the continuous white noise process $\omega(t)$, the sampling period T, and the parameters of the corresponding continuous shaping filter.

Consider a first-order continuous case

$$\dot{x}(t) = -a_1 x(t) + a_1 \omega(t) \tag{1.1}$$

Let the variance of colored noise process x(t) be designated as $P_c(t)$, where $P_c(t)$ obeys the differential equation

$$\dot{P}_c(t) = -2a_1 P_c(t) + a_1^2 Q_c \tag{1.2}$$

Similarly, for the discrete case, let the variance of the noise process $x_d(t_k)$ be defined as $P_d(t_k)$. Replacing a_1 by α_1 in (1.1) yields

$$x_d(t_{k+1}) = e^{-\alpha_1 T} x_d(t_k) + (1 - e^{-\alpha_1 T})\omega_d(t_k) \tag{1.3}$$

Thus, $P_d(t_{k+1})$ is given by

$$P_d(t_{k+1}) = e^{-2\alpha_1 T} P_d(t_k) + (1 - e^{-\alpha_1 T})^2 Q_d \tag{1.4}$$

It is assumed that the random processes x(t) and $x_d(t_k)$ are stationary. In steady-state $\dot{P}_c(t) = 0$ and $P_d(t_{k+1}) = P_d(t_k)$. Therefore, the steady-state values are

$$P_c\Big|_{ss} = \frac{a_1}{2} Q_c \tag{1.5}$$

$$P_d\Big|_{ss} = \frac{(1 - e^{-\alpha_1 T})^2 Q_d}{(1 - e^{-2\alpha_1 T})} \tag{1.6}$$

Since the objective is to optimally discretize the continuous correlated random process x(t), the right-hand sides of (1.5) and (1.6) are equated to give

$$Q_d = \frac{a_1(1 + e^{-\alpha_1 T})Q_c}{2(1 - e^{-\alpha_1 T})} \tag{1.7}$$

The relation (1.7) was obtained by requiring only that the variance of the modeling discrete-time series process be equivalent to that of the continuous process. The autocorrelation functions for the two cases may also be matched. Consider the autocorrelation function for the discrete case at the sampling instants $\tau = nT$, i.e.

$$\begin{aligned} R_{x_d x_d}(\tau)\Big|_{\tau=nT} &= E\{x_d(kT)x_d(\overline{k+n}\ T)\} \\ &= E\Big\{x_d(kT)\Big[(e^{-\alpha_1 T})^n x_d(kT) \\ &\quad + \sum_{m=0}^{n}(1 - e^{-\alpha_1 T})^{n-m+1}\omega_d(\overline{k+m}\ T)\Big]\Big\} \end{aligned} \tag{1.8}$$

where the notation kT has been used to replace t_k. Since $x_d(kT)$ is uncorrelated with the white noise input $\omega_d(\overline{k+m}\ T)$, which is applied to the digital shaping filter either at $t = kT$ or afterwards, (1.8) may be expressed as

$$R_{x_d x_d}(nT) = e^{-\alpha_1 (nT)} E\{x_d^2(kT)\} \tag{1.9}$$

Therefore, the autocorrelation function for the discrete case decays exponentially with a time constant of $1/\alpha_1$. The autocorrelation function for the continuous case is given by

$$R_{xx}(\tau) = e^{-a_1|\tau|} P_c\Big|_{ss}$$

$$= \frac{a_1}{2} Q_c e^{-a_1|\tau|} \tag{1.10}$$

It may be concluded then that setting α_1 equal to a_1 matches the auto-correlation functions exactly when the variance relationship is given by (1.7) with $\alpha_1 = a_1$ gives

$$\frac{Q_c}{Q_d} = \frac{2(1 - e^{-a_1 T})}{a_1(1 + e^{-a_1 T})} = T\left\{1 - \frac{(a_1 T)^2}{12} + \frac{(a_1 T)^4}{72} - \ldots\right\} \tag{1.11}$$

Since (1.3) yields an exact discrete realization of the given continuous process, one may determine the errors resulting from earlier approximations. Figure 1 shows the percent error obtained by using $Q_d = Q_c/T$ as a function of $a_1 T$ for the scalar example in (1.1).

Outline of the Thesis

The major emphasis of this thesis research was the development of optimal discrete representations of continuous filtering algorithms for nonlinear stochastic systems. The approach to this problem was based on the joint development of the estimation algorithm and the digital mechanization procedure. The system trajectory for nonlinear applications was optimized along with the digital mechanization. Chapter II deals with the mathematical formulation of the problem. A steady-state optimization approach is used in this chapter and the results are compared with the existing discretization methods. In Chapter III the optimal discrete representations are extended to the whole

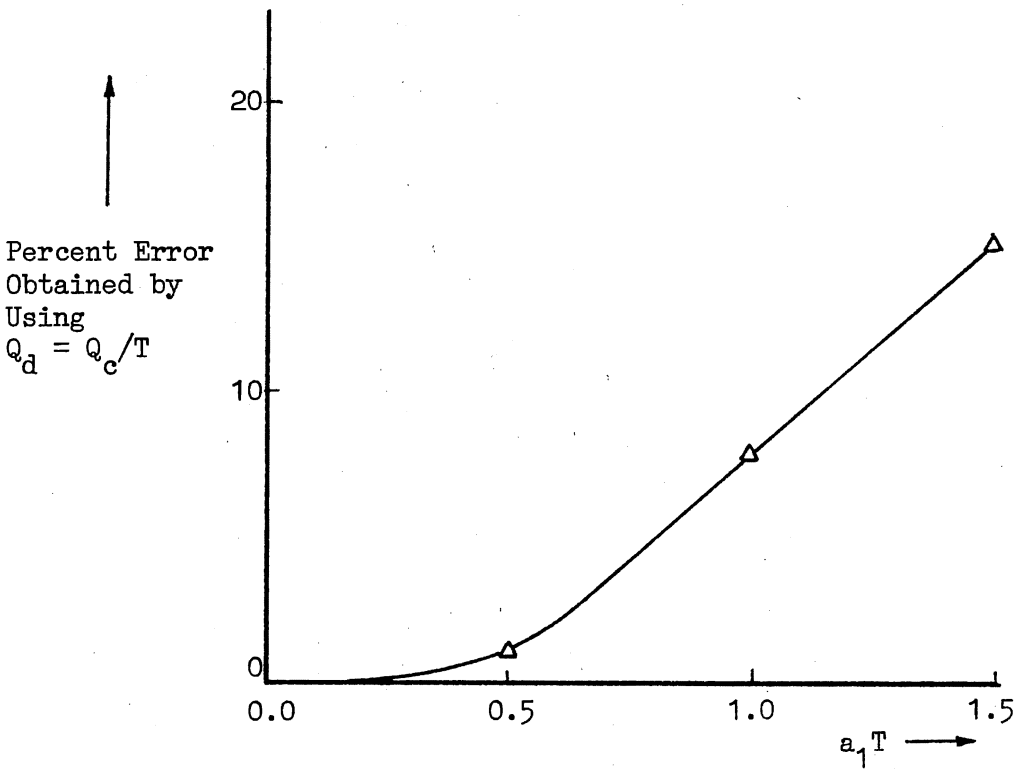

Figure 1. Percent Error Obtained by Using the Approximate Relationship for Variance Ratio

trajectory and results are compared with other discretization methods. The optimization procedure developed is expanded to include algorithm accuracy and computational speed tradeoffs in Chapter IV. The simultaneous optimization of the nominal trajectory, the incremental filtering algorithm parameters, and the discrete representation based on speed-versus-accuracy considerations are handled in Chapter V. Finally, in Chapter VI conclusions and recommendations are presented.

CHAPTER II

PRELIMINARY COMPARISON STUDIES

This chapter deals with the mathematical development of the optimal discrete representations. A first-order example is used to compare the optimal discrete representation results with the Euler Method results. The steady-state optimizations of this chapter are extended to the transient regions in Chapter III.

Mathematical Problem Statement

The nonlinear dynamic system is described by

$$\dot{\underline{x}}(t) = \underline{f}(\underline{x}(t),t) + B(t)\underline{\omega}(t) \tag{2.1}$$

$$\underline{z}(t) = \underline{h}(\underline{x}(t),t) + \underline{v}(t) \tag{2.2}$$

where $\underline{x}(t)$ is the n-vector representing the system state, $\underline{f}$ and $\underline{h}$ are vector functionals, and $B(t)$ is an n by m weighting matrix for the zero-mean white noise input $\underline{\omega}(t)$. The measurement vector $\underline{z}(t)$ is an r-vector. The system noise m-vector $\underline{\omega}(t)$ and measurement noise r-vector $\underline{v}(t)$ have covariance matrices $Q_{\omega}(t)$ and $Q_{v}(t)$, respectively, which are defined by

$$\begin{aligned} E\{\underline{\omega}(t)\underline{\omega}^{T}(\tau)\} &= Q_{\omega}(t)\delta(t - \tau) \\ E\{\underline{v}(t)\underline{v}^{T}(\tau)\} &= Q_{v}(t)\delta(t - \tau) \end{aligned} \tag{2.3}$$

It is assumed that $\underline{x}(t_0)$, $\underline{\omega}(t)$, and $\underline{v}(t)$ are all uncorrelated and that $Q_\omega(t)$ and $Q_v(t)$ are symmetric, positive-definite matrices.

The linearized (or variational) Kalman filter is based on an incremental linearization about a nominal trajectory. Both $\underline{f}(\underline{x}(t),t)$ and $\underline{h}(\underline{x}(t),t)$ are expanded in Taylor series about the nominal deterministic trajectory given by

$$\dot{\underline{x}}_N(t) = \underline{f}(\underline{x}_N(t),t) \tag{2.4}$$

where $\underline{x}_N(t)$ is the noise-free nominal trajectory and $\delta\underline{x}(t)$ is the small variation about $\underline{x}_N(t)$ caused by the disturbance noise $\underline{\omega}(t)$. Then

$$\begin{aligned} \delta\underline{x}(t) &= \underline{x}(t) - \underline{x}_N(t) \\ \delta\underline{z}(t) &= \underline{z}(t) - \underline{z}_N(t) \end{aligned} \tag{2.5}$$

and

$$\begin{aligned} \delta\dot{\underline{x}}(t) &= A(t)\delta\underline{x}(t) + B(t)\underline{\omega}(t) \\ \delta\underline{z}(t) &= C(t)\delta\underline{x}(t) + \underline{v}(t) \end{aligned} \tag{2.6}$$

For the linearized Kalman filter, A(t) and C(t) are given by

$$\begin{aligned} A(t) &\triangleq \left.\frac{\partial \underline{f}(\underline{x}(t),t)}{\partial \underline{x}(t)}\right|_{\underline{x}(t)=\underline{x}_N(t)} \\ C(t) &\triangleq \left.\frac{\partial \underline{h}(\underline{x}(t),t)}{\partial \underline{x}(t)}\right|_{\underline{x}(t)=\underline{x}_N(t)} \end{aligned} \tag{2.7}$$

The linearized continuous Kalman filtering equations are given by

$$\dot{\delta\hat{\underline{x}}}(t) = A(t)\delta\hat{\underline{x}}(t) + K(t)[\delta\underline{z}(t) - C(t)\delta\hat{\underline{x}}(t)] \tag{2.8}$$

$$K(t) = P_e(t)C^T(t)Q_v^{-1}(t) \tag{2.9}$$

where the error covariance equation is

$$P_e(t) = A(t)P_e(t) + P_e(t)A^T(t) - P_e(t)C^T(t)Q_v^{-1}C(t)P_e(t)$$
$$+ B(t)Q_\omega(t)B^T(t) \tag{2.10}$$

The linearized Kalman filter in (2.8)-(2.10) yields the least mean-square estimation error for the incremental variation $\underline{\delta x}(t)$ in (2.6). The sum of $\underline{\delta \hat{x}}(t)$ and $\underline{x}_N(t)$, denoted by $\underline{\hat{x}}(t)$, is only an approximate estimate of the system state $\underline{x}(t)$ in (2.1) because higher-order terms were neglected in forming (2.6). This approximation provides a nearly optimal estimate when $\underline{\delta x}(t)$ is sufficiently small over the time interval of interest. Trajectory optimization has been described in a later section of this thesis as one means of improving the accuracy of the resulting state estimate.

The problem investigated in this thesis research is to obtain an optimal discrete filtering model according to a given cost functional. Let a discrete representation of ℓ components of $\underline{\delta \hat{x}}(t)$, where $\ell \leq n$, be given by

$$\underline{\delta \hat{x}}_d(t_{k+1}) = \alpha(t_k)\underline{\delta \hat{x}}_d(t_k) + \beta(t_k)\underline{\delta z}(t_k) \tag{2.11}$$

The ℓ-vector $\underline{\delta \hat{x}}_d(t_k)$ represents the discrete filtering model state, and $\alpha(t_k)$ and $\beta(t_k)$ are ℓ by ℓ and ℓ by r matrices composed of free optimization parameters. While the $\alpha(t_k)$ and $\beta(t_k)$ matrices in (2.11) are indicated as functions of t_k only, they are actually functions of the complete system response over its entire range of operation and

their optimal values will be determined as part of the optimization procedure. A schematic diagram is shown in Figure 2.

A cost functional J is selected such that the minimization of J results in a suitable discrete representation of the continuous variational Kalman filter by the discrete model in (2.11). It is required that if the discrete model order ℓ is equal to the system order n and if a sufficiently small discretization interval T is selected, then the discrete modeling error in representing (2.8) by (2.11) should be arbitrarily small at $t = t_k$ for all k. If ℓ equals n but T is not sufficiently small, then the form of the discrete model should be the same as a direct discretization of (2.8) except different values of $\alpha(t_k)$ and $\beta(t_k)$ will be obtained.

Two approaches are commonly used to obtain an estimate of $\underline{\delta x}(t)$ at discrete points in time. First, the continuous linearized Kalman filtering equations in (2.8) may be integrated on the digital computer by using either single-step (Runge-Kutta) or multi-step (Adams-Bashforth or Adams-Moulton) numerical integration formulas. Second, the continuous equations in (2.6) may be discretized directly, and an optimal discrete Kalman filtering algorithm may be applied to the resulting discrete equations. In this thesis research a generalized optimization format which includes the two approaches above as special cases when ℓ equals n and T is sufficiently small was investigated. Two approaches toward this more general discrete optimization is to define a cost functional J as either

$$J = \text{Trace} \sum_{k=0}^{K-1} \frac{1}{2} E\{[\underline{\delta\hat{x}}_{\ell}(t_{k+1}) - \underline{\delta\hat{x}}_{d}(t_{k+1})][\underline{\delta\hat{x}}_{\ell}(t_{k+1}) - \underline{\delta\hat{x}}_{d}(t_{k+1})]^T\} \tag{2.12}$$

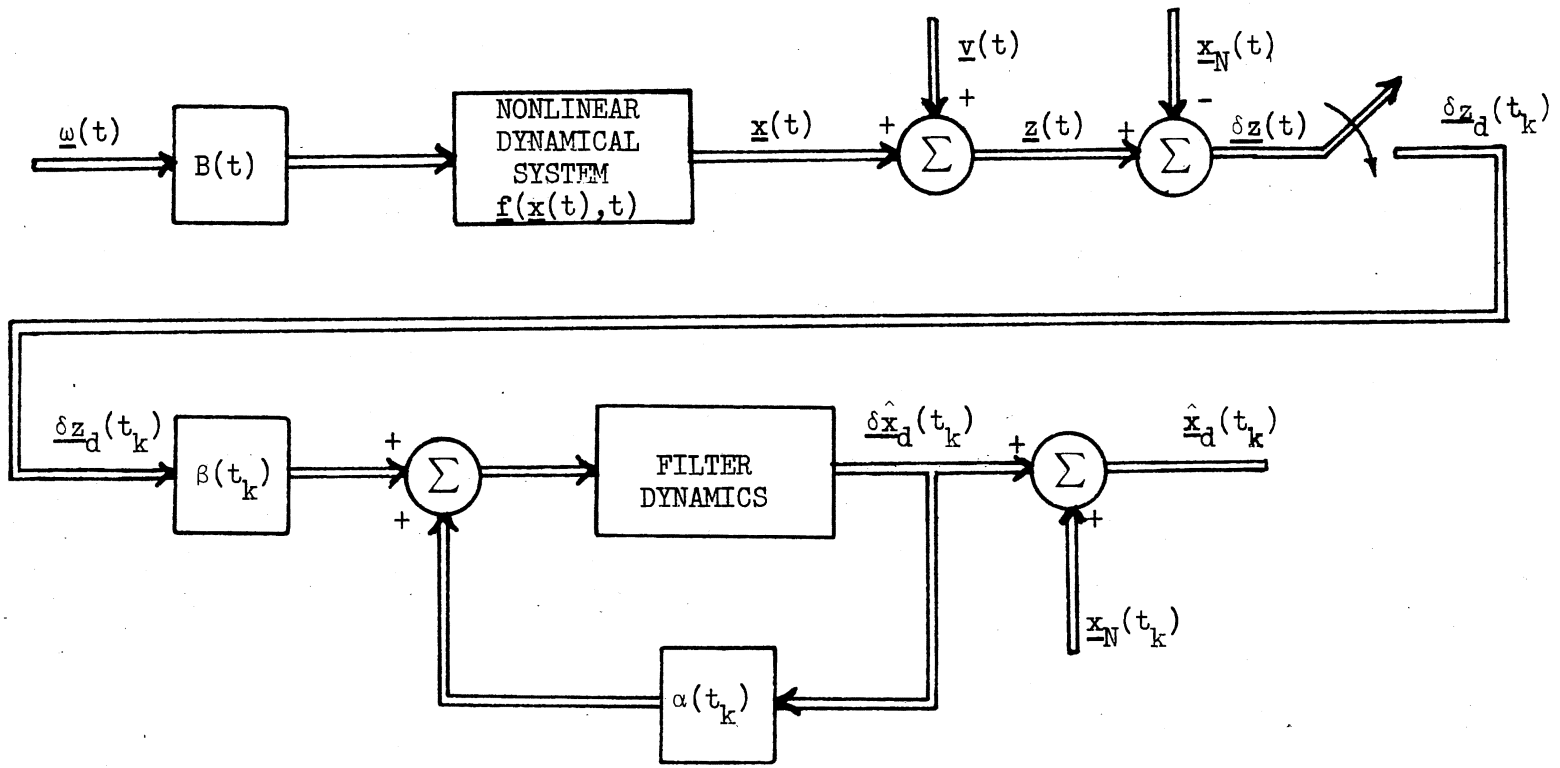

Figure 2. A Schematic Diagram of Filtering Equations with Optimization Parameters Included in α and β Matrices

or as

$$J = \text{Trace} \sum_{k=0}^{K-1} \frac{1}{2} E\{[\underline{\delta x}_{\ell}(t_{k+1}) - \underline{\delta \hat{x}}_{d}(t_{k+1})][\underline{\delta x}_{\ell}(t_{k+1}) - \underline{\delta \hat{x}}_{d}(t_{k+1})]^{T}\} \tag{2.13}$$

where $\underline{\delta x}_{\ell}$ contains the ℓ ordered states from $\underline{\delta x}$ corresponding to $\underline{\delta \hat{x}}_{d}$. The J in (2.12) is based on forming an optimal discrete model (2.11) for the continuous variational Kalman filter in (2.8). On the other hand, the J in (2.13) attempts to obtain an optimal discrete fixed-configuration filter for estimating the $\underline{\delta x}(t)$ in (2.6). The problem is to obtain optimal values of $\alpha(t_k)$ and $\beta(t_k)$ in (2.11) to minimize the J in (2.12) or (2.13) subject to (2.5)-(2.10).

Steady-State Optimizations

The mathematical problem stated in the previous section was approached initially by considering a first-order linear system. The first step towards obtaining the optimal stochastic representations was achieved by comparing the results for the steady-state portions. These results were then extended for the general case by also comparing the transient portion results. The steady-state equations were obtained for the continuous case by equating the derivative portion to zero. For the discrete case the (k+1)th stage was equated to the kth stage.

Let the first-order system be

$$\dot{x}(t) = -x(t) + \omega(t) \tag{2.14}$$

and its state estimate $\hat{x}(t)$ be given by

$$\dot{\hat{x}}(t) = -\hat{x}(t) + K(t)[x(t) + v(t) - \hat{x}(t)] \tag{2.15}$$

where

$$K(t) = \frac{P_e(t)}{Q_v}$$

$$P_e(t) = E\{(x - \hat{x})^2\} \tag{2.16}$$

The discrete representations of (2.14) and (2.15) may be written as

$$x_d(t_{k+1}) = e^{-T}x_d(t_k) + (1 - e^{-T})\omega_d(t_k)$$

$$\hat{x}(t_{k+1}) = (e^{-T} - e^{-(1+K(t_k))T})x_d(t_k) + e^{-(1+K(t_k))T}\hat{x}(t_k) \tag{2.17}$$

$$- \frac{1}{(1+K(t_k))}(1 - e^{-(1+K(t_k))T})\omega_d(t_k) + (1 - e^{-T})\omega_d(t_k)$$

$$+ \frac{1}{(1+K(t_k))}(1 - e^{-(1+K(t_k))T})v_d(t_k)$$

The optimal discrete representation of (2.15) may be written as

$$\hat{x}_\alpha(t_{k+1}) = \alpha(t_k)\hat{x}_\alpha(t_k) + \beta(t_k)x_d(t_k) + \beta(t_k)v_d(t_k) \tag{2.18}$$

The covariance equations for (2.14) and (2.15) are given by

$$\dot{P}_{11} = -2P_{11} + Q_\omega$$

$$\dot{P}_{12} = P_{11} - 3P_{12} \tag{2.19}$$

$$\dot{P}_{22} = 2P_{12} - 4P_{22} + Q_v$$

In steady-state $\dot{P}_{11} = \dot{P}_{12} = \dot{P}_{22} = 0$, which gives

$$P_{11} = \frac{Q_\omega}{2}$$

$$P_{12} = \frac{Q_\omega}{6} \tag{2.20}$$

$$P_{22} = \frac{Q_\omega}{12} + \frac{Q_v}{4}$$

Also, the covariance equations for (2.17) for $K(t_k) = 1$ may be written as

$$\begin{aligned} P_{d11}(t_{k+1}) &= E\{x_d^2(t_{k+1})\} \\ &= (1 - e^{-2T})P_{d11}(t_k) + (1 - e^{-T})^2 Q_{\omega d} \end{aligned} \tag{2.21}$$

$$\begin{aligned} P_{d1\alpha}(t_{k+1}) &= E\{x_d(t_{k+1})\hat{x}_\alpha(t_{k+1})\} \\ &= \alpha e^{-T} P_{d1\alpha}(t_k) + \beta e^{-T} P_{d11}(t_k) \end{aligned} \tag{2.22}$$

and

$$\begin{aligned} P_{d\alpha\alpha}(t_{k+1}) &= E\{\hat{x}_\alpha^2(t_{k+1})\} \\ &= \alpha^2 P_{d\alpha\alpha}(t_k) + \beta^2 P_{d11}(t_k) + 2\alpha\beta P_{d1\alpha}(t_k) + \beta^2 Q_{vd} \end{aligned} \tag{2.23}$$

In steady-state

$$\begin{aligned} P(t_{k+1}) &= P(t_k) \\ P_{d11}(t_k) &= \frac{(1 - e^{-T})}{(1 + e^{-T})} Q_{\omega d} \\ P_{d1\alpha}(t_k) &= \frac{0.5\beta e^{-T} Q_\omega}{1 - \alpha e^{-T}} \\ P_{d\alpha\alpha}(t_k) &= \frac{\beta^2[(0.5Q_\omega + Q_{vd})(1 - \alpha e^{-T}) + \alpha e^{-T} Q_\omega]}{(1 - \alpha^2)(1 - \alpha e^{-T})} \end{aligned} \tag{2.24}$$

These equations are matched term-by-term in the next section to obtain

an optimal steady-state discrete representation of the filtering algorithm.

Numerical Comparisons with the Euler Method

The mathematical development of the steady-state equations and their comparisons are discussed in this section. The results obtained from the optimal discrete representation and the Euler Method are plotted in several figures.

The covariance equations in steady-state form, (2.20) and (2.24), are matched to obtain the optimal coefficients for an optimal discrete representation.

$$P_{d11}(t_k) = \frac{1 - e^{-T}}{1 + e^{-T}} Q_{\omega d} = \frac{Q_\omega}{2}$$

$$\frac{Q_\omega}{Q_{\omega d}} = \frac{2(1 - e^{-T})}{(1 + e^{-T})} \tag{2.25}$$

which gives the exact discrete realization (33). Also

$$P_{d1\alpha}(t_k) = P_{12}(t_k)$$

$$\frac{0.5\beta e^{-T} Q_\omega}{1 - \alpha e^{-T}} = \frac{Q_\omega}{6} \tag{2.26}$$

and

$$P_{d\alpha\alpha}(t_k) = P_{22}(t_k)$$

$$\frac{\beta^2[(0.5Q_\omega + Q_{vd})(1 - \alpha e^{-T}) + \alpha e^{-T} Q_\omega]}{(1 - \alpha^2)(1 - \alpha e^{-T})} = \frac{Q_\omega}{12} + \frac{Q_v}{4} \tag{2.27}$$

To obtain the exact digital representation of Q_v in steady-state for $K(t_k) = 1.0$, the covariance equations for (2.17) in the discrete form may be written as

$$P(t_{k+1}) = \Phi P(t_k)\Phi^T + HQH^T \tag{2.28}$$

where

$$\Phi = \begin{bmatrix} e^{-T} & 0 \\ \frac{1}{2}(1 - e^{-2T}) & e^{-2T} \end{bmatrix}$$

$$H = \begin{bmatrix} 1 - e^{-T} & 0 \\ 0 & \frac{1}{2}(1 - e^{-2T}) \end{bmatrix}$$

and

$$Q = \begin{bmatrix} Q_{\omega d} & 0 \\ 0 & Q_{vd} \end{bmatrix}$$

or

$$P_{11}(t_{k+1}) = \phi_{11}(\phi_{11}P_{11}(t_k) + \phi_{12}P_{12}(t_k)) + \phi_{12}(\phi_{11}P_{12}(t_k) + \phi_{12}P_{22}(t_k)) + (1 - e^{-T})^2 Q_{\omega d}$$

$$P_{12}(t_{k+1}) = \phi_{11}(\phi_{21}P_{11}(t_k) + \phi_{22}P_{12}(t_k)) + \phi_{12}(\phi_{21}P_{12}(t_k) + \phi_{22}P_{22}(t_k))$$

$$P_{22}(t_{k+1}) = \phi_{21}(\phi_{21}P_{11}(t_k) + \phi_{22}P_{12}(t_k)) + \phi_{22}(\phi_{21}P_{12}(t_k) + \phi_{22}P_{22}(t_k)) + \frac{1}{4}(1 - e^{-2T})Q_{vd} \tag{2.29}$$

In steady-state

$$P_{22}(t_{k+1}) = P_{22}(t_k) \tag{2.30}$$

From the third equation in (2.29)

$$P_{22}(t_k) = \frac{\phi_{21}^2 P_{11}(t_k) + 2\phi_{21}\phi_{22}P_{12}(t_k) + \frac{1}{4}(1 - e^{-2T})^2 Q_{vd}}{1 - \phi_{22}^2}$$

$$= \frac{(3 + e^{-2T})Q_\omega + 6(1 - e^{-2T})Q_{vd}}{24(1 + e^{-2T})} \tag{2.31}$$

Matching the right hand sides of (2.20) and (2.31) yields

$$\frac{(3 + e^{-2T})Q_\omega + 6(1 - e^{-2T})Q_{vd}}{24(1 + e^{-2T})} = \frac{Q_\omega}{12} + \frac{Q_v}{4} \tag{2.32}$$

Solving for Q_{vd} gives

$$Q_{vd} = \frac{6Q_v(1 + e^{-2T}) - Q_\omega(1 - e^{-2T})}{6(1 - e^{-2T})} \tag{2.33}$$

The difference in modeling Q_v as Q_v/T and by (2.33) are evident in Figure 3. It can be observed that a small modeling error would be introduced if Q_v/T were used instead of the value of Q_{vd} given by (2.33).

Returning now to the original problem with this optimal value of Q_{vd}, there are two unknowns, α and β, and two equations, (2.26) and (2.27). These two equations can be rewritten to yield

$$\alpha + 3\beta - e^T = 0 \tag{2.34}$$

$$(\alpha^2 - 1)(\frac{Q_\omega}{12} + \frac{Q_v}{4})(1 - \alpha e^{-T}) + \beta^2((0.5Q_\omega + Q_{vd})(1 - \alpha e^{-T}) + \alpha e^{-T}Q_\omega) = 0 \tag{2.35}$$

These equations can further be solved in terms of β to obtain

$$\beta = \frac{(e^T - \alpha)}{3} \tag{2.36}$$

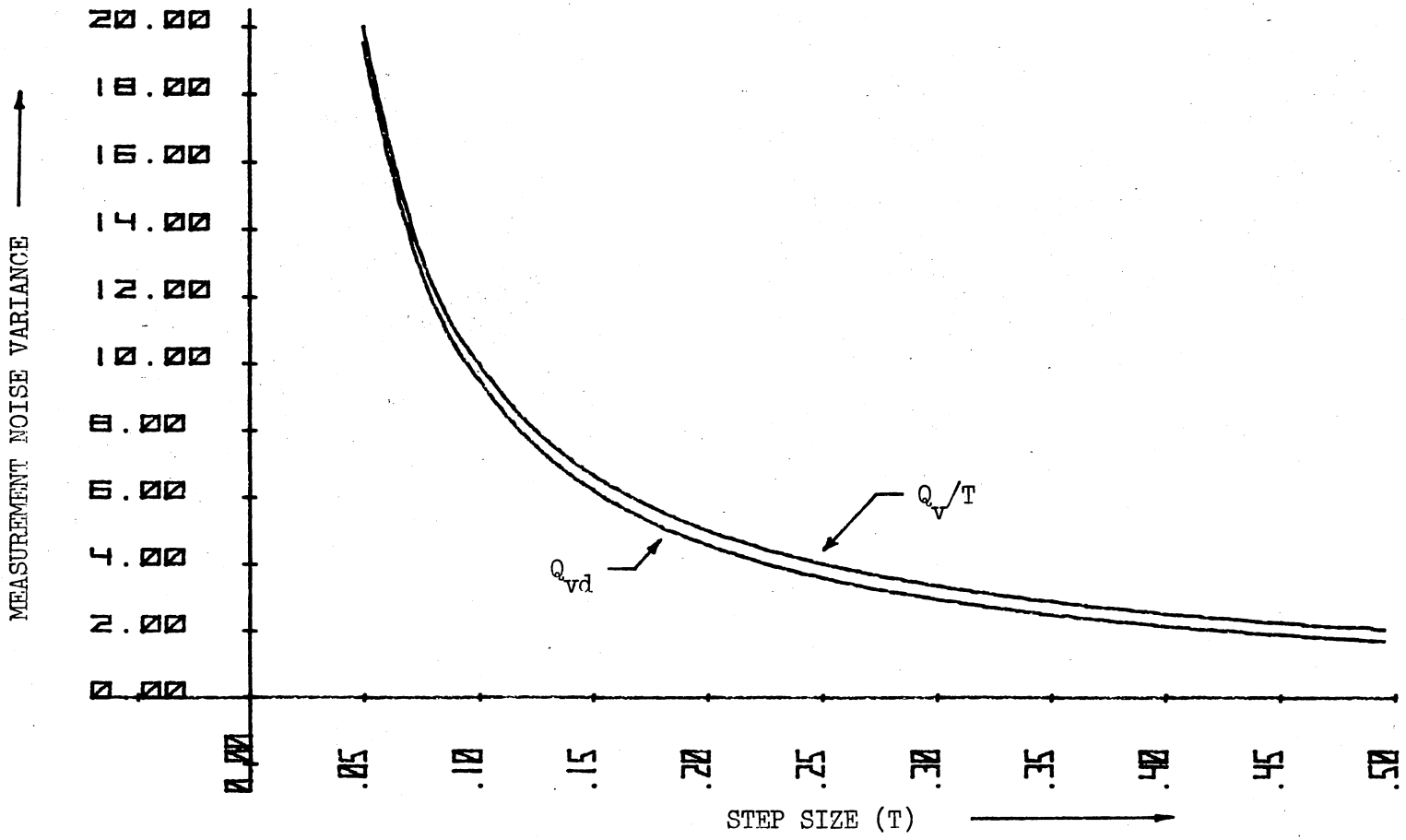

Figure 3. The difference in Modeling Q_v as Q_v/T and by (2.33) for the First-Order Linear System

and

$$\beta = \sqrt{\frac{\left(\frac{Q_\omega}{12} + \frac{Q_v}{4}\right)(1 - \alpha^2)(1 - \alpha e^{-T})}{(0.5Q_\omega + Q_{vd})(1 - \alpha e^{-T}) + \alpha e^{-T} Q_\omega}}$$

The cost functional for the first-order example given by (2.14) may be written as

$$J = \frac{1}{2}\left[P_{d11}(t_{k+1}) + P_{d\alpha\alpha}(t_{k+1}) - 2P_{d1\alpha}(t_{k+1})\right] \tag{2.37}$$

In steady-state

$$J = \frac{1}{2}\left[P_{d11}(t_k) + P_{d\alpha\alpha}(t_k) - 2P_{d1\alpha}(t_k)\right] \tag{2.38}$$

Also, the error covariance matrix

$$\begin{aligned} P_e(t) &= E\{(x - \hat{x})^2\} \\ &= P_{11}(t) + P_{22}(t) - 2P_{12}(t) \end{aligned} \tag{2.39}$$

Now

$$\dot{P}_e(t) = -2P_e(t) - \frac{P_e^2}{Q_v} + Q_\omega \tag{2.40}$$

In steady-state, setting $\dot{P}_e(t)$ to 0 yields

$$\frac{P_e^2}{Q_v} + 2P_e - Q_\omega = 0$$

$$P_e = \frac{-2 \pm \sqrt{4 + 4\frac{Q_\omega}{Q_v}}}{\frac{2}{Q_v}}$$

or

$$P_e = Q_v\left(-1 \pm \sqrt{1 + \frac{Q_\omega}{Q_v}}\right) \tag{2.41}$$

As an example, choosing $Q_\omega = 3.0$ and $Q_v = 1.0$, one has

$$P_e = 1 \tag{2.42}$$

From (2.38), (2.39) and (2.42) at $t = t_k$, one has

$$J = 0.5 \tag{2.43}$$

Now the equations of β in terms of α in (2.36) are plotted in Figure 4. It is assumed that $Q_\omega = 3.0$, $Q_v = 1.0$, and $T = 0.1$. Since the two curves do not intersect, the exact discrete representation of the filtering algorithm is not possible. In other words, the cost functional will not be exactly 0.5 for this example as required by (2.43).

To obtain the minimum value of performance index based on the optimal values of α and β for given T, Q_ω, and Q_v, Fletcher and Powell's unconstrained minimization technique is used (37,38). The cost functional obtained from optimal (α,β) values and the Euler Method are plotted in Figure 5 for three values of T. This figure shows that a smaller cost functional is obtained by using the coefficients of the optimal discrete representation of the filtering algorithm.

These values of α and β were used in (2.18) and (2.38) for 100 Monte Carlo simulation runs which were ensemble-averaged to obtain error covariance results. These results are compared with the same number of Monte Carlo simulation runs for the Euler Method in Figure 6 through 8 using step sizes T = 0.1, 0.25, and 0.5. These curves verify the optimal discrete representation of the filtering technique for the first-order linear system in the steady-state for the cost functional J given by (2.13). In Figures 9 through 11, the curves are plotted for the cost functional J given by (2.12) by using the optimal

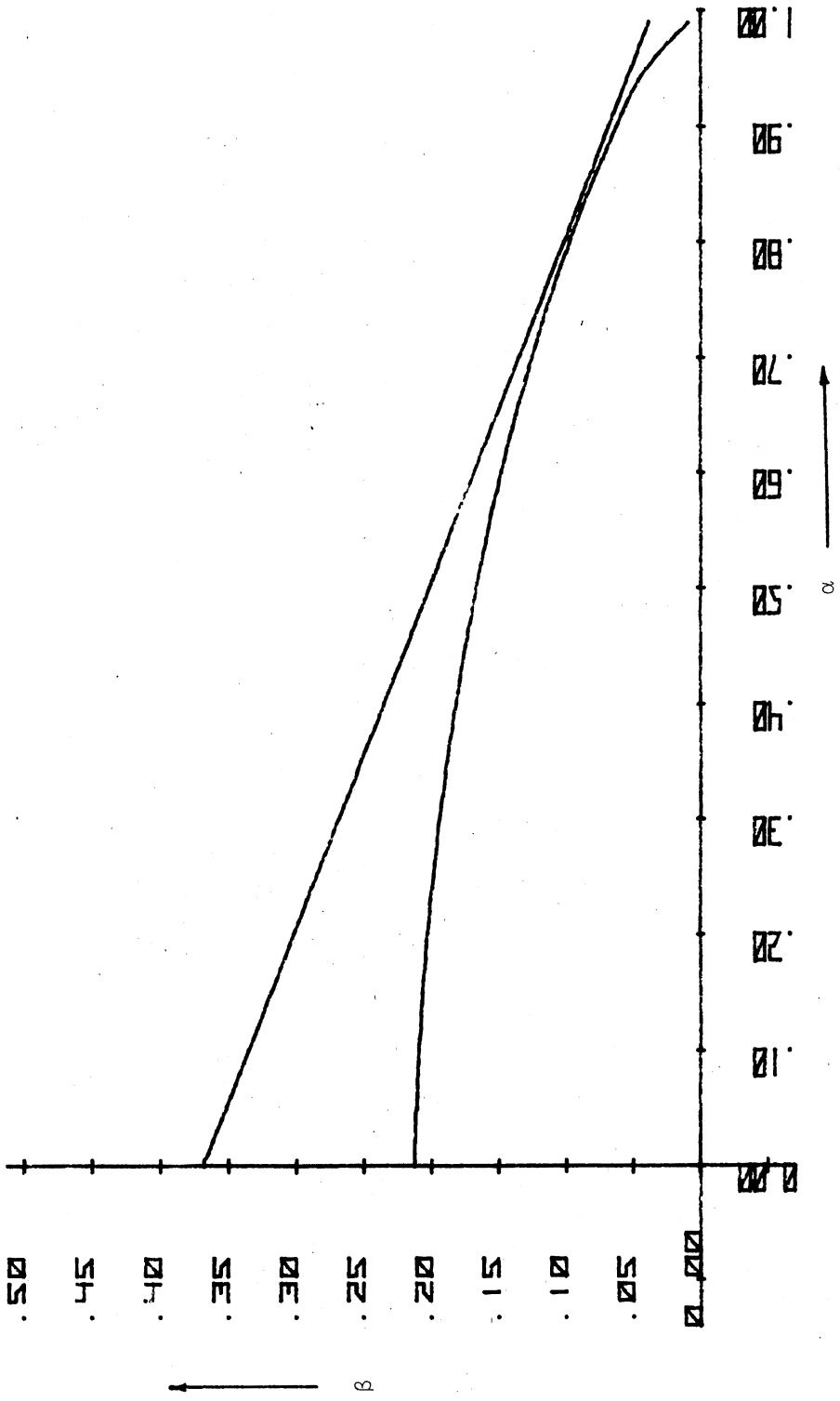

Figure 4. The Parameter β Plotted for Different Values of α in Steady-State for T = 0.1

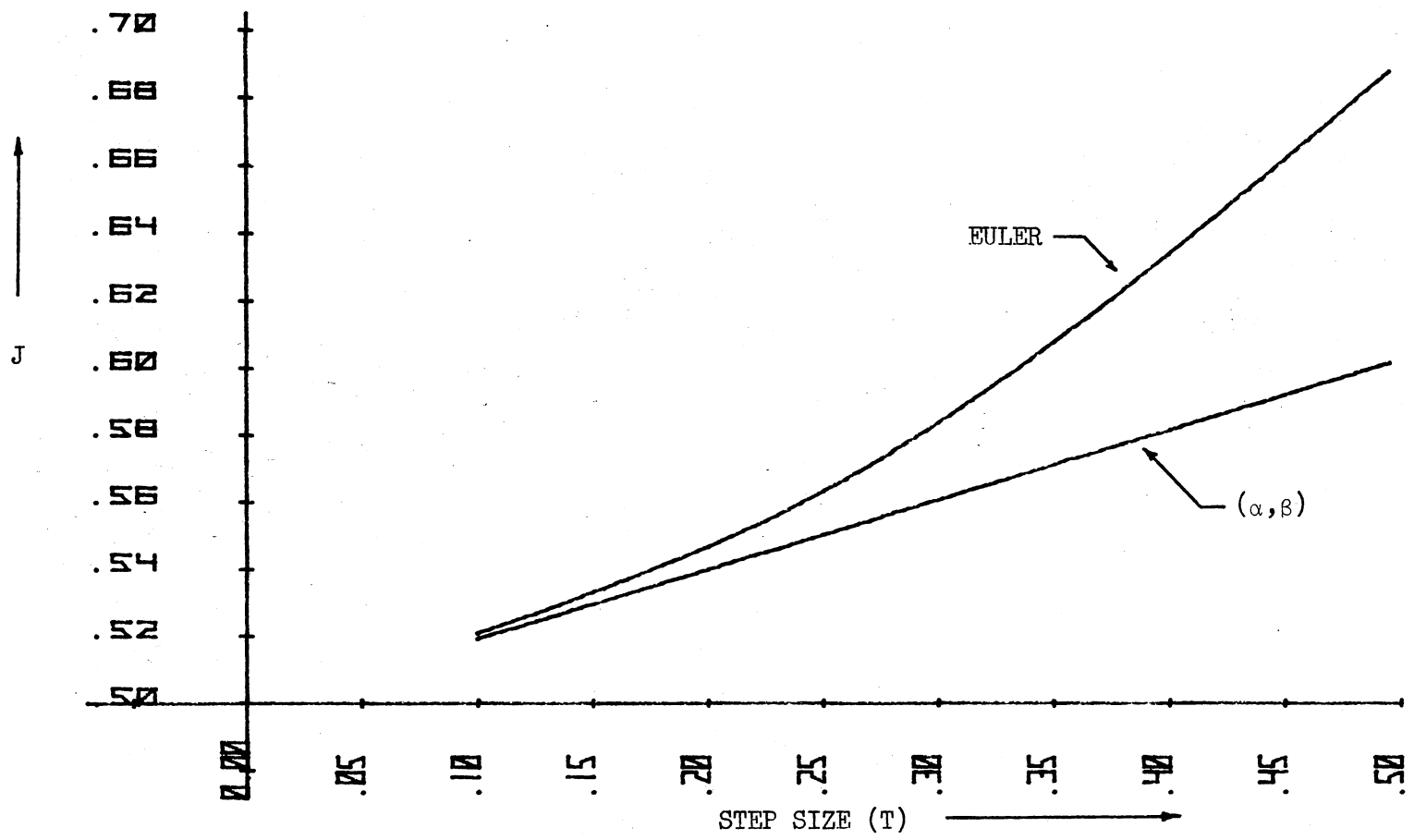

Figure 5. The Cost Functionals from Optimal (α,β) Values and the Euler Method for the First-Order Linear System

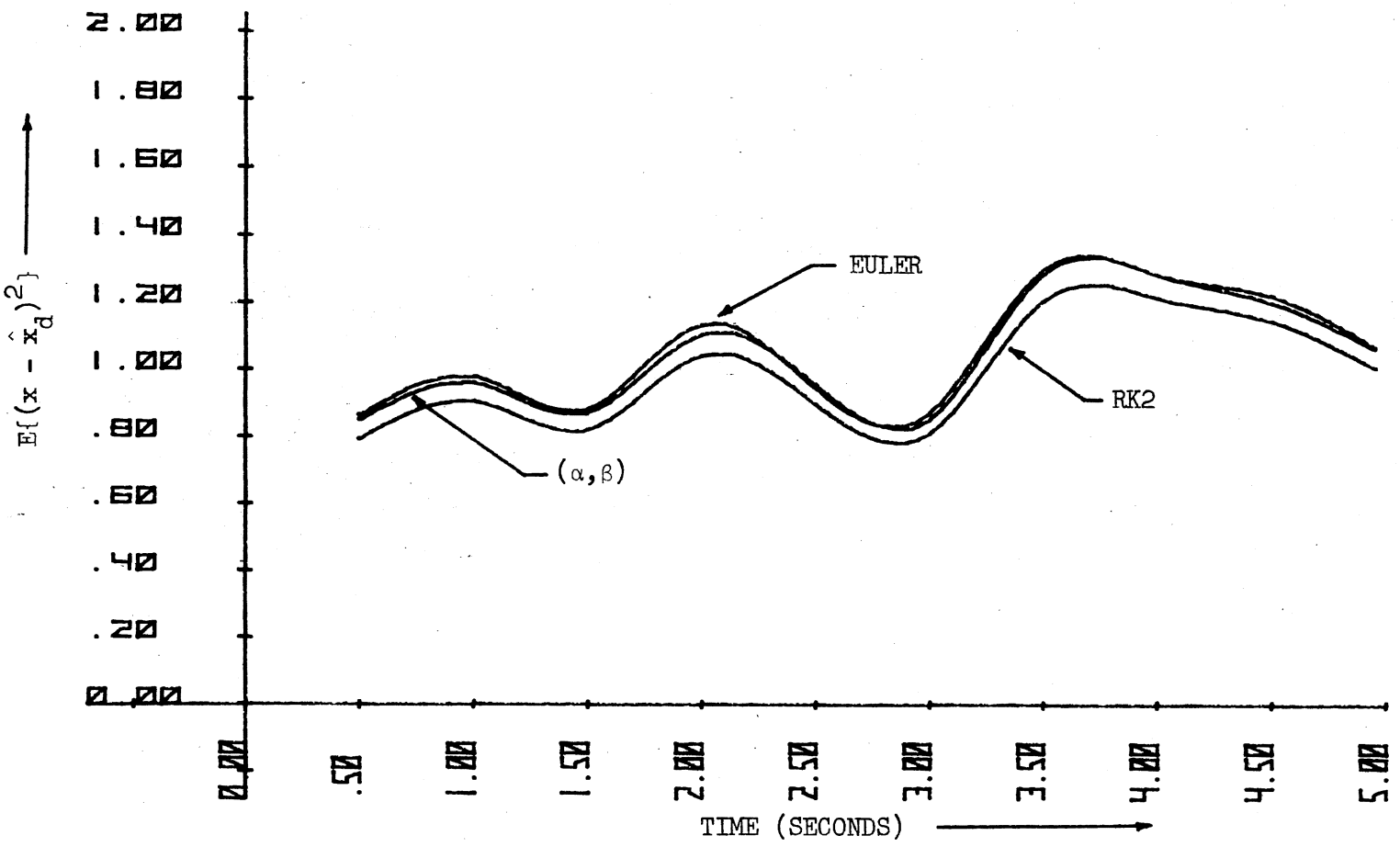

Figure 6. Comparisons of Error Covariance $E\{(x - \hat{x}_d)^2\}$ for Steady-State Optimizations for the First-Order Linear System for T = 0.1

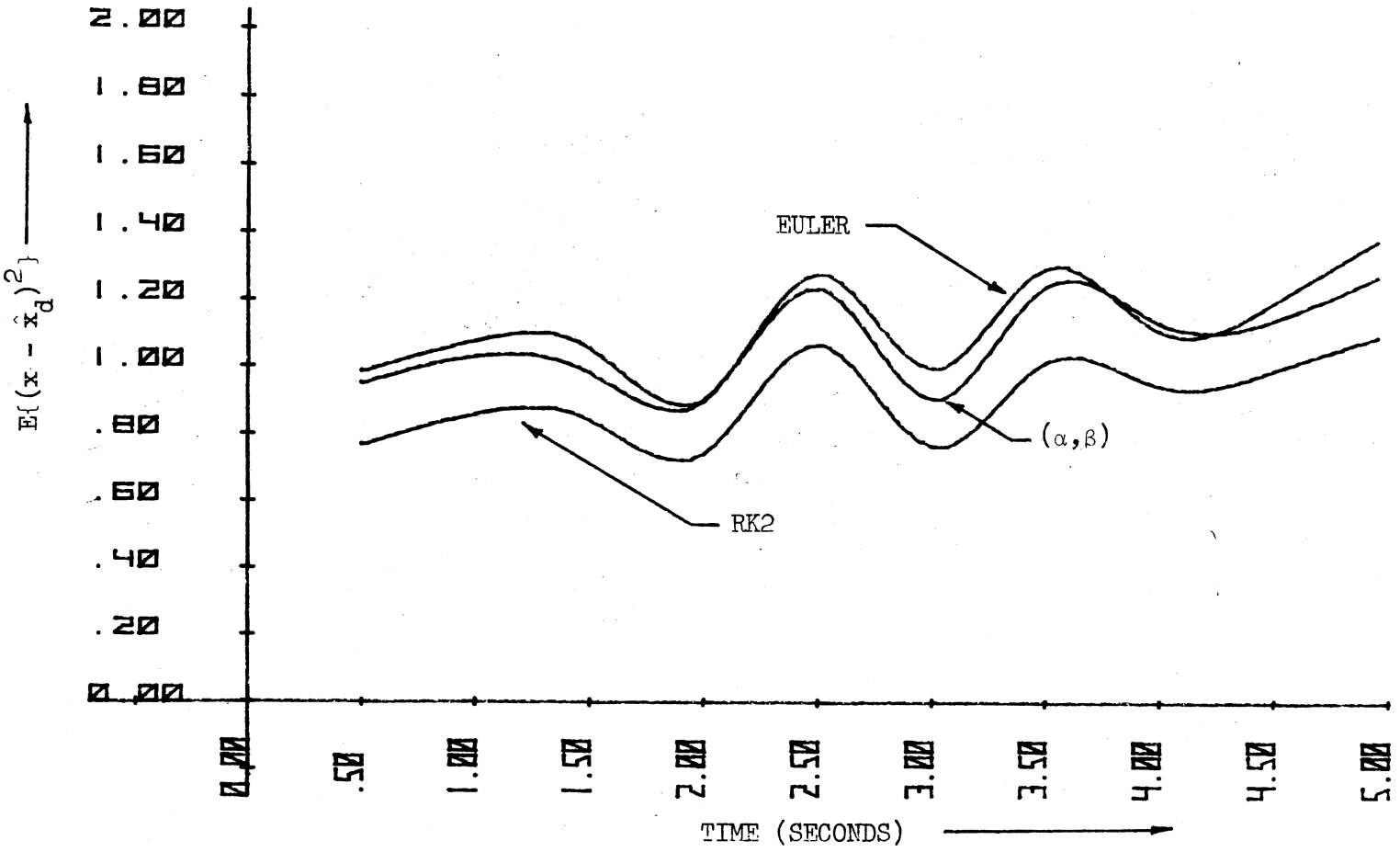

Figure 7. Comparisons of Error Covariance $E\{(x - \hat{x}_d)^2\}$ for Steady-State Optimizations for the First-Order Linear System for T = 0.25

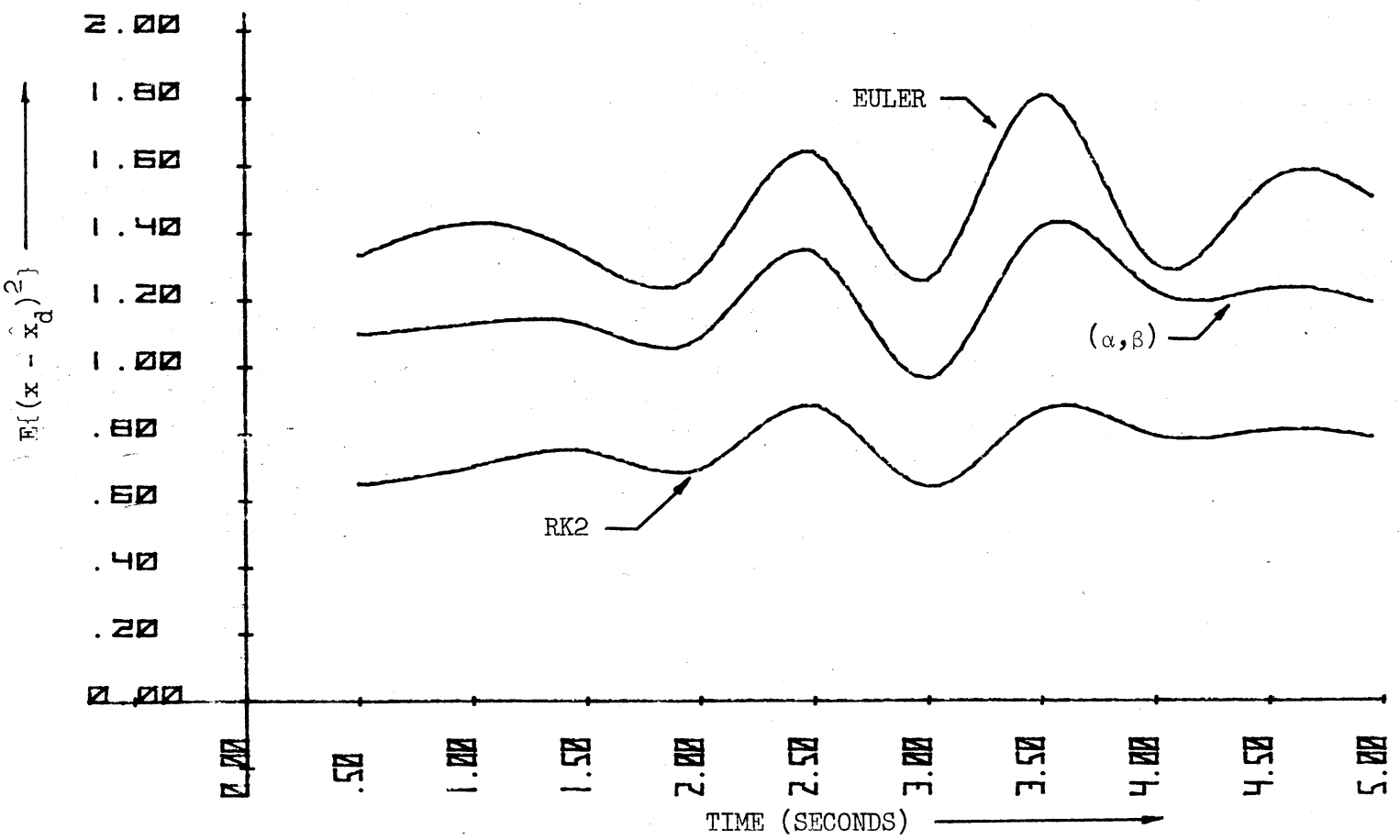

Figure 8. Comparisons of Error Covariance $E\{(x - \hat{x}_d)^2\}$ for Steady-State Optimizations for the First-Order Linear System for T = 0.5

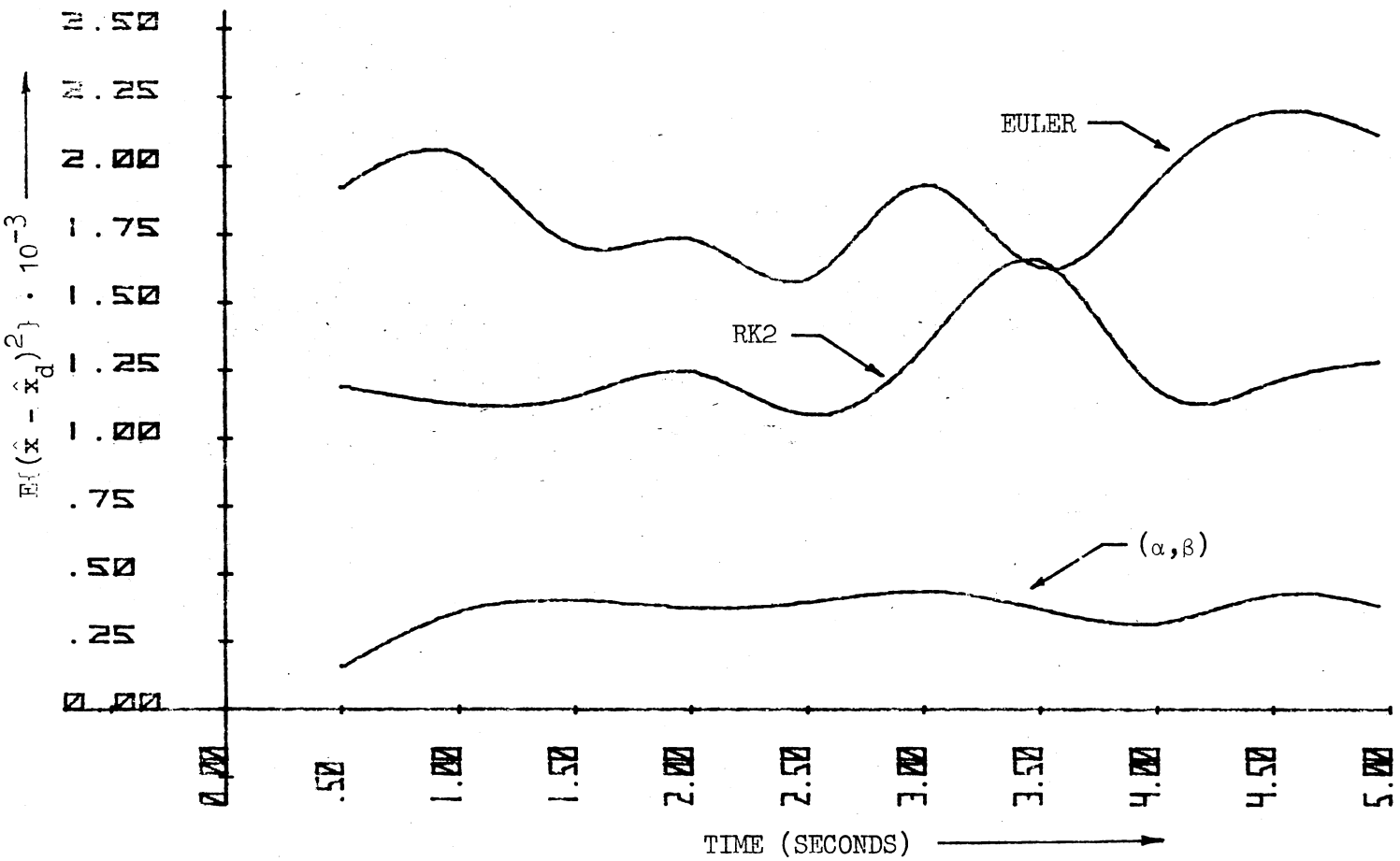

Figure 9. Comparisons of Error Covariance $E\{(\hat{x} - \hat{x}_d)^2\}$ for Steady-State Optimizations for the First-Order Linear System for T = 0.1

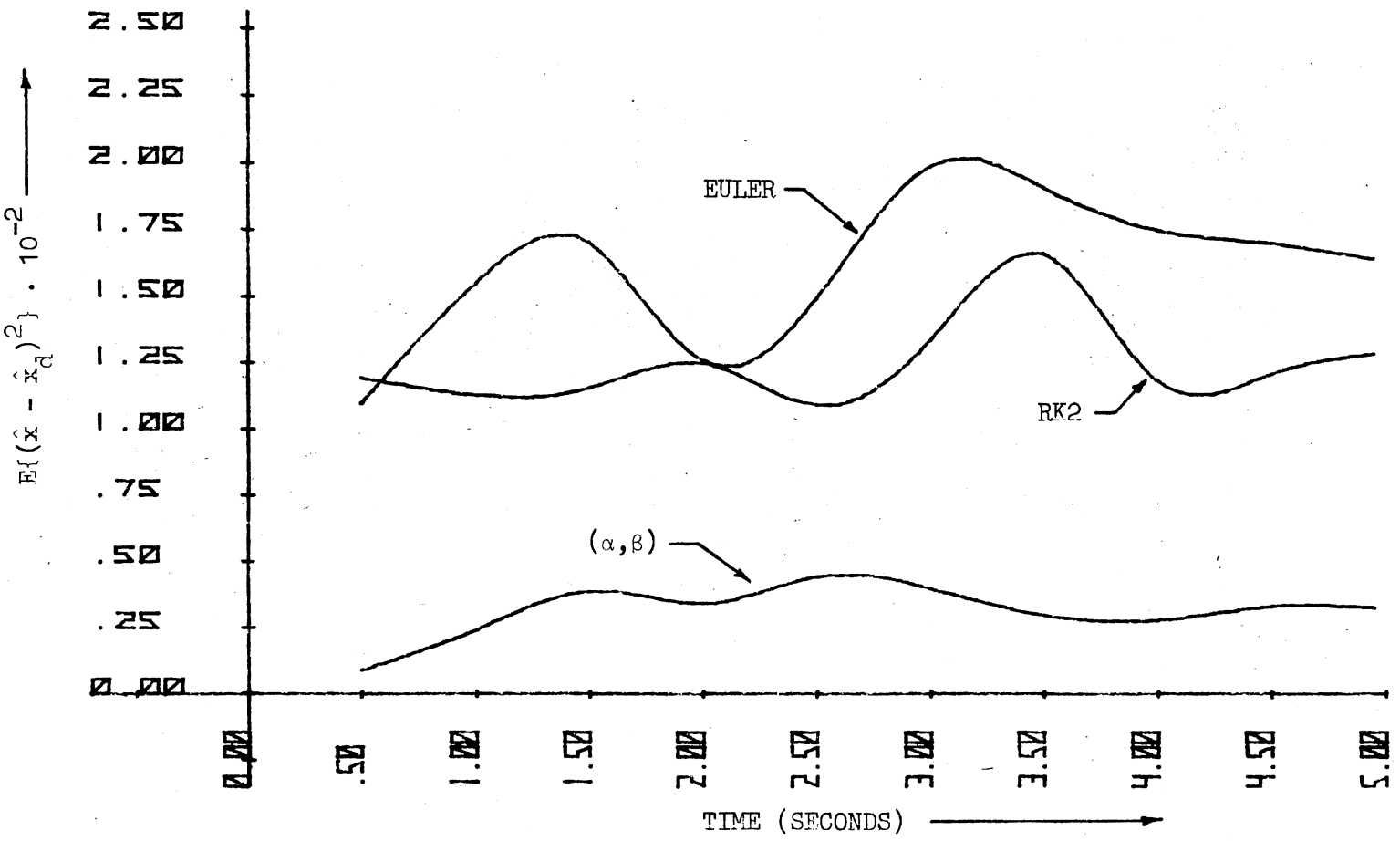

Figure 10. Comparisons of Error Covariance $E\{(\hat{x} - \hat{x}_d)^2\}$ for Steady-State Optimizations for the First-Order Linear System for T = 0.25

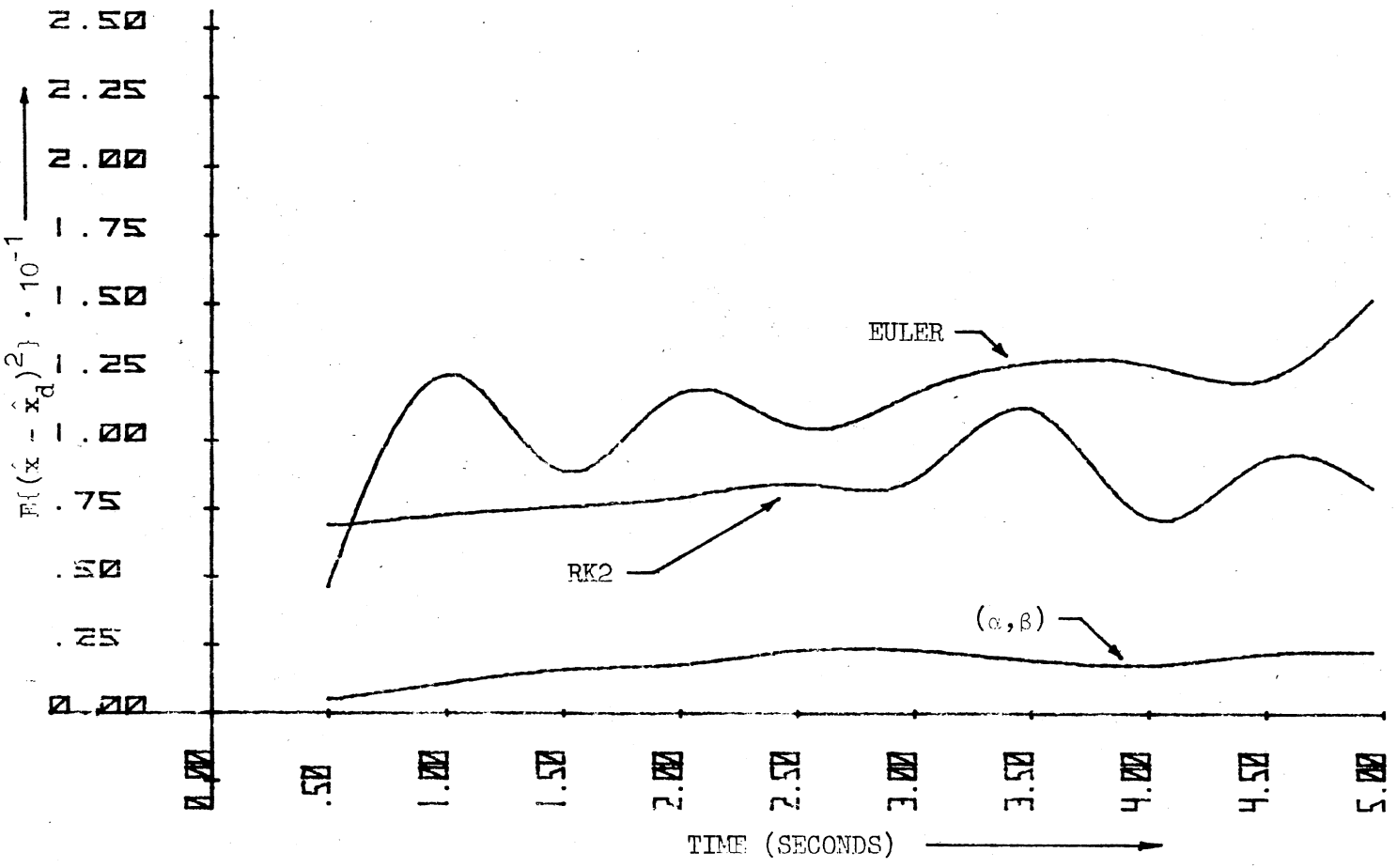

Figure 11. Comparisons of Error Covariance $E\{(\hat{x} - \hat{x}_d)^2\}$ for Steady-State Optimizations for the First-Order Linear System for T = 0.5

α and β parameters determined from (2.13).

Numerical Comparisons with the RK2 Integration Formula

The optimal discrete representations may also be compared with the second-order Runge-Kutta method (RK2). The recursive relation for the general case using RK2 may be written for the integration interval T as

$$\underline{x}(t_{k+1}) = \underline{x}(t_k) + \frac{T}{2}\left[\underline{g}(\underline{x}(t_k),t_k) + \underline{g}(\underline{x}(t_{k+1}),t_{k+1})\right] \qquad (2.44)$$

where

$$\dot{\underline{x}}(t) = \underline{g}(\underline{x}(t),t) \qquad (2.45)$$

The recursive relation for the state using the above method for the first-order system given by (2.14) may be written as

$$\hat{x}_d(t_{k+1}) = (1 - T(1+K) + 0.5T^2(1+K)^2)\hat{x}_d(t_k) + 0.5TK((1 - T(1+K))z(t_k) + z(t_{k+1})) \qquad (2.46)$$

The error covariance curves are plotted for 100 Monte Carlo runs using the above method and using the optimal discrete representation in Figures 6 through 8 for T = 0.1, 0.25, and 0.5 for the cost functional J in (2.13). The results obtained using the cost functional given by (2.12) are plotted in Figures 9 through 11 for T = 0.1, 0.25, and 0.5. It can be concluded from the curves that the second-order Runge-Kutta integration method is better than the first-order optimal discrete representation results. A second-order optimal discrete representation using Fletcher and Powell's method of minimization failed to converge. Another method of minimization is developed in Chapter III for the

general, time-varying case by converting the problem to a two-point boundary value problem.

Summary

In this chapter the basic problem was defined. A first-order example was selected and steady-state optimization results were compared with the results from Euler and RK2 integration methods. It was shown that considerable improvement was obtained in the cost functional J over the Euler Method of integration by using the optimal discrete representation.

CHAPTER III

OPTIMAL DISCRETE REPRESENTATIONS

This chapter deals with the development of the optimization procedure for both transient and steady-state regions using Lagrange multipliers. The cost functionals defined in the previous chapter as the difference between the discrete filter states of interest and the corresponding continuous filter states or system states are utilized. In both cases matrix difference equations are formed for the appropriate covariance matrices, and the optimization is performed to minimize J subject to the constraint equations. A second-order nonlinear system is selected to illustrate the procedure.

Development of the Optimization Procedure

The J defined in (2.13) is repeated again here

$$J = \text{Trace} \sum_{k=0}^{K-1} \frac{1}{2} E\{[\underline{\delta x}_\ell(t_{k+1}) - \underline{\delta \hat{x}}_d(t_{k+1})][\underline{\delta x}_\ell(t_{k+1}) - \underline{\delta \hat{x}}_d(t_{k+1})]^T\} \tag{3.1}$$

Taking expected values as indicated, (3.1) may be written as

$$J = \text{Trace} \sum_{k=0}^{K-1} \frac{1}{2} [E\{\underline{\delta x}_\ell(t_{k+1})\underline{\delta x}_\ell^T(t_{k+1})\} + E\{\underline{\delta \hat{x}}_d(t_{k+1})\underline{\delta \hat{x}}_d^T(t_{k+1})\} - E\{\underline{\delta x}_\ell(t_{k+1})\underline{\delta \hat{x}}_d^T(t_{k+1})\} - E\{\underline{\delta \hat{x}}_d(t_{k+1})\underline{\delta x}_\ell^T(t_{k+1})\}] \tag{3.2}$$

$$J = \text{Trace} \sum_{k=0}^{K-1} \frac{1}{2} [P_{11}(t_{k+1}) + P_{22}(t_{k+1}) - P_{12}(t_{k+1}) - P_{12}^T(t_{k+1})] \tag{3.3}$$

where the P_{ij}'s in (3.3) are yet to be determined. Let

$$\begin{aligned} P'_{11}(t_{k+1}) &\triangleq E\{\underline{\delta x}(t_{k+1})\underline{\delta x}^T(t_{k+1})\} \\ P'_{12}(t_{k+1}) &\triangleq E\{\underline{\delta x}(t_{k+1})\underline{\hat{\delta x}}_d^T(t_{k+1})\} \end{aligned} \tag{3.4}$$

The ℓ by ℓ matrix $P_{11}(t_{k+1})$, which is the covariance matrix of $\underline{\delta x}_\ell(t_{k+1})$, is obtained from the n by n matrix $P'_{11}(t_{k+1})$ by selecting only those elements corresponding to the ℓ by ℓ entries in $P_{22}(t_{k+1})$, which is the covariance matrix of $\underline{\hat{\delta x}}_d(t_{k+1})$. Similarly, the ℓ by ℓ matrix $P_{12}(t_{k+1})$, defined as $E\{\underline{\delta x}_\ell(t_{k+1})\underline{\hat{\delta x}}_d^T(t_{k+1})\}$, is obtained from $P'_{12}(t_{k+1})$ by retaining appropriate entries. An example is included later in this section to illustrate these details.

The optimization approach to be used here first requires that matrix difference equations be formed for $P_{12}(t_{k+1})$ and $P_{22}(t_{k+1})$ in terms of $\alpha(t_k)$ and $\beta(t_k)$. In addition, a matrix difference equation can be determined for $P_{11}(t_{k+1})$. The problem of minimizing J in (2.13) subject to the difference equation constraints on $P_{12}(t_{k+1})$ and $P_{22}(t_{k+1})$ is solved by using Fletcher and Powell's minimization technique.

The matrix difference equation for $P'_{11}(t_{k+1})$ may be obtained by using (2.6) in $\underline{\delta x}(t_{k+1})$ to form

$$\underline{\delta x}(t_{k+1}) = \Phi(t_{k+1},t_k)\underline{\delta x}(t_k) + \int_{t_k}^{t_{k+1}} \Phi(t_{k+1},\tau)B(\tau)\underline{\omega}(\tau)d\tau \tag{3.5}$$

where $\Phi(t_{k+1},t_k)$ is the state transition matrix. Therefore, from (3.4)

$$P'_{11}(t_{k+1}) = E\{\underline{\delta x}(t_{k+1})\underline{\delta x}^T(t_{k+1})\}$$

$$= E\{[\Phi(t_{k+1},t_k)\underline{\delta x}(t_k) + \int_{t_k}^{t_{k+1}} \Phi(t_{k+1},\tau)B(\tau)\underline{\omega}(\tau)d\tau]\cdot$$

$$[\Phi(t_{k+1},t_k)\underline{\delta x}(t_k) + \int_{t_k}^{t_{k+1}} \Phi(t_{k+1},\tau)B(\tau)\underline{\omega}(\tau)d\tau]^T\} \quad (3.6)$$

Since $\underline{\delta x}(t_k)$ and $\underline{\omega}(t)$ are uncorrelated

$$P'_{11}(t_{k+1}) = \Phi(t_{k+1},t_k)E\{\underline{\delta x}(t_k)\underline{\delta x}^T(t_k)\}\Phi^T(t_{k+1},t_k)$$

$$+ \int_{t_k}^{t_{k+1}}\int_{t_k}^{t_{k+1}} \Phi(t_{k+1},\tau)B(\tau)E\{\underline{\omega}(\tau)\underline{\omega}^T(\rho)\}B^T(\rho)\Phi^T(t_{k+1},\rho)d\tau d\rho. \quad (3.7)$$

Using (2.3) and the sifting property of the delta function

$$P'_{11}(t_{k+1}) = \Phi(t_{k+1},t_k)P'_{11}(t_k)\Phi^T(t_{k+1},t_k)$$

$$+ \int_{t_k}^{t_{k+1}} \Phi(t_{k+1},\tau)B(\tau)Q_\omega(\tau)B^T(\tau)\Phi^T(t_{k+1},\tau)d\tau. \quad (3.8)$$

The matrix difference equation for $P_{22}(t_{k+1})$ may be obtained by using (2.11) to yield

$$P_{22}(t_{k+1}) \triangleq E\{\underline{\delta\hat{x}}_d(t_{k+1})\underline{\delta\hat{x}}_d^T(t_{k+1})\}$$

$$= E\{[\alpha(t_k)\underline{\delta\hat{x}}_d(t_k) + \beta(t_k)C(t_k)\underline{\delta x}(t_k) + \beta(t_k)\underline{y}_d(t_k)]\cdot$$

$$[\alpha(t_k)\underline{\delta\hat{x}}_d(t_k) + \beta(t_k)C(t_k)\underline{\delta x}(t_k) + \beta(t_k)\underline{y}_d(t_k)]^T\}$$

$$P_{22}(t_{k+1}) = \alpha(t_k)P_{22}(t_k)\alpha^T(t_k) + \beta(t_k)C(t_k)P'_{11}(t_k)C^T(t_k)\beta^T(t_k)$$
$$+ \beta(t_k)Q_{vd}(t_k)\beta^T(t_k) + \alpha(t_k)P'_{12}(t_k)C^T(t_k)\beta^T(t_k)$$
$$+ \beta(t_k)C(t_k)P'_{12}(t_k)\alpha^T(t_k). \tag{3.10}$$

Similarly,

$$P'_{12}(t_{k+1}) \triangleq E\{\underline{\delta x}(t_{k+1})\underline{\delta \hat{x}}_d^T(t_{k+1})\} \tag{3.11}$$

$$= E\{[\Phi(t_{k+1},t_k)\underline{\delta x}(t_k) + \int_{t_k}^{t_{k+1}} \Phi(t_{k+1},\tau)B(\tau)\underline{\omega}(\tau)d\tau] \cdot$$
$$[\alpha(t_k)\underline{\delta \hat{x}}_d(t_k) + \beta(t_k)C(t_k)\underline{\delta x}(t_k) + \beta(t_k)\underline{v}_d(t_k)]^T\}$$
$$= \Phi(t_{k+1},t_k)P'_{12}(t_k)\alpha^T(t_k) + \Phi(t_{k+1},t_k)P'_{11}(t_k)C^T(t_k)\beta^T(t_k). \tag{3.12}$$

The matrix $P'_{11}(t_{k+1})$ in (3.8) is a known time-varying matrix which serves as a forcing function in (3.10) and (3.12).

Let two ℓ by ℓ matrices $\lambda_{12}(t_k)$ and $\lambda_{22}(t_k)$ of Lagrange multipliers for $P_{12}(t_k)$ and $P_{22}(t_k)$, respectively, be introduced. It is known that $\lambda_{12}(t_k)$ and $\lambda_{22}(t_k)$ satisfy adjoint difference equations which have the boundary conditions

$$\lambda_{12}(t_K) = 0$$
$$\lambda_{22}(t_K) = 0 \tag{3.13}$$

where t_K is the terminal time. One method for obtaining the adjoint equation is to define the Hamiltonian H as

$$H = \text{Trace}\ \{\ \frac{1}{2}\ [P_{11}(t_{k+1}) + P_{22}(t_{k+1}) - P_{12}(t_{k+1}) - P_{12}^{T}(t_{k+1})]$$

$$+ P_{12}(t_{k+1})\lambda_{12}^{T}(t_{k+1}) + P_{22}(t_{k+1})\lambda_{22}^{T}(t_{k+1})\} \qquad (3.14)$$

The procedure for optimization is to substitute (3.10) and (3.12) into (3.14) and then minimize the resulting H with respect to the entries in the $\alpha(t_k)$ and $\beta(t_k)$ matrices. If the minimized H is represented by H^*, then

$$\lambda_{12}(t_k) = \frac{\partial H^*}{\partial P_{12}(t_k)}$$

$$\lambda_{22}(t_k) = \frac{\partial H^*}{\partial P_{22}(t_k)}\ . \qquad (3.15)$$

The right hand sides of the equations in (3.15) include terms involving $\lambda_{12}(t_{k+1})$ and $\lambda_{22}(t_{k+1})$ and, therefore, the optimization result may be obtained by solving simultaneously (3.10), (3.12), and (3.15). The resulting two-point boundary value problem has boundary values specified in (3.13) at $t = t_K$ for $\lambda_{12}(t_k)$ and $\lambda_{22}(t_k)$ and some known initial conditions for $P_{12}(t_k)$ and $P_{22}(t_k)$.

The three types of errors which occur in forming optimal discrete representations are filtering error due to signal and measurement noise, discretization errors in modeling the filter, and errors in using a reduced-order filter. The first of these is inherent in all filtering problems, but its effect can sometimes be reduced by using improved continuous filtering algorithms, e.g., using the extended Kalman filter or trajectory optimization. The second type of error can be handled on accuracy alone by minimizing the cost functional in (2.12) and (2.13). The third error has been investigated extensively for reduced-

order, fixed-configuration filters by Sims and Melsa (39,40).

Example

Consider the second-order nonlinear system described by

$$\begin{aligned} \dot{x}_1 &= -2x_1 + x_2 + \gamma x_2^{\rho} \\ \dot{x}_2 &= -x_2 + \omega(t) \\ z(t) &= x_1 + v(t) \end{aligned} \tag{3.16}$$

where $\gamma > 0$, $\rho > 1$, and $\omega(t)$ and $v(t)$ are zero-mean, Gaussian, white noise processes with variances $Q_{\omega}(t) = 1.0$ and $Q_{v}(t) = 0.1$, respectively. Let the known initial conditions be $x_1(0) = 0.0$ and $x_2(0) = 0.1$.

The linearized equation for $\underline{\delta x}(t)$ about the noise-free nominal trajectory is obtained from (2.6) as

$$\begin{aligned} \delta\dot{x}_1 &= -2\delta x_1 + \delta x_2 + (\rho\gamma x_{2N}^{\rho-1}(t))\delta x_2 \\ \delta\dot{x}_2 &= -\delta x_2 + \omega(t) \end{aligned} \tag{3.17}$$

where $x_{2N}(t)$ may be determined as $x_2(0)e^{-t}$ from (2.4). Using (2.8)-(2.10), the variational Kalman filter is given by

$$\begin{aligned} \delta\dot{\hat{x}}_1 &= -2\delta\hat{x}_1 + \delta\hat{x}_2 + \rho\gamma(x_2(0)e^{-t})^{\rho-1}\delta\hat{x}_2 + K_1(t)[\delta z(t) - \delta\hat{x}_1] \\ \delta\dot{\hat{x}}_2 &= -\delta\hat{x}_2 + K_2(t)[\delta z(t) - \delta\hat{x}_1] \end{aligned} \tag{3.18}$$

where

$$\dot{P}_e(t) = A(t)P_e(t) + P_e(t)A^T(t) - P_e(t)\begin{pmatrix}0\\1\end{pmatrix}Q_v^{-1}(t)(0\ 1)P_e(t) + \begin{pmatrix}0\\1\end{pmatrix}Q_{\omega}(t)(0\ 1) \tag{3.19}$$

$$K(t) \triangleq \begin{pmatrix} K_1(t) \\ K_2(t) \end{pmatrix}$$

$$= P_e(t)\begin{pmatrix} 0 \\ 1 \end{pmatrix} Q_v^{-1}(t)$$

and

$$A(t) = \begin{pmatrix} -2 & 1+\rho\gamma(x_2(0)e^{-t})^{\rho-1} \\ 0 & -1 \end{pmatrix} \tag{3.20}$$

The discrete representation in (2.11) may be written as

$$\delta\hat{x}_d(t_{k+1}) = \alpha(t_k)\delta\hat{x}_d(t_k) + \beta(t_k)\delta z(t_k)$$

$$= \alpha(t_k)\delta\hat{x}_d(t_k) + \beta(t_k)\delta x_1(t_k) + \beta(t_k)v_d(t_k) \tag{3.21}$$

where $\ell = 1$ and $n = 2$ in this example. Let the cost functional J corresponding to (3.1) be written as

$$J = \frac{1}{2}\sum_{k=0}^{K-1} E\{[\delta x_1(t_{k+1}) - \delta\hat{x}_d(t_{k+1})]^2\} \tag{3.22}$$

which, as in (3.3), simplifies to

$$J = \frac{1}{2}\sum_{k=0}^{K-1} [P_{11}(t_{k+1}) + P_{22}(t_{k+1}) - 2P_{12}(t_{k+1})] \tag{3.23}$$

The state transition matrix $\Phi(t_{k+1},t_k)$ satisfies the matrix differential equation

$$\dot{\Phi}(t,t_k) = A(t)\Phi(t,t_k)$$

$$\Phi(t_k,t_k) = I \tag{3.24}$$

where I is the 2 by 2 identity matrix and A(t) is defined in (3.20).

Let $\Phi(t_{k+1},t_k)$ be expressed in component form for this problem as

$$\Phi(t_{k+1},t_k) = \begin{bmatrix} \phi_{11} & \phi_{12} \\ \phi_{21} & \phi_{22} \end{bmatrix} \tag{3.25}$$

Numerical values for the component ϕ_{ij}'s for each t_k is determined by sufficiently accurate digital computer programs for numerical integration.

The $P'_{11}(t_{k+1})$ matrix is determined numerically by integrating the matrix differential equation (15)

$$\dot{P}'_{11}(t) = A(t)P'_{11}(t) + P'_{11}(t)A^T(t) + \begin{pmatrix} 0 \\ 1 \end{pmatrix} Q_\omega(t)(0\ 1) \tag{3.26}$$

Let $P'_{11}(t_k)$ be denoted as

$$P'_{11}(t_k) = \begin{bmatrix} p'_{11}(t_k) & p'_{12}(t_k) \\ p'_{12}(t_k) & p'_{22}(t_k) \end{bmatrix} \tag{3.27}$$

The time function $P'_{11}(t_k)$ is used as a forcing function in the vector difference equation for $P'_{12}(t_{k+1})$ from (3.12) and scalar difference equation for $P_{22}(t_{k+1})$ from (3.10). Let $P'_{12}(t_k)$ be denoted as

$$P'_{12}(t_k) \triangleq \begin{pmatrix} p'_{12a}(t_k) \\ p'_{12b}(t_k) \end{pmatrix} \tag{3.28}$$

From (3.12)

$$P'_{12}(t_{k+1}) = \begin{pmatrix} \phi_{11} & \phi_{12} \\ \phi_{21} & \phi_{22} \end{pmatrix} \begin{pmatrix} p'_{12a}(t_k) \\ p'_{12b}(t_k) \end{pmatrix} \alpha(t_k)$$

$$+ \begin{pmatrix} \phi_{11} & \phi_{12} \\ \phi_{21} & \phi_{22} \end{pmatrix} \begin{pmatrix} p'_{11}(t_k) & p'_{12}(t_k) \\ p'_{12}(t_k) & p'_{22}(t_k) \end{pmatrix} \begin{pmatrix} 1 \\ 0 \end{pmatrix} \beta(t_k) \tag{3.29}$$

Using (3.10) yields

$$P_{22}(t_{k+1}) = \alpha^2(t_k)P_{22}(t_k) + \beta^2(t_k)p'_{11}(t_k) + \beta^2(t_k)Q_{vd}(t_k)$$

$$+ 2\alpha(t_k)\beta(t_k)p'_{12a}(t_k) \tag{3.30}$$

The problem of determining just which of these difference equations should be treated as constraint equations for optimization may be resolved by forming the covariance matrix of the augmented vector $(\underline{\delta x}(t_k) \quad \delta\hat{x}_d(t_k))^T$

$$\text{Cov} \begin{pmatrix} \underline{\delta x}(t_k) \\ \delta\hat{x}_d(t_k) \end{pmatrix} = \begin{pmatrix} p'_{11}(t_k) & p'_{12}(t_k) & p'_{12a}(t_k) \\ p'_{12}(t_k) & p'_{22}(t_k) & p'_{12b}(t_k) \\ p'_{12a}(t_k) & p'_{12b}(t_k) & P_{22}(t_k) \end{pmatrix} \tag{3.31}$$

Since only the first incremental state $\delta x_1(t)$ is to be modeled by the discrete filter in (2.11), the second row and second column of the matrix in (3.31) are deleted and all other entries retained to give

$$\begin{bmatrix} P_{11}(t_k) & P_{12}(t_k) \\ P_{12}(t_k) & P_{22}(t_k) \end{bmatrix} = \begin{bmatrix} p'_{11}(t_k) & p'_{12a}(t_k) \\ p'_{12a}(t_k) & P_{22}(t_k) \end{bmatrix} \tag{3.32}$$

Therefore, the scalar difference equation in (3.30) and the equation for $P_{12}(t_k) = p'_{12a}(t_k)$ in (3.29) serve as the required constraint equations. Note that if only $\delta x_2(t)$ had been modeled by the discrete filter, then the first row and first column would have been deleted in (3.31) and all other entries retained. In that case the constraint equations would have been for $P_{22}(t_k)$ from (3.30) and for $p'_{12b}(t_k)$ from (3.29).

The Hamiltonian is defined as

$$H = \frac{1}{2}\,[P_{11}(t_{k+1}) + P_{22}(t_{k+1}) - 2P_{12}(t_{k+1})] + P_{12}(t_{k+1})\lambda_{12}(t_{k+1}) + P_{22}(t_{k+1})\lambda_{22}(t_{k+1}) \tag{3.33}$$

Substituting (3.29) and (3.30) into (3.33) yields

$$\begin{aligned} H = {} & \frac{1}{2}\,p'_{11}(t_{k+1}) + [\,\tfrac{1}{2} + \lambda_{22}(t_{k+1})][\alpha^2(t_k)P_{22}(t_k) + \beta^2(t_k)p'_{11}(t_k) \\ & + \beta^2(t_k)Q_{vd}(t_k) + 2\alpha(t_k)\beta(t_k)p'_{12a}(t_k)] \\ & + [-1 + \lambda_{12}(t_{k+1})][(\phi_{11}p'_{12a}(t_k) + \phi_{12}p'_{12b}(t_k))\alpha(t_k) \\ & + \beta(t_k)\phi_{11}p'_{11}(t_k) + \beta(t_k)\phi_{12}p'_{12}(t_k)] \end{aligned} \tag{3.34}$$

H^* (optimum) is found by setting

$$\begin{aligned} \frac{\partial H}{\partial \alpha(t_k)} = 0 = {} & [\,\tfrac{1}{2} + \lambda_{22}(t_{k+1})][2\alpha(t_k)P_{22}(t_k) + 2\beta(t_k)p'_{12a}(t_k)] \\ & + [-1 + \lambda_{12}(t_{k+1})][\phi_{11}p'_{12a}(t_k) + \phi_{12}p'_{12b}(t_k)] \end{aligned} \tag{3.35}$$

$$\frac{\partial H}{\partial \beta(t_k)} = 0 = [\frac{1}{2} + \lambda_{22}(t_{k+1})][2\beta(t_k)p'_{11}(t_k) + 2\beta(t_k)Q_{vd}(t_k)$$
$$+ 2\alpha(t_k)p'_{12a}(t_k)]$$
$$+ [-1 + \lambda_{12}(t_{k+1})][\phi_{11}p'_{11}(t_k) + \phi_{12}p'_{12}(t_k)] \qquad (3.36)$$

and substituting values of $\alpha(t_k)$ and $\beta(t_k)$ into (3.34). Therefore, the adjoint difference equations may be determined from (3.15) as

$$\lambda_{12}(t_k) = \frac{\partial H^*}{\partial p'_{12a}(t_k)} = [\frac{1}{2} + \lambda_{22}(t_{k+1})][2\alpha(t_k)\beta(t_k)]$$
$$+ [-1 + \lambda_{12}(t_{k+1})]\phi_{11}\alpha(t_k) \qquad (3.37)$$

$$\lambda_{22}(t_k) = \frac{\partial H^*}{\partial P_{22}(t_k)} = [\frac{1}{2} + \lambda_{22}(t_{k+1})]\alpha^2(t_k) \qquad (3.38)$$

The optimal discrete filter, constrained to be of the form in (2.11), may be determined by solving the two-point boundary value problem specified by the difference equations for $p'_{12a}(t_k)$, $P_{22}(t_k)$, $\lambda_{12}(t_k)$, and $\lambda_{22}(t_k)$ in (3.29), (3.30), (3.37), and (3.38), respectively. Observe that the use of H instead of H^* in (3.37) and (3.38) requires that the algebraic equations (3.35) and (3.36) must also be satisfied. The standard formulation for the two-point boundary value problem requires the inversion of the algebraic equations in (3.37) and (3.38) to express the λ's at time t_{k+1} in terms of the λ's at time t_k. The gradient technique is used to solve the constraint equations in (3.29) and (3.30) and the adjoint equations in (3.37) and (3.38) without inverting (3.37) and (3.38) or even solving (3.35) and (3.36) for $\alpha(t_k)$ and $\beta(t_k)$. In (34) a simpler problem was solved in which only the discrete representation of system noise ($\underline{\omega}(t)$) covariance matrix $Q_{\omega d}(t_k)$

was to be determined. The initial starting value was chosen as $Q_{\omega d}(t_k) = Q_\omega/T$, where T was the integration step size, and the term $-\varepsilon[\partial H/\partial Q_{\omega d}(t_k)]$ was added to the previous value of $Q_{\omega d}(t_k)$ to obtain the next iteration value. In this thesis research, arbitrary values were assigned to $\alpha(t_k)$ and $\beta(t_k)$ and then the constraint equations in (3.29) and (3.30) were solved forward in time from t = 0 to $t = t_K$. Thereafter, (3.37) and (3.38) were solved backwards in time from $t = t_K$ using $\lambda_{12}(t_K) = \lambda_{22}(t_K) = 0$. The values of $\alpha(t_k)$ and $\beta(t_k)$ for the next iteration were obtained by adding to the previous corresponding values the terms $-\varepsilon_1[\partial H/\partial\alpha(t_k)]$ and $-\varepsilon_2[\partial H/\partial\beta(t_k)]$, respectively, which were evaluated by using the p's and λ's from the last iteration in (3.35) and (3.36).

Numerical Results

This section deals with the comparison of optimal discrete representation results obtained using the two optimization techniques described earlier. These results are compared for the first-order example. The optimal discrete representations for the first and second-order examples are presented using the optimization technique developed in the last section.

The optimization technique developed in last section was applied to the first-order example given by (2.14). The example is rewritten here as

$$\begin{aligned} \dot{x}(t) &= -x(t) + \omega(t) \\ z(t) &= x(t) + v(t) \end{aligned} \tag{3.39}$$

The Hamiltonian for the cost functional given by (2.13) may be written as

$$H = \frac{1}{2}\left[P_{11}(t_{k+1}) + P_{22}(t_{k+1}) - 2P_{12}(t_{k+1})\right] + P_{12}(t_{k+1})\lambda_{12}(t_{k+1}) + P_{22}(t_{k+1})\lambda_{22}(t_{k+1}) \tag{3.40}$$

where

$$\begin{aligned} P_{12}(t_{k+1}) &= e^{-(t_{k+1}-t_k)}\left[\alpha(t_k)P_{12}(t_K) + \beta(t_k)P_{11}(t_k)\right] \\ P_{22}(t_{k+1}) &= \alpha^2(t_k)P_{22}(t_k) + \beta^2(t_k)P_{11}(t_k) + \beta^2(t_k)Q_{vd}(t_k) \\ &\quad + 2\alpha(t_k)\beta(t_k)P_{12}(t_k) \end{aligned} \tag{3.41}$$

and $P_{11}(t_k)$ is a known time-varying covariance of $x(t)$ at $t = t_k$. Now

$$\begin{aligned} \frac{\partial H}{\partial \alpha(t_k)} = 0 &= \left[\frac{1}{2} + \lambda_{22}(t_{k+1})\right]\left[2\alpha(t_k)P_{22}(t_k) + 2\beta(t_k)P_{12}(t_k)\right] \\ &\quad + \left[-1 + \lambda_{12}(t_{k+1})\right]\left[e^{-(t_{k+1}-t_k)}P_{12}(t_k)\right] \\ \frac{\partial H}{\partial \beta(t_k)} = 0 &= \left[\frac{1}{2} + \lambda_{22}(t_{k+1})\right]\left[2\beta(t_k)P_{11}(t_k) + 2\beta(t_k)Q_{vd}(t_k)\right. \\ &\quad \left. + 2\alpha(t_k)P_{12}(t_k)\right] + \left[-1 + \lambda_{12}(t_{k+1})\right]\left[e^{-(t_{k+1}-t_k)}P_{11}(t_k)\right] \end{aligned} \tag{3.42}$$

The adjoint difference equations now may be written as

$$\begin{aligned} \lambda_{12}(t_k) = \frac{\partial H^*}{\partial P_{12}(t_k)} &= \left[\frac{1}{2} + \lambda_{22}(t_{k+1})\right]\left[2\alpha(t_k)\beta(t_k)\right] \\ &\quad + \left[-1 + \lambda_{12}(t_{k+1})\right]\left[e^{-(t_{k+1}-t_k)}\right] \\ \lambda_{22}(t_k) = \frac{\partial H^*}{\partial P_{22}(t_k)} &= \left[\frac{1}{2} + \lambda_{22}(t_{k+1})\right]\alpha^2(t_k) \end{aligned} \tag{3.43}$$

The results obtained by using the above optimization procedure and from Fletcher and Powell's optimization technique are plotted in Figures 12

and 13 for T = 0.1 and 0.5. The new optimization technique shows results that are better or at least as good as those obtained from Fletcher and Powell's technique. The results corresponding to the cost functionals given by (2.12) and (2.13) are plotted in Figures 14 through 19 and are compared with the results obtained using the Euler Method. The optimal parameters α and β were determined by using only (2.13) in all cases. For all these results 100 Monte Carlo results were ensemble-averaged at 10 points between zero and five seconds. It can be observed that a considerable reduction in the error covariance was obtained by using these optimal discrete representations.

The results of the second-order nonlinear example given by (3.16) are now compared with the results obtained by the Euler Method for $\rho = 3.0$ and $\gamma = 0.5$. The results of these two are plotted in Figures 20 through 25 for the cost functionals given by (2.12) and (2.13). Again, only (2.13) was used in solving for the optimal values of α and β. For this second-order nonlinear example, the optimal discrete representations results also showed a considerable reduction in the error covariance.

Summary

This chapter dealt with the development of the optimization procedure which showed results that either surpassed or were as good as those obtained using Fletcher and Powell's optimization technique. The first-order linear and second-order nonlinear examples were used to compare the optimal discrete representations with the results from the Euler Method. A considerable improvement was obtained by using the optimal discrete representations.

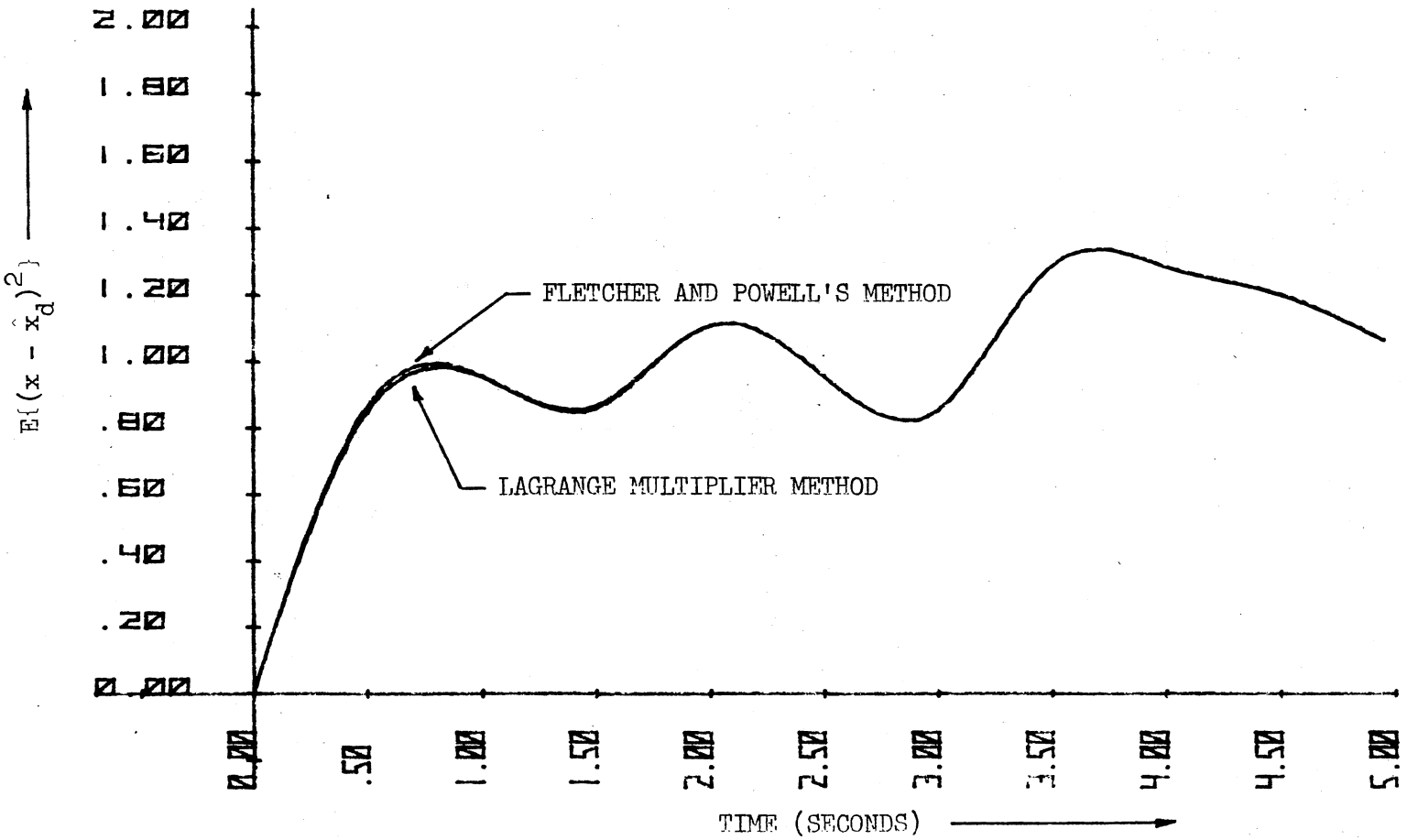

Figure 12. Comparisons of the Error Covariance $E\{(x - \hat{x}_d)^2\}$ Obtained by Using Fletcher and Powell's and Optimal Discrete Representation Methods for T = 0.1

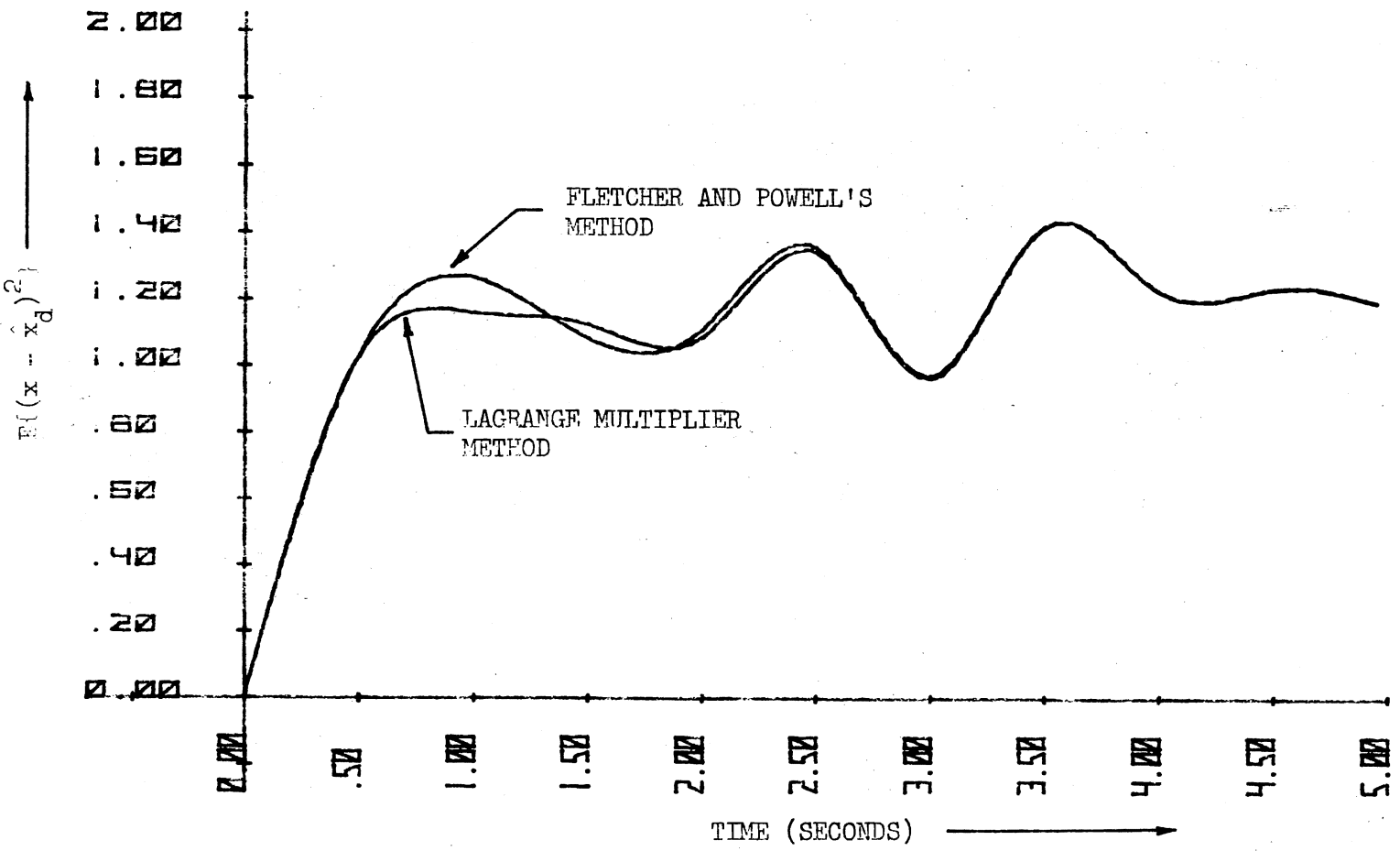

Figure 13. Comparisons of the Error Covariance $E\{(x - \hat{x}_d)^2\}$ Obtained by Using Fletcher and Powell's and Optimal Discrete Representation Methods for T = 0.5

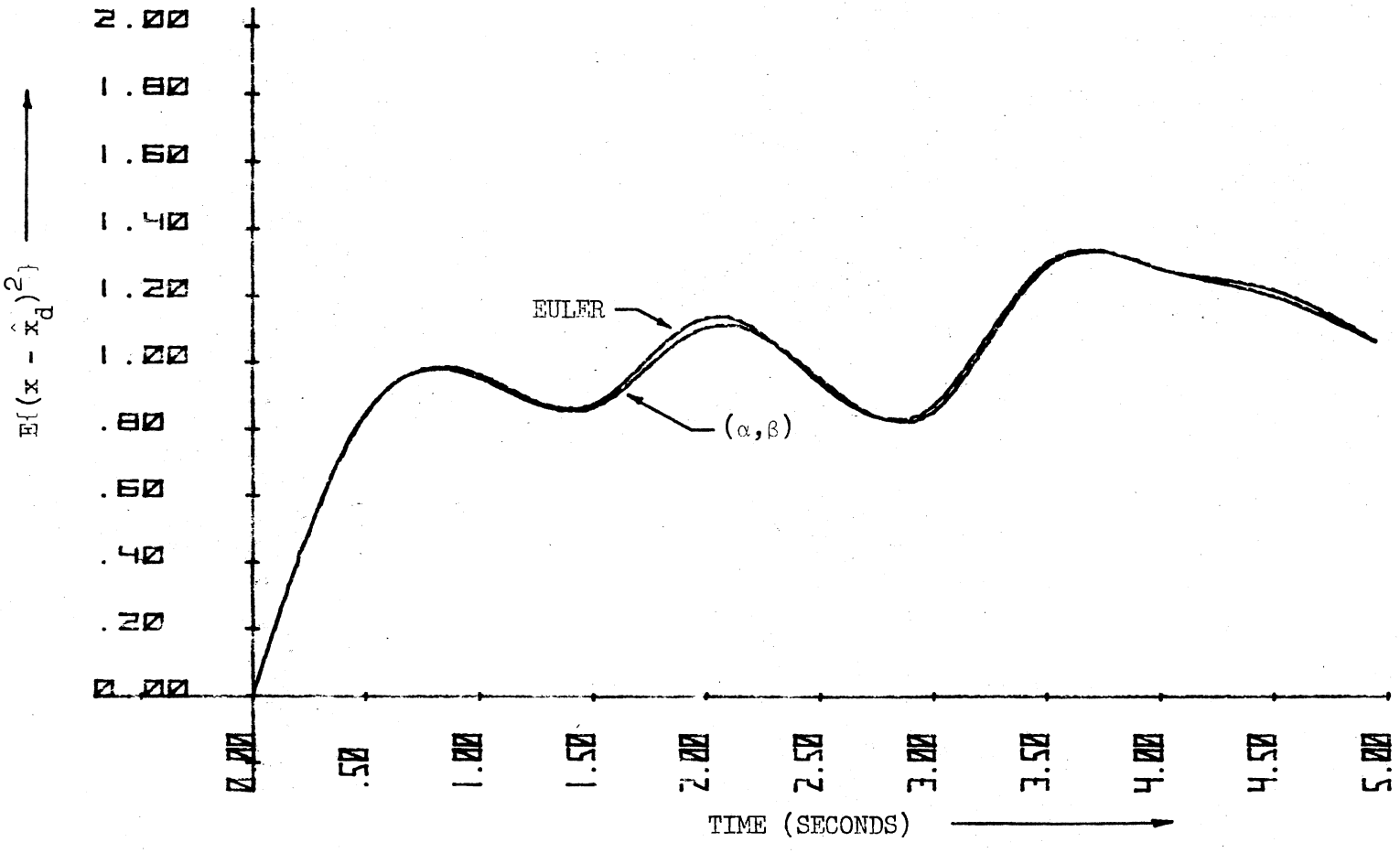

Figure 14. Error Covariance $E\{(x - \hat{x}_d)^2\}$ for the First-Order Linear System for T = 0.1

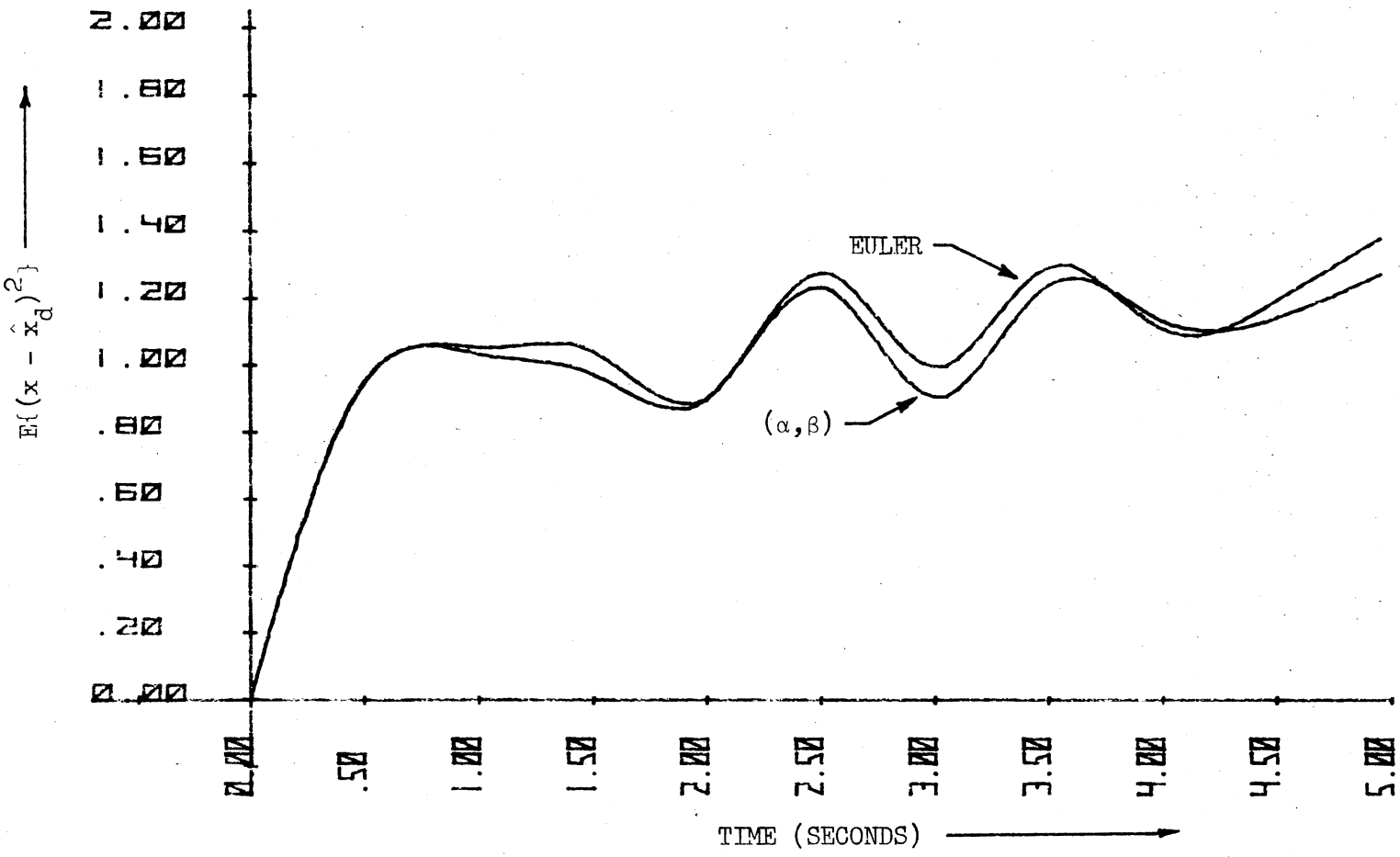

Figure 15. Error Covariance $E\{(x - \hat{x}_d)^2\}$ for the First-Order Linear System for T = 0.25

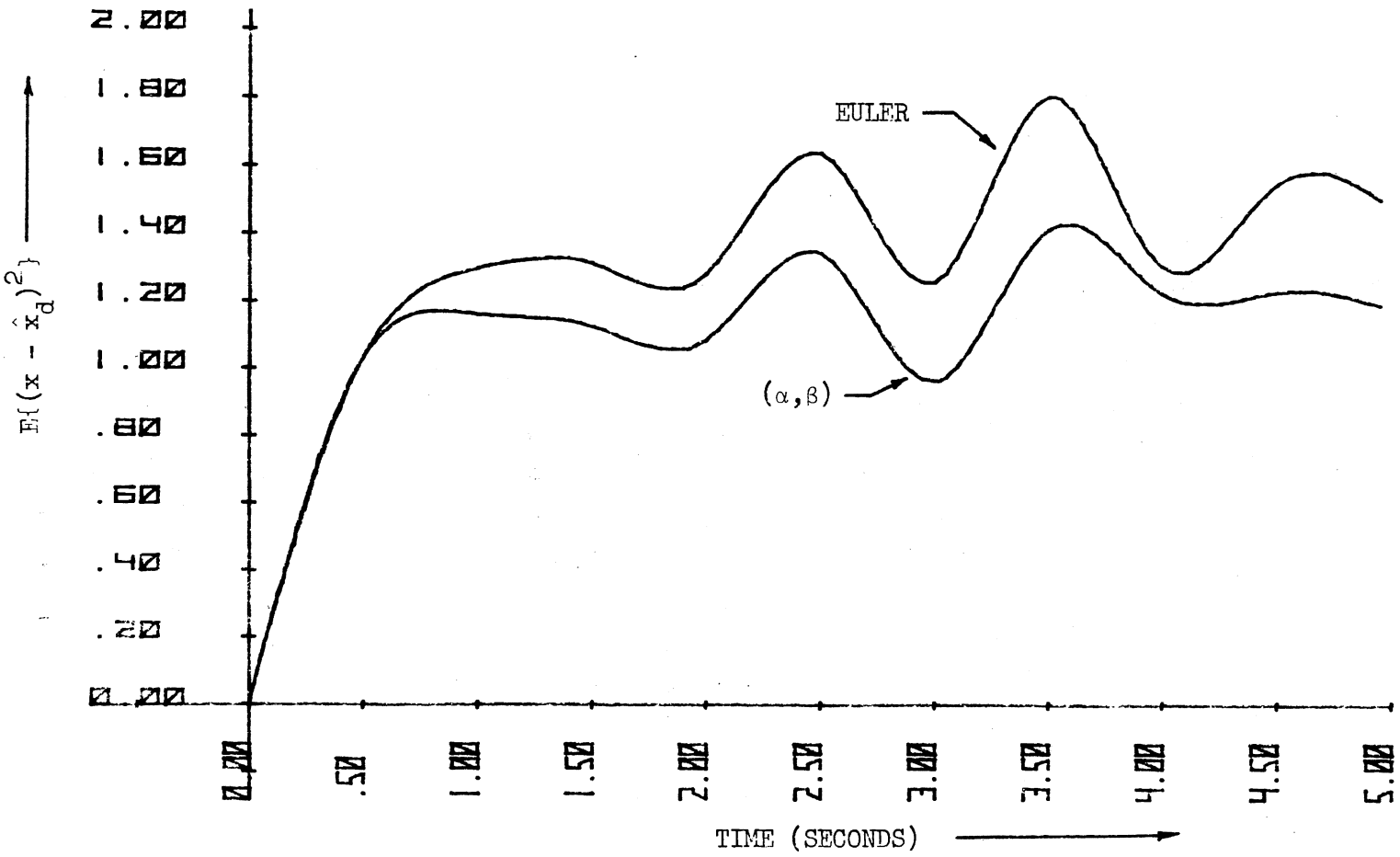

Figure 16. Error Covariance $E\{(x - \hat{x}_d)^2\}$ for the First-Order Linear System for T = 0.5

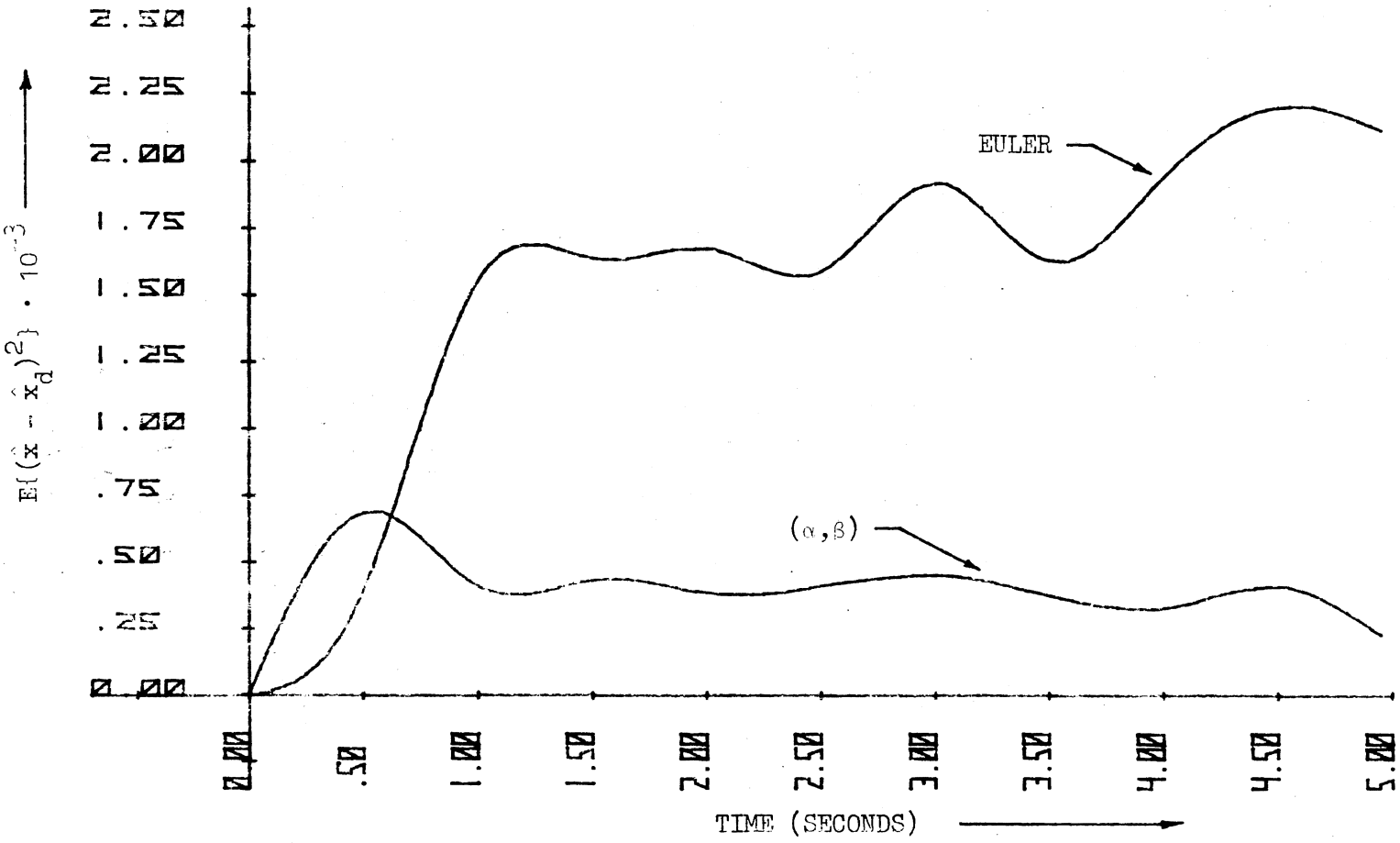

Figure 17. Error Covariance $E\{(\hat{x} - \hat{x}_d)^2\}$ for the First-Order Linear System for T = 0.1

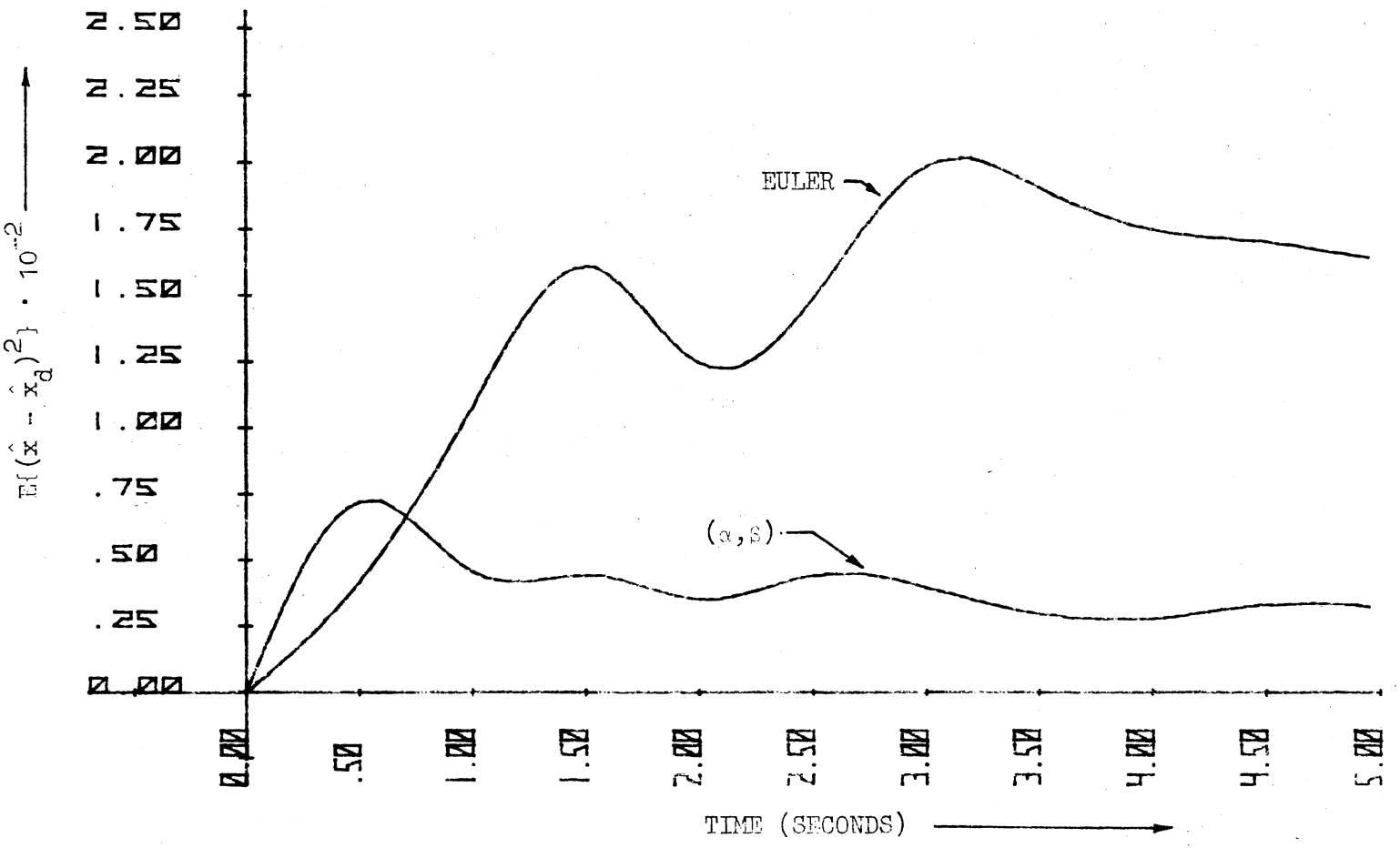

Figure 18. Error Covariance $E\{(\hat{x} - \hat{x}_d)^2\}$ for the First-Order Linear System for T = 0.25

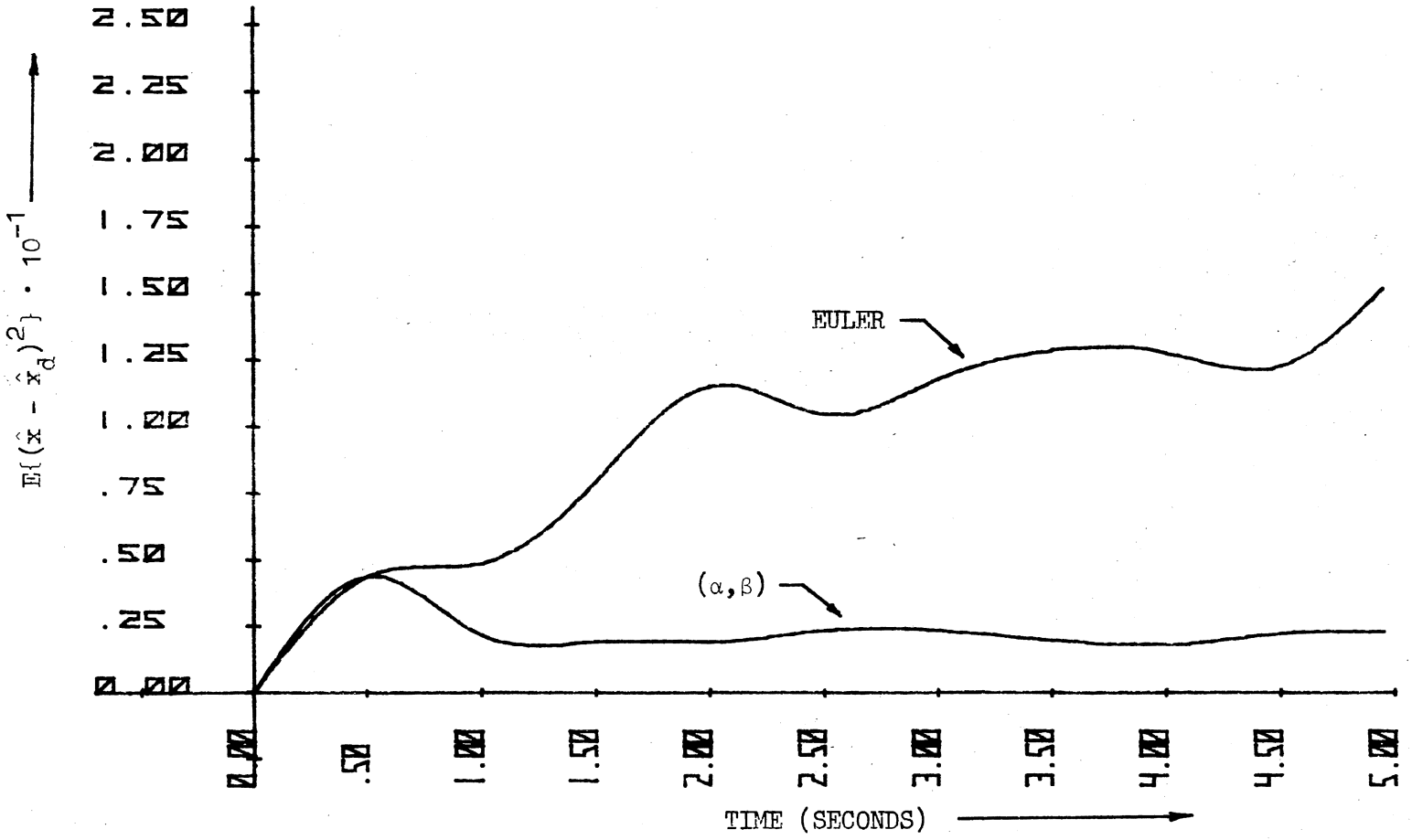

Figure 19. Error Covariance $E\{(\hat{x} - \hat{x}_d)^2\}$ for the First-Order Linear System for T = 0.5

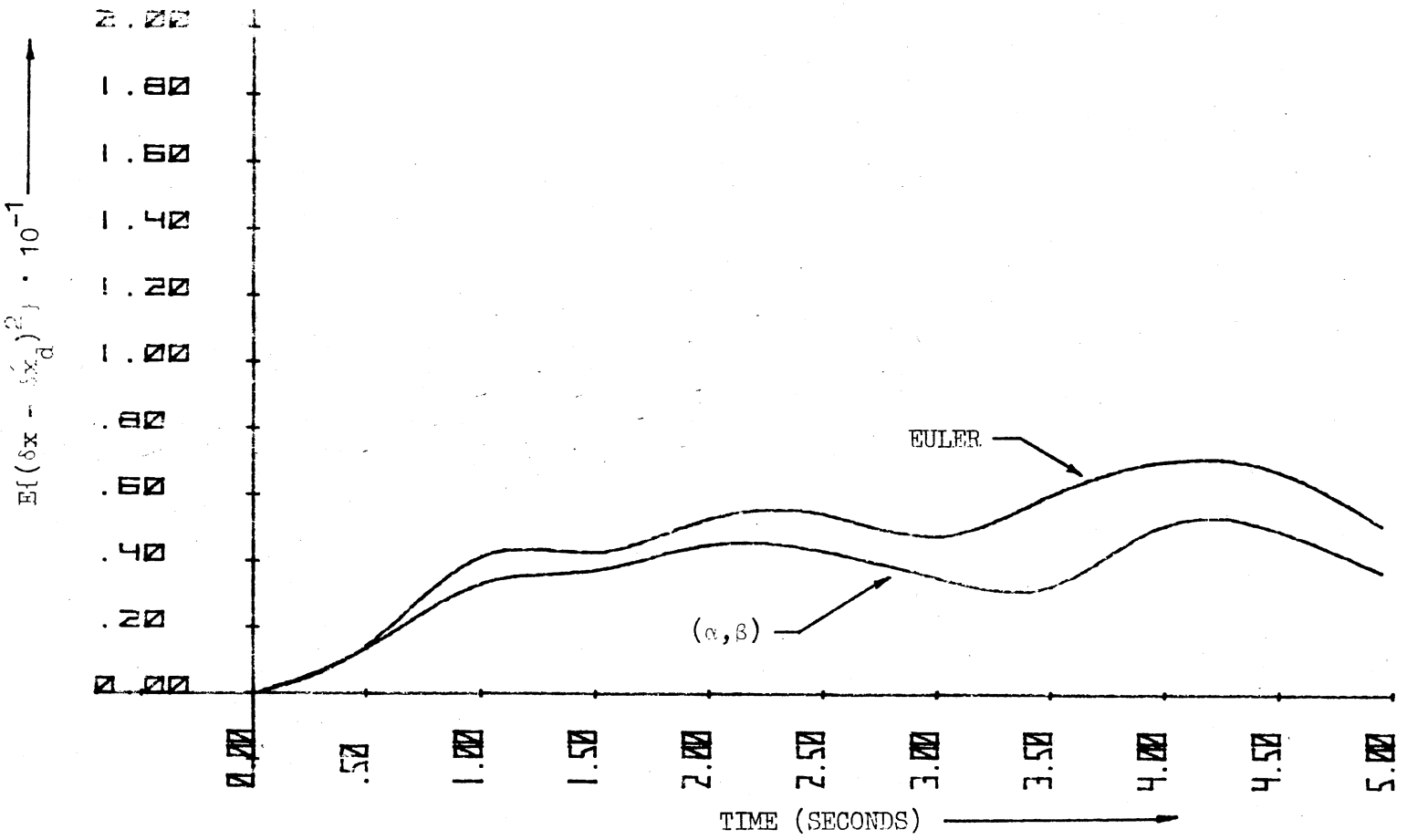

Figure 20. Error Covariance $E\{(\delta x - \delta\hat{x}_d)^2\}$ for the Second-Order Nonlinear System for T = 0.1

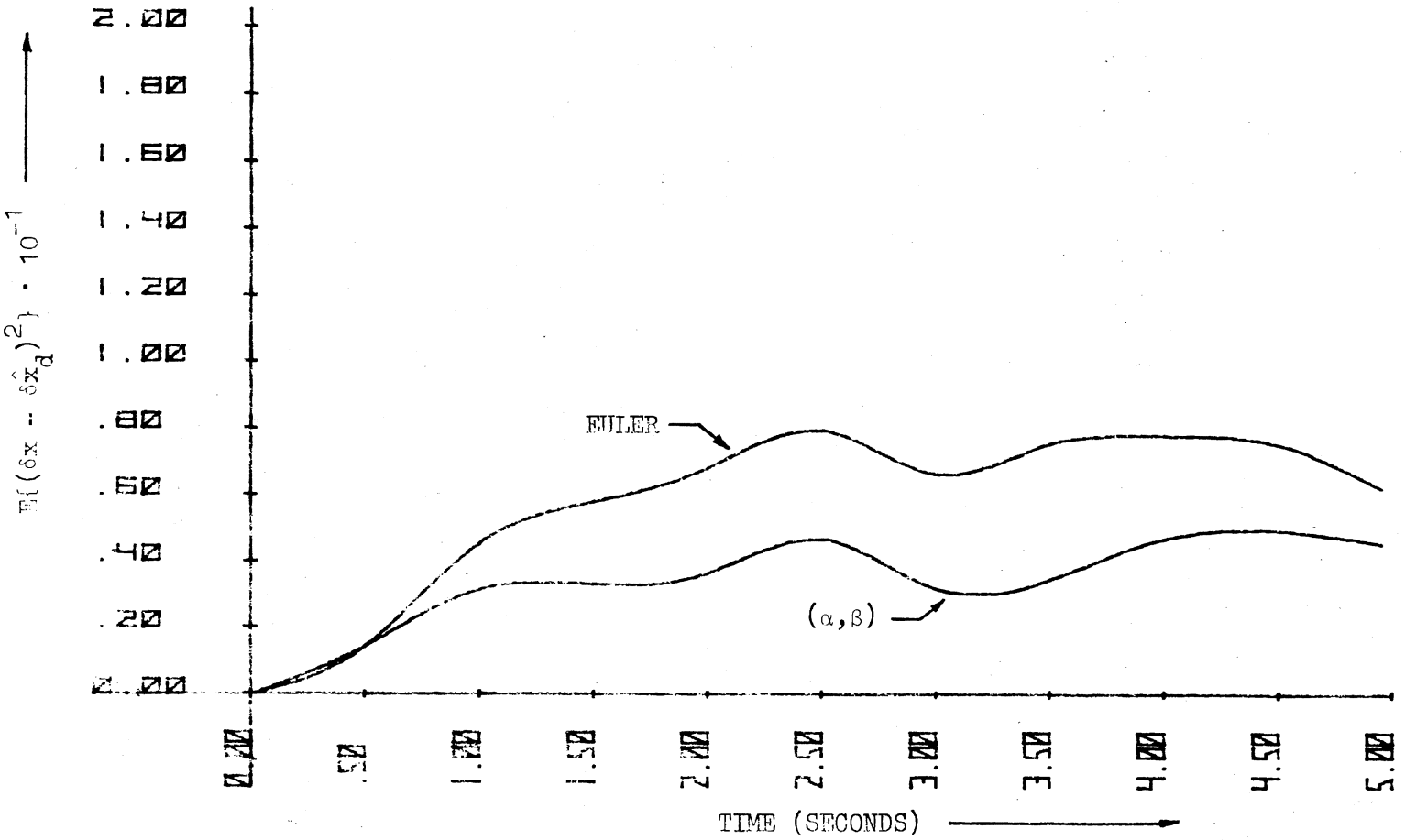

Figure 21. Error Covariance $E\{(\delta x - \delta\hat{x}_d)^2\}$ for the Second-Order Nonlinear System for T = 0.25

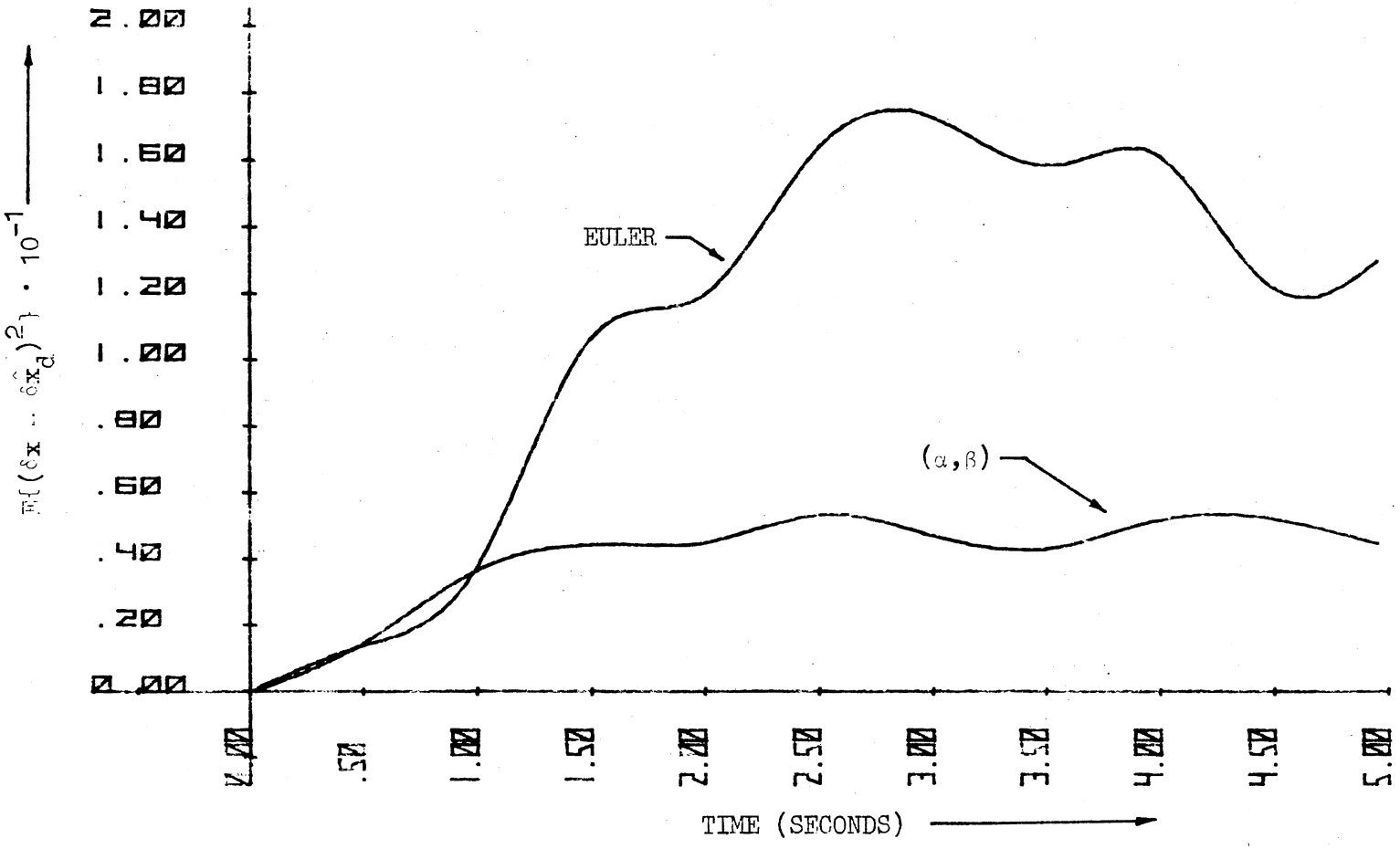

Figure 22. Error Covariance $E\{(\delta x - \delta\hat{x}_d)^2\}$ for the Second-Order Nonlinear System for T = 0.5

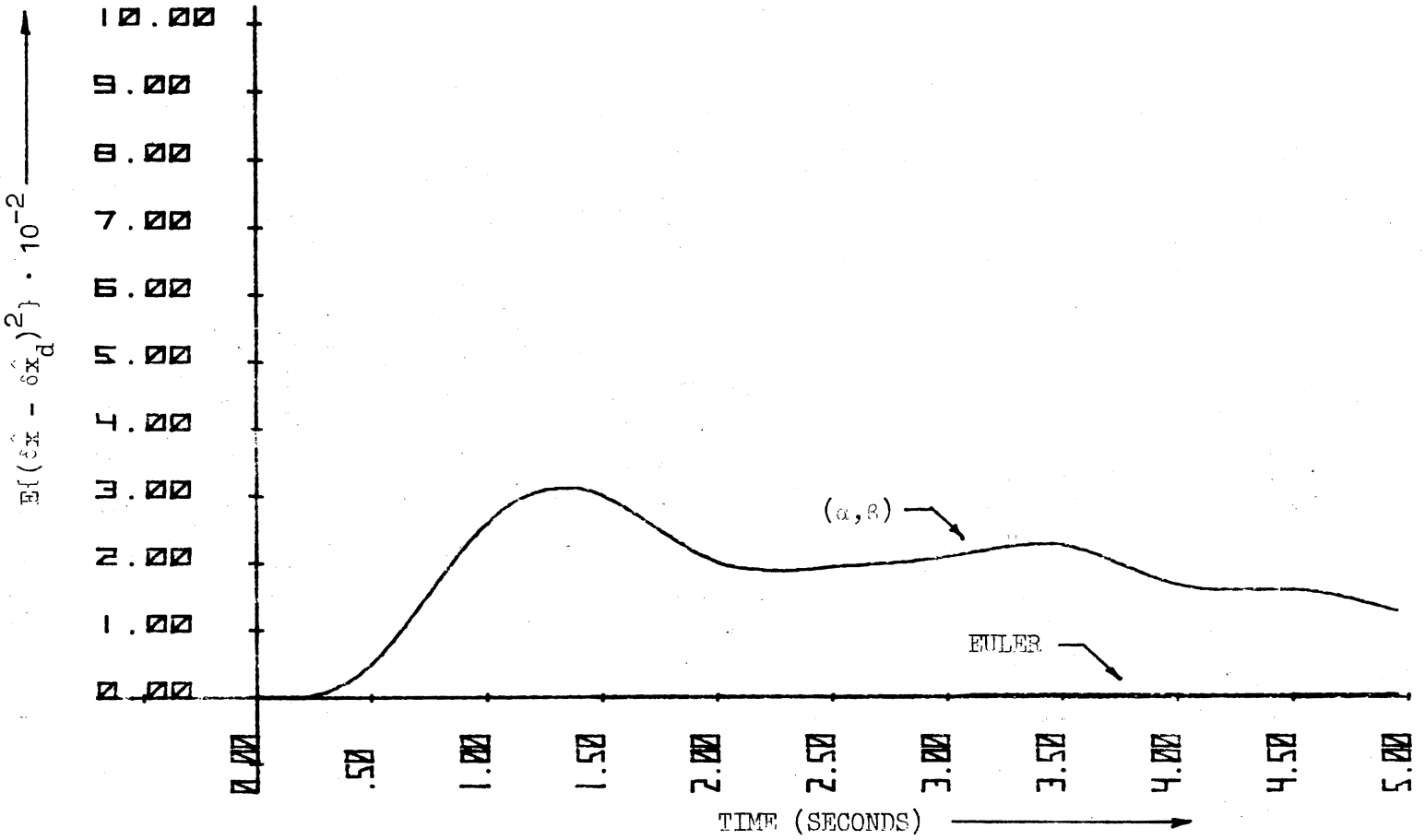

Figure 23. Error Covariance $E\{(\delta\hat{x} - \delta\hat{x}_d)^2\}$ for the Second-Order Nonlinear System for T = 0.1

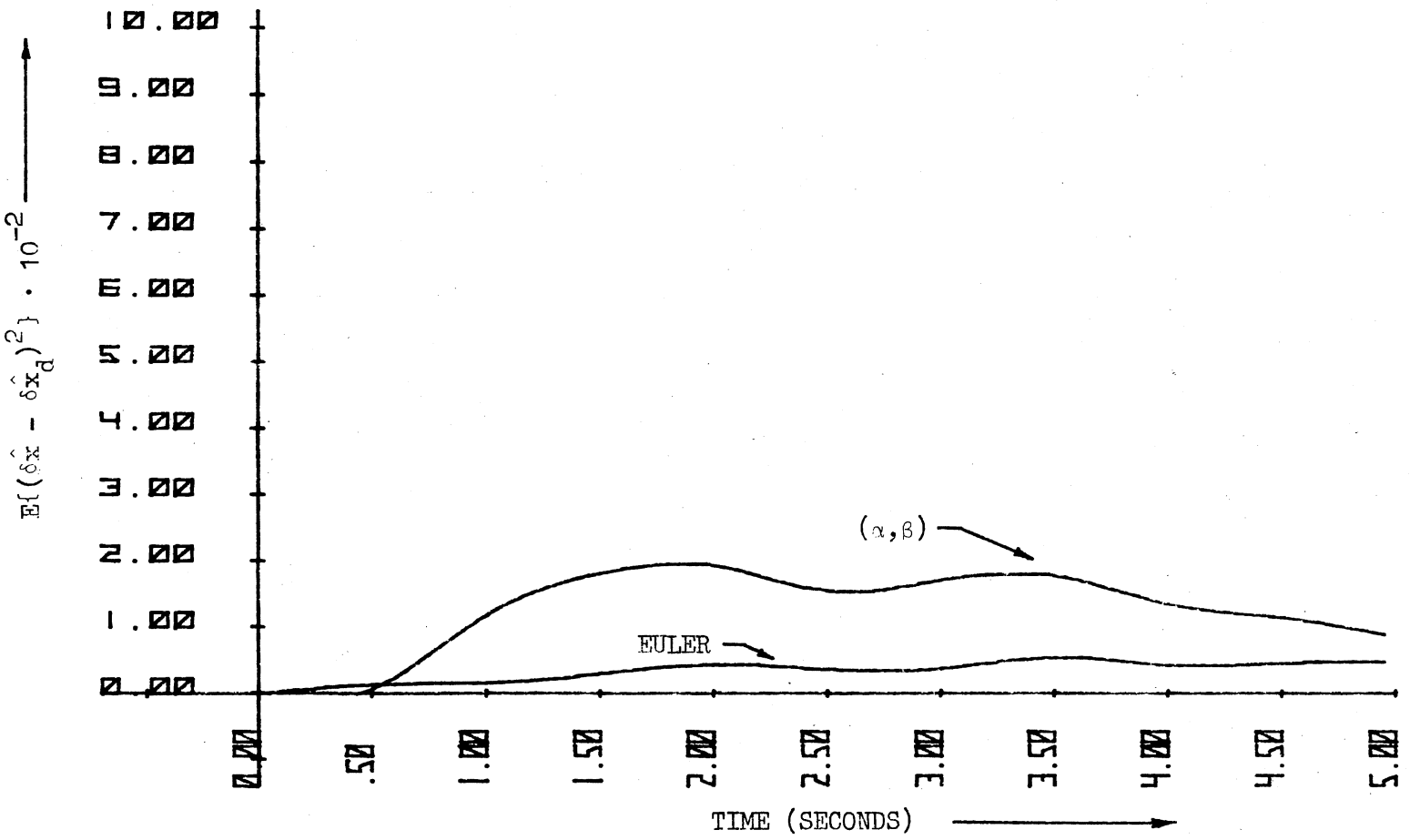

Figure 24. Error Covariance $E\{(\delta\hat{x} - \delta\hat{x}_d)^2\}$ for the Second-Order Nonlinear System for T = 0.25

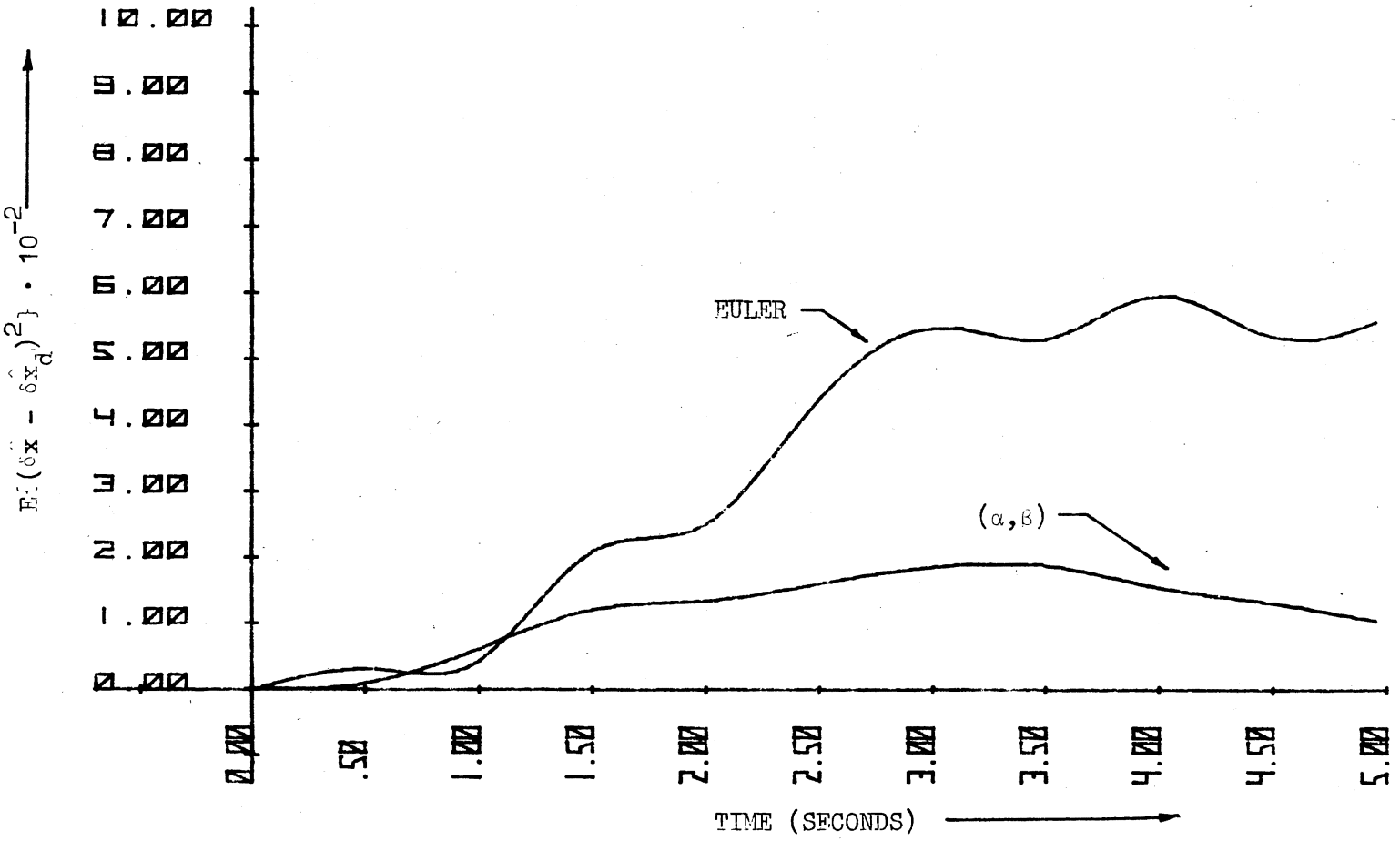

Figure 25. Error Covariance $E\{(\delta\hat{x} - \delta\hat{x}_d)^2\}$ for the Second-Order Nonlinear System for T = 0.5

CHAPTER IV

ACCURACY-VERSUS-SPEED TRADEOFFS

In this chapter, accuracy-versus-speed comparisons are made for the optimal discrete representation method developed in the previous chapter. A procedure is developed for obtaining an acceptable accuracy and speed under constraint conditions. The developed procedure is illustrated by an example. A new cost functional is defined to allow these tradeoffs between accuracy and computational speed.

Constraint Concepts

The search for extrema in optimization problems usually is restricted by the parameters which define the region of search. Thus, the goal is to obtain the best possible solution within the defined region for search. Constraints in an optimization problem may be classified as either soft constraints or hard constraints. For the problems considered in this thesis, the cost functionals defined by (2.12) and (2.13) are functions of the sampling period T. In the earlier chapters, the value of T was assumed to be fixed. This assumption is replaced by a constraint condition in this chapter. If the sampling period T was restricted, e.g. $T \leq 0.2$, then this constraint is referred to as a "hard" constraint, as it is imposed directly on T. This restriction reduces the region of search for the minimum value of the cost functional. Under this condition the search direction is

modified, if any violation of the constraint is made, to obtain the constrained minimum. On the other hand, if T appears in an added penalty term in the performance index, as in (4.3) below, the constraint on T is indirect and is referred to as a "soft" constraint. Under this condition the minimum value of J based on some given weighting parameter K_c is to be obtained.

The Hard Constraint Case

As indicated in the previous section, the accuracy-versus-speed problem may be treated in the context of a hard constraint. The cost functionals defined in (2.12) and (2.13) were based on algorithm accuracy for a fixed step size T. It is important to be able to incorporate the computational speed requirement into the optimization format. The computational speed is directly proportional to the step size T. For a fixed speed, i.e. $\geq$ some minimum speed, T must be as large as possible, i.e. since

$$\text{Speed} \geq \text{Minimum speed} \tag{4.1}$$

then

$$T \geq T_{min} \tag{4.2}$$

Since the J's in (2.12) and (2.13) are also directly proportional to T, then the smallest T possible yields best accuracy, i.e. least error and smallest J. Thus, a suitable tradeoff between algorithm accuracy and computational speed would yield minimum J. The consequence is that if computational speed is treated as a hard constraint, then the step size should be chosen as T_{min} to yield the best accuracy, i.e. minimum value

of J. Therefore, the results obtained in Chapter III are valid for this case if the fixed step size T for the two examples corresponded to T_{min}. The speed of the particular digital processor being utilized in any given application will determine T_{min}.

The Soft Constraint Case

Let a new cost functional J which treats computational speed as a soft constraint be defined by

$$J(\alpha,\beta,T) = J_{ERROR}(\alpha,\beta,T) + J_{EXEC}(T) \tag{4.3}$$

where J_{ERROR} is defined by (2.12) or (2.13) and J_{EXEC} is some monotonically decreasing function of T, e.g. $J_{EXEC} = K_c/T$. The subscript on J_{EXEC} indicates that a penalty is incurred if the algorithm execution time is too large. Observe that, for fixed curves of α and β, J_{ERROR} is a monotonically increasing function of T, since the error increases as the step size increases. Since J_{ERROR} is directly proportional to T and J_{EXEC} is inversely proportional to T, a suitable choice should be made to obtain the minimum J in (4.3). If T is chosen to be smaller than the optimal value, then the execution time would be high, which corresponds to a lower computational speed. While the accuracy would be improved somewhat, corresponding to a lower value of J_{ERROR}, the higher value of J_{EXEC} would result in an overall higher value of J, as shown in Figure 26. On the upper side of the optimal T, J_{ERROR} is higher and J_{EXEC} is lower, resulting again in a higher value of J than its minimum. These curves of J were plotted for the first-order example given by (3.39) for three different values of the weighting parameter K_c. Observe that as the value of the weighting parameter K_c increases, the

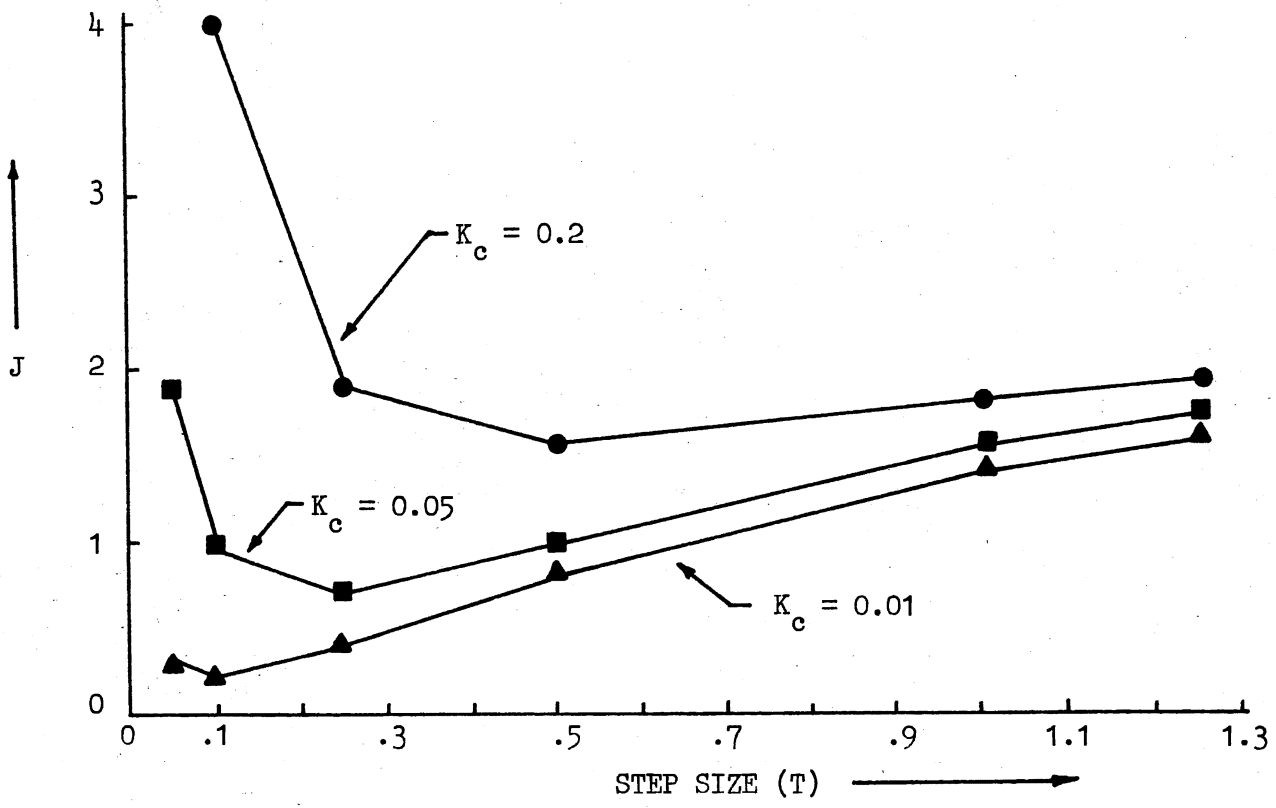

Figure 26. Cost Functional J in (4.3) Versus T for K_c = 0.01, 0.05, and 0.2

value of the optimal T also increases, indicating that a faster operating speed of the filtering algorithm is required.

An Example

To further illustrate the hard constraint case, digital computer simulation results using 100 Monte Carlo runs are shown in Figure 27 for the optimal constrained (first-order) filter obtained by applying the optimization algorithm to the second-order nonlinear example given by (3.16). Comparisons are made with the second-order Adams-Bashforth (AB2) and Runge-Kutta (RK2) formulas integrating the continuous variational Kalman filter equations and with the RK2 formula integrating the continuous extended Kalman filter equations (25,41). It was assumed in the case of the optimal constrained filter that the choice of T was T_{min}. Observe that the value of T for the three comparison curves ($AB2_{var}$, $RK2_{var}$, and $RK2_{ext}$) was selected to yield approximately the same filter computational time. On the other hand, the optimal constrained filter had a value of T = 0.1 seconds, which operated eight times faster than the other filters. Thus, it can be concluded that the use of the optimal constrained filter for on-line applications will yield a lower error variance and will operate much faster than the others filters.

Summary

This chapter dealt with the problem of speed and accuracy tradeoffs for the optimal discrete representation developed in Chapter III. A new cost functional J was defined to take into account the computational time required by the filter. It was shown in this soft constraint case

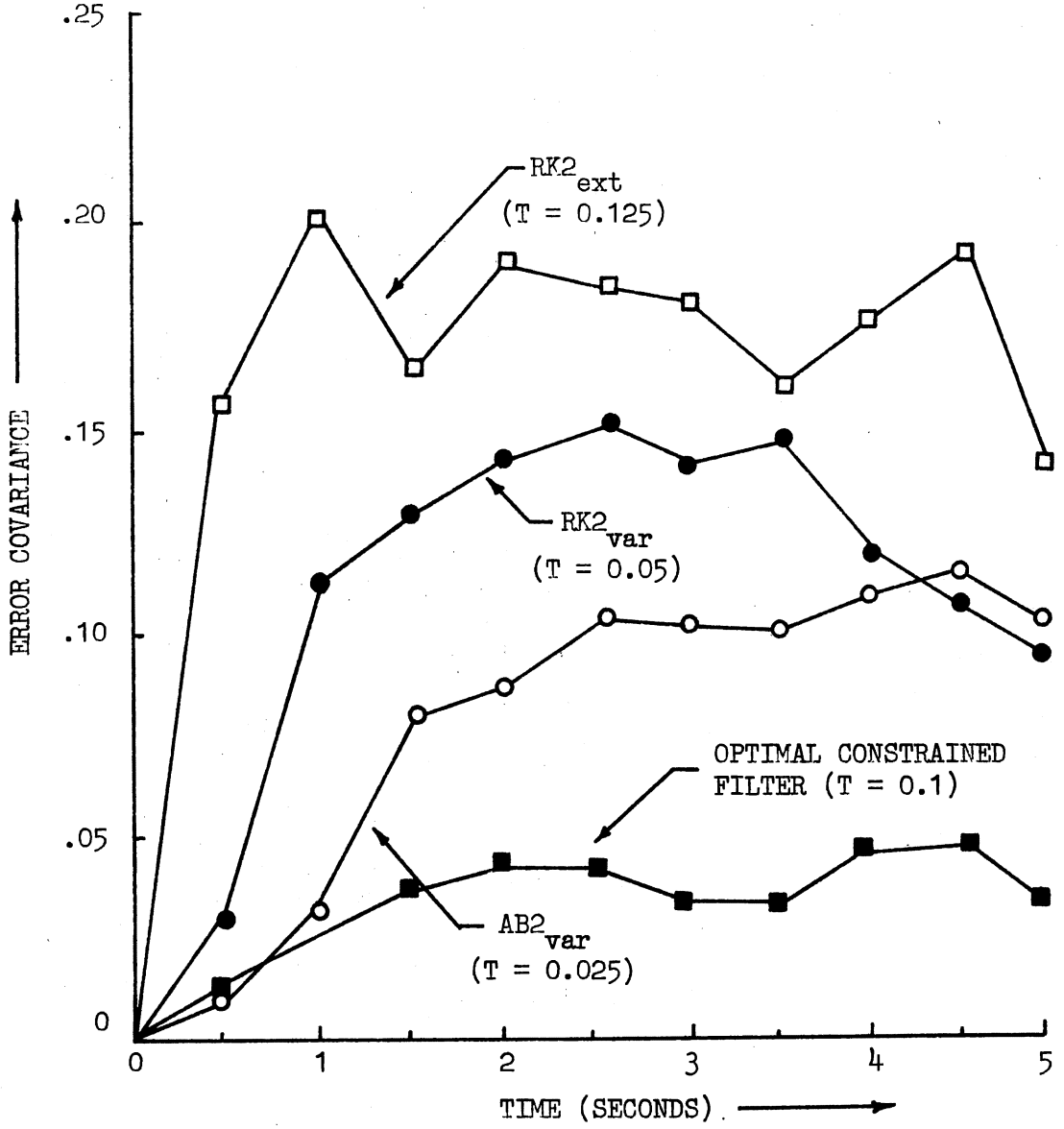

Figure 27. Comparison of Optimal Constrained Filter with $AB2_{var}$, $RK2_{var}$, and $RK2_{ext}$

that an optimal value of T may be used to obtain the minimum J. However, the use of a different weighting parameter in the cost functional yielded different optimal values of T. The arbitrariness in selecting this parameter suggests that the computational speed-versus-accuracy problem should be treated more properly as a hard constraint case. An example was included for this case with comparisons between $AB2_{var}$, $RK2_{var}$, and $RK2_{ext}$ and the optimal constrained filter using T_{min}.

CHAPTER V

TRAJECTORY OPTIMIZATION

The simultaneous optimization of the nominal trajectory, the incremental filtering algorithm parameters, and the discrete representation itself for a fixed value of $T = T_{min}$ is handled in this chapter. Nonlinear examples are included to illustrate the procedure. The coefficients $\alpha(t_k)$ and $\beta(t_k)$ are simultaneously optimized with the nominal trajectory to obtain the minimum cost functionals defined in Chapter II.

Mathematical Development

The basic approach used here is the minimization of (2.13) subject to (2.1)-(2.4), (2.6) and (2.11). As Bryson and Ho (42) and Denham (43) indicated that the "best" nominal trajectory is not necessarily the deterministic optimal trajectory, a procedure for obtaining an improved nominal trajectory is developed in this section. The Hamiltonian in (3.14) is redefined with another ℓ by ℓ Lagrange multiplier $\lambda_{11}(t_k)$ for $P_{11}(t_{k+1})$ which satisfies the boundary condition $\lambda_{11}(t_K) = 0$. The Hamiltonian is defined as

$$H = \text{Trace} \{ \frac{1}{2} [P_{11}(t_{k+1}) + P_{22}(t_{k+1}) - P_{12}(t_{k+1}) - P_{12}^T(t_{k+1})] + P_{11}(t_{k+1})\lambda_{11}^T(t_{k+1}) + P_{12}(t_{k+1})\lambda_{12}^T(t_{k+1}) + P_{22}(t_{k+1})\lambda_{22}^T(t_{k+1})\} \tag{5.1}$$

Using (3.8), (3.25), (3.29), and (3.30) in the above equation yields (3.35) through (3.38) by minimizing the Hamiltonian with respect to $\alpha(t_k)$, $\beta(t_k)$, $P_{12}(t_k)$ and $P_{22}(t_k)$. Further,

$$\lambda_{11}(t_k) = \frac{\partial H^*}{\partial P_{11}(t_k)} \tag{5.2}$$

$$\frac{\partial H}{\partial x_N(t_k)} = 0 \tag{5.3}$$

where $\underline{x}_N(t_k)$ is the optimal deterministic trajectory.

Example

A second-order example given by (3.16) for $\rho = 3.0$ and $\gamma = 0.5$ is considered here again for trajectory optimization. The Hamiltonian in (5.1) may be written as

$$H = [\frac{1}{2} + \lambda_{11}(t_{K+1})]P_{11}(t_{k+1}) + [\frac{1}{2} + \lambda_{22}(t_{k+1})]P_{22}(t_{k+1}) + [-1 + \lambda_{12}(t_{k+1})]P_{12}(t_{k+1}) \tag{5.4}$$

Using (3.8), (3.24), (3.29), and (3.30) in the above equation yields

$$\begin{aligned} H = {} & [\frac{1}{2} + \lambda_{11}(t_{k+1})][\phi_{11}^2 p'_{11}(t_k) + 2\phi_{12}\phi_{11}p'_{12}(t_k) + \phi_{12}^2 p'_{22}(t_k) \\ & + Q_\omega \int_{t_k}^{t_{k+1}} \phi_{12}^2(t_{k+1},\tau)d\tau] + [\frac{1}{2} + \lambda_{22}(t_{k+1})][\alpha^2(t_k)P_{22}(t_k) \\ & + \beta^2(t_k)p'_{11}(t_k) + \beta^2(t_k)Q_{vd}(t_k) + 2\alpha(t_k)\beta(t_k)p'_{12a}(t_k)] \\ & + [-1 + \lambda_{12}(t_{k+1})][(\phi_{11}p'_{12a}(t_k) + \phi_{12}p'_{12b}(t_k))\alpha(t_k) \\ & + \beta(t_k)(\phi_{11}p'_{11}(t_k) + \phi_{12}p'_{12}(t_k))] \end{aligned} \tag{5.5}$$

The minimization of the above Hamiltonian with respect to $\alpha(t_k)$, $\beta(t_k)$,

$p'_{12a}(t_k)$, and $P_{22}(t_k)$ yields (3.35) through (3.38) and with respect to $x_{2N}(t_k)$ and $p'_{11}(t_k)$ gives

$$\frac{\partial H}{\partial x_{2N}(t_k)} = \frac{\partial \phi_{12}}{\partial x_{2N}(t_k)} \Big[\left(\frac{1}{2} + \lambda_{11}(t_{k+1})\right) [2\phi_{11}p'_{12}(t_k) + 2\phi_{12}p'_{22}(t_k) + 3Q_\omega x_{2N}(t_k)\left(1 + 1.5x^2_{2N}(t_k)\right)\left(\frac{2}{3}e^{-3T} - \frac{e^{-2T}}{2} - \frac{e^{-4T}}{4} - \frac{11}{12}\right)] + (-1 + \lambda_{12}(t_{k+1}))(\alpha(t_k)p'_{12b}(t_k) + \beta(t_k)p'_{12}(t_k)\Big] = 0 \quad (5.6)$$

and

$$\frac{\partial H^*}{\partial p'_{11}(t_k)} = \left[\frac{1}{2} + \lambda_{11}(t_{k+1})\right]\phi^2_{11} + \left[\frac{1}{2} + \lambda_{22}(t_{k+1})\right]\beta^2(t_k) + \left[-1 + \lambda_{12}(t_{k+1})\right]\beta(t_k)\phi_{11} = \lambda_{11}(t_k) \quad (5.7)$$

where, from (3.24),

$$\dot{\Phi}(t,t_k) = A(t)\Phi(t,t_k)$$
$$\Phi(t_k,t_k) = I \quad (5.8)$$

Therefore,

$$\Phi(t,t_k) = \begin{bmatrix} -2 & 1+1.5x^2_{2N}(t) \\ 0 & -1 \end{bmatrix}\begin{bmatrix} \phi_{11} & \phi_{12} \\ \phi_{21} & \phi_{22} \end{bmatrix} \quad (5.9)$$

Assuming that $x_{2N}(t)$ is held constant over the sampling interval $T = t_{k+1}-t_k$, one has

$$\phi_{11}(t_{k+1},t_k) = e^{-2T}$$
$$\phi_{12}(t_{k+1},t_k) = \left[1 + 1.5x^2_{2N}(t_k)\right]e^{-T}(1 - e^{-T}) \quad (5.10)$$
$$\phi_{21}(t_{k+1},t_k) = 0$$

$$\phi_{22}(t_{k+1},t_k) = e^{-T}$$

Therefore,

$$\frac{\partial\phi_{12}(t_{k+1},t_k)}{\partial x_{2N}(t_k)} = 3.0x_{2N}(t_k)e^{-T}(1 - e^{-T}) \qquad (5.11)$$

The numerical results obtained by using trajectory optimization are compared with the results obtained from the optimal discrete representation and the Euler Method in Figures 28 through 31. These results correspond to the cost functionals given by (2.12) and (2.13) and are plotted for sampling times of T = 0.1 and 0.5. It should be noted that the results obtained by using trajectory optimizations are not exact because of the approximations involved. It was assumed that $x_{2N}(t)$ was constant over the sampling period T in obtaining (5.10) from (5.9). It can be observed that except for one point in Figure 28, the trajectory optimization method shows an improvement over the basic optimal discrete representation. For higher step sizes, the results from trajectory optimizations approach the results obtained from the optimal discrete representations (Figure 29). Figures 30 and 31 compare the results obtained corresponding to the cost functional in (2.12). This amounts to comparing the state estimate obtained from the trajectory optimization and optimal discrete representation with the results obtained from the variational Kalman filter. Since the variational Kalman filter is not the best filter, because of the approximations involved, the results from the trajectory optimization and the optimal discrete representation are different from the results obtained by using the Euler Method. As the step size T increases

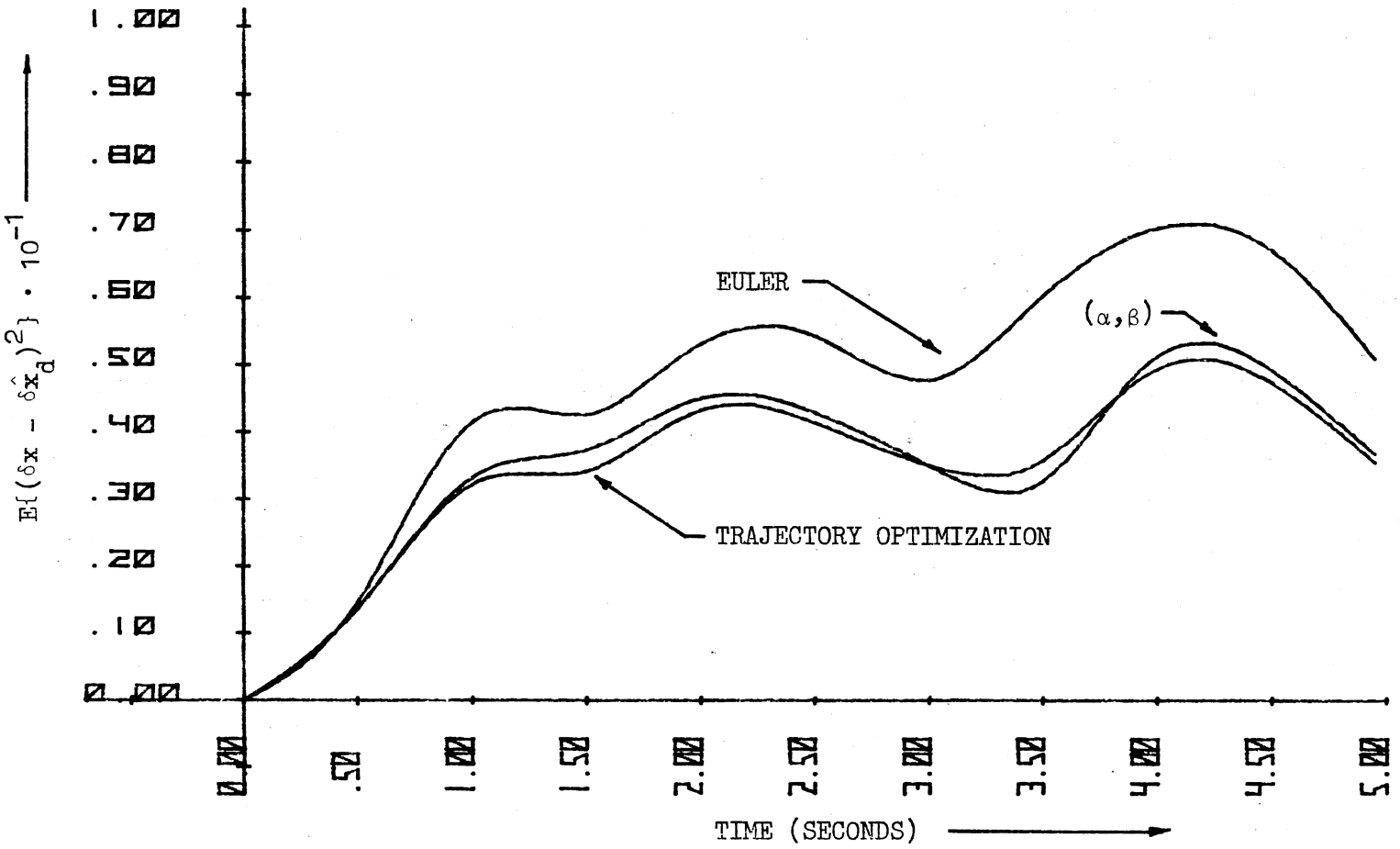

Figure 28. Comparisons of Error Covariance $E\{(\delta x - \delta\hat{x}_d)^2\}$ Obtained from Trajectory Optimization, Optimal Discrete Representation and Euler Methods for the Second-Order Nonlinear System for T = 0.1

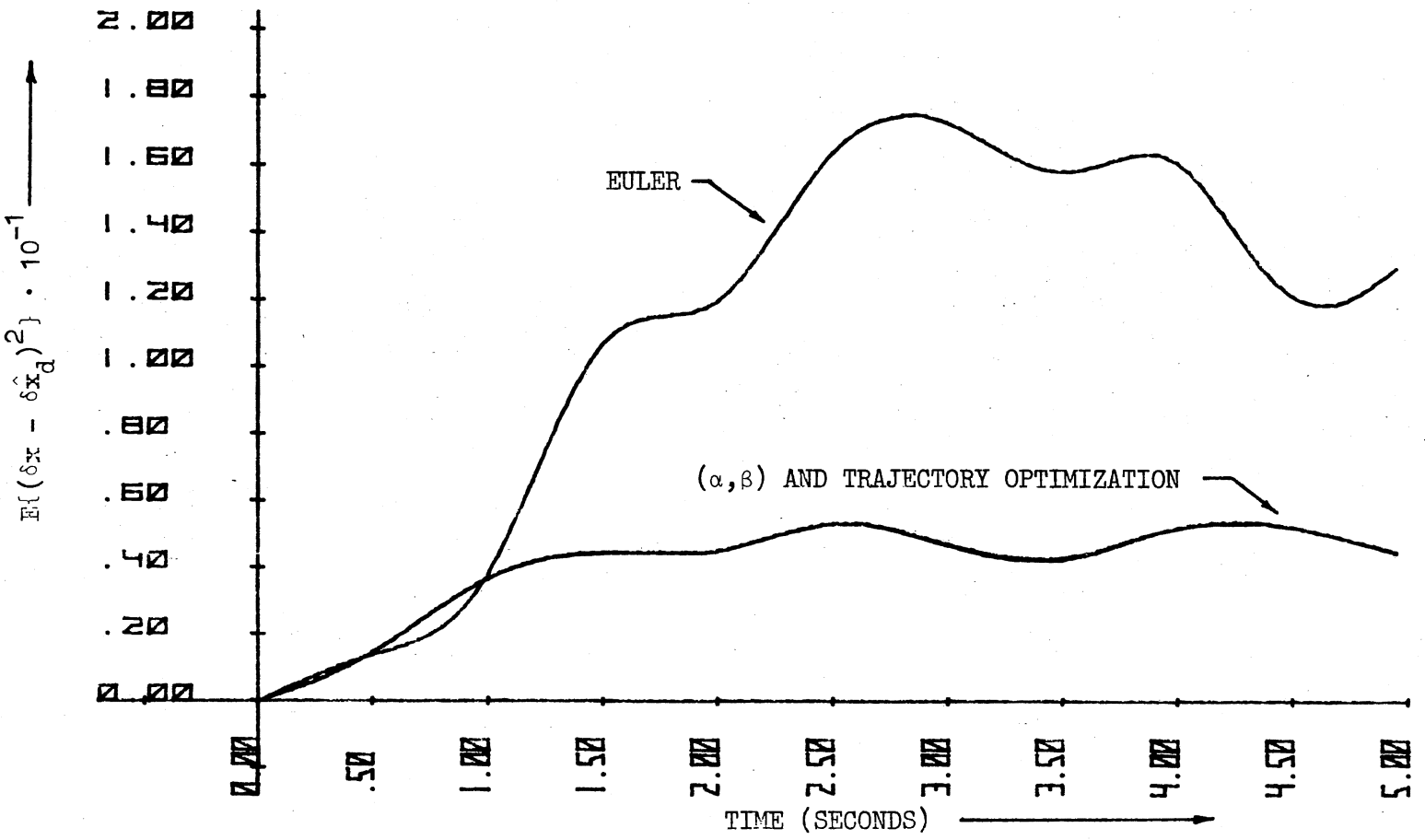

Figure 29. Comparisons of Error Covariance $E\{(\delta x - \delta\hat{x}_d)^2\}$ Obtained from Trajectory Optimization, Optimal Discrete Representation and Euler Methods for the Second-Order Nonlinear System for T = 0.5

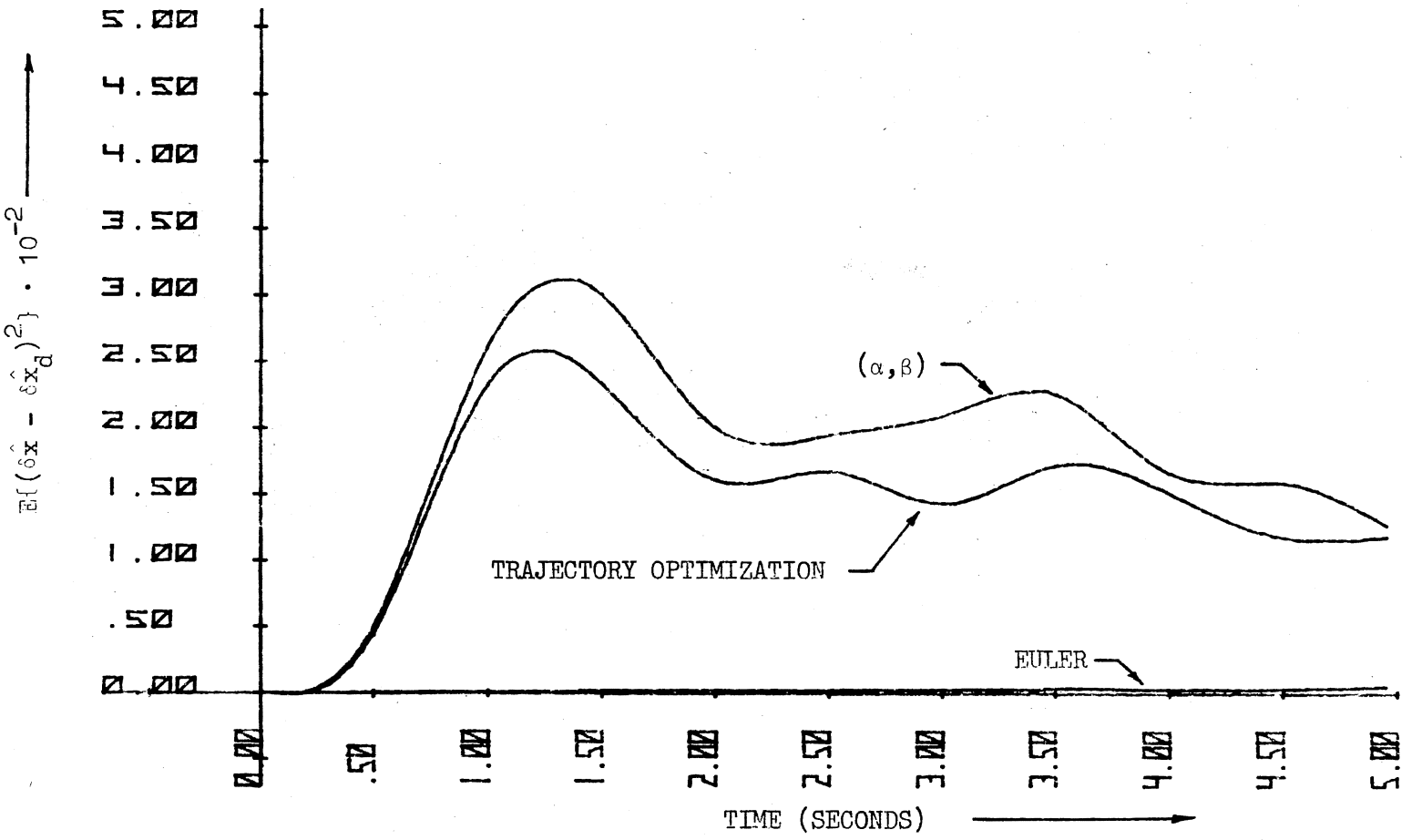

Figure 30. Comparisons of Error Covariance $E\{(\delta\hat{x} - \delta\hat{x}_d)^2\}$ Obtained from Trajectory Optimization, Optimal Discrete Representation and Euler Methods for the Second-Order Nonlinear System for T = 0.1

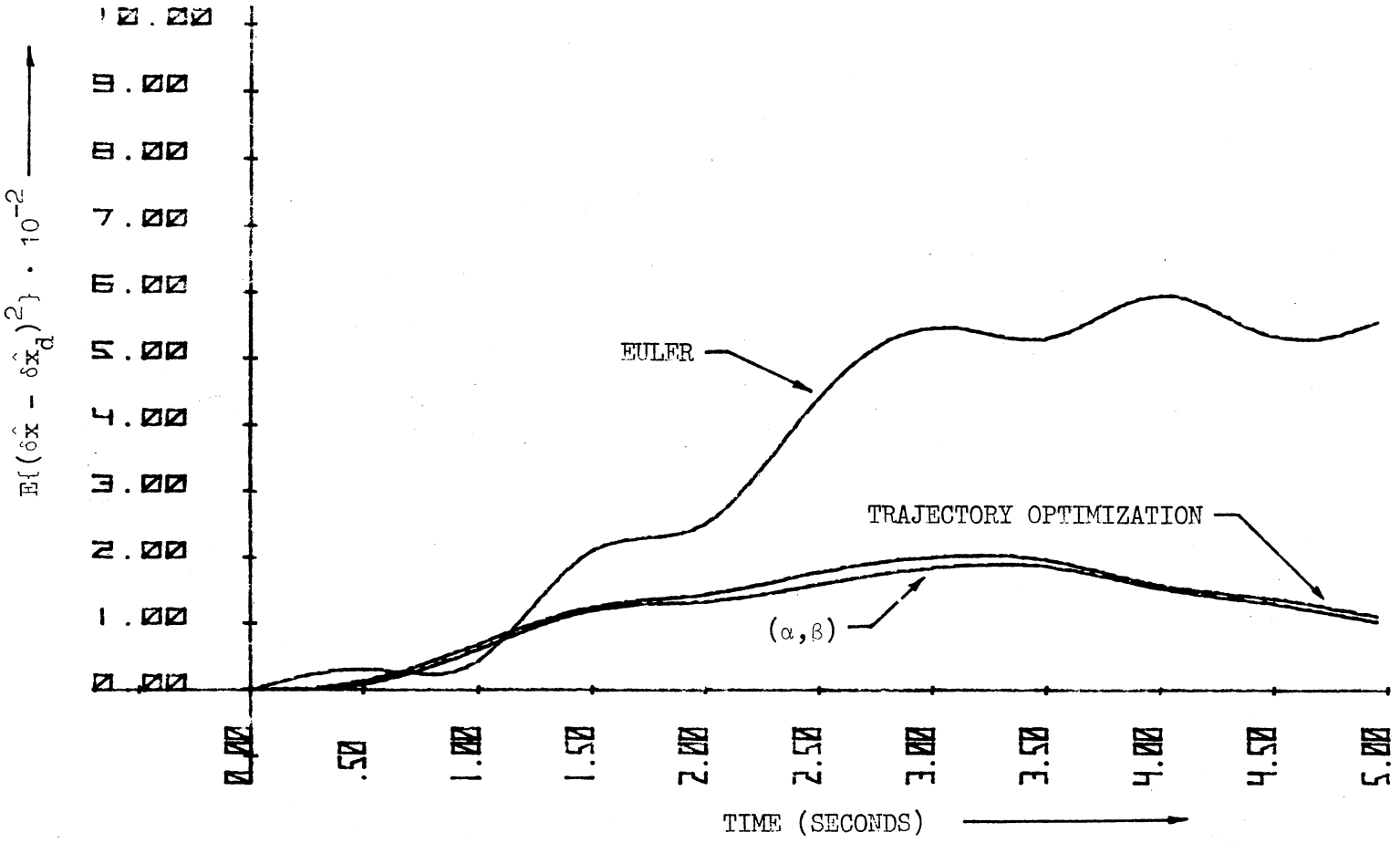

Figure 31. Comparisons of Error Covariance $E\{(\delta\hat{x} - \delta\hat{x}_d)^2\}$ Obtained from Trajectory Optimization, Optimal Discrete Representation and Euler Methods for the Second-Order Nonlinear System for T = 0.5

(Figure 31), it can be seen that the percent error increase in the results of Euler Method is much higher than that of trajectory optimization or the basic optimal discrete representation. Another example of a highly nonlinear system with a non-Gaussian noise input is chosen to illustrate the improved results obtained by using trajectory optimization as compared to the Euler Method and optimal discrete representation results.

Example

A first-order nonlinear system (35,36) is given by

$$\dot{x} = -0.5x + 0.25x^3 - 0.035x^5 + \omega(t)$$
$$z = x + v(t) \tag{5.12}$$

with $x(0) = 1.5$, $Q_\omega = 3.0$, $Q_v = 0.1$, $t_0 = 0.0$, and $t_f = 1.5$. The probability density of the discrete samples was chosen according to the non-Gaussian probability density function given by

$$p_{\omega_d}(\omega_d) = \begin{cases} 6.5\sqrt{Q_{\omega d}}\,\omega_d^{12} & \text{for } \dfrac{-1}{(\sqrt{Q_{\omega d}})^{\frac{1}{13}}} \le \omega_d \le \dfrac{1}{(\sqrt{Q_{\omega d}})^{\frac{1}{13}}} \\ 0 & \text{otherwise} \end{cases} \tag{5.13}$$

The linearized equation for $\delta x(t)$ about the noise-free nominal trajectory is obtained from (2.6) as

$$\delta\dot{x}(t) = (-0.5 + 0.75x_N^2(t) - 0.175x_N^4(t))\delta x(t) + \omega(t) \tag{5.14}$$

and the variational Kalman filter using (2.8) is given by

$$\dot{\delta\hat{x}}(t) = (A(t) - K(t))\delta\hat{x}(t) + K(t)\delta z(t) \tag{5.15}$$

where

$$\dot{P}_e(t) = 2A(t)P_e(t) - \frac{P_e^2(t)}{Q_v} + Q_\omega$$

$$A(t) = -0.5 + 0.75x_N^2(t) - 0.175x_N^4(t) \tag{5.16}$$

and

$$K(t) = \frac{P_e(t)}{Q_v}$$

Using the Hamiltonian defined in (5.4) with

$$P_{11}(t_{k+1}) = \phi^2 P_{11}(t_k) + Q_\omega \frac{(e^{2A(t_k)T} - 1)}{2A(t_k)} \tag{5.17}$$

where it is assumed that $A(t_k)$ is constant over the sampling interval $T = t_{k+1} - t_k$, yields

$$\begin{aligned} H = {} & [\tfrac{1}{2} + \lambda_{11}(t_{k+1})][\phi^2 P_{11}(t_k) + Q_\omega \frac{(\phi^2 - 1)}{2A(t_k)}] + \\ & [\tfrac{1}{2} + \lambda_{22}(t_{k+1})][\alpha^2(t_k)P_{22}(t_k) + \beta^2(t_k)P_{11}(t_k) + \beta^2(t_k)Q_{vd} \\ & + 2\alpha(t_k)\beta(t_k)P_{12}(t_k)] + [-1 + \lambda_{12}(t_{k+1})][\phi(\alpha(t_k)P_{12}(t_k) \\ & + \beta(t_k)P_{11}(t_k)] \end{aligned} \tag{5.18}$$

where

$$\phi(t_{k+1}, t_k) = e^{A(t_k)T} \tag{5.19}$$

An average value of x_N was selected for the calculation of $A(t_k)$ over the sampling interval T. The resulting $A(t_k)$ was

$$A(t_k) = -0.5 + 0.75\left(\frac{x_N(t_{k+1}) + x_N(t_k)}{2}\right)^2 - 0.175\left(\frac{x_N(t_{k+1}) + x_N(t_k)}{2}\right)^4 \tag{5.20}$$

The minimization of the Hamiltonian in (5.18) with respect to $\alpha(t_k)$, $\beta(t_k)$, $P_{11}(t_k)$, $P_{12}(t_k)$, $P_{22}(t_k)$, and $x_N(t_k)$ yields

$$\frac{\partial H(t_{k+1},t_k)}{\partial \alpha(t_k)} = [\ \frac{1}{2} + \lambda_{11}(t_{k+1})][2\alpha(t_k)P_{22}(t_k) + 2\beta(t_k)P_{12}(t_k)]$$
$$+ [-1 + \lambda_{12}(t_{k+1})]\phi(t_{k+1},t_k)P_{12}(t_k) \tag{5.21}$$

$$\frac{\partial H(t_{k+1},t_k)}{\partial \beta(t_k)} = 2[\ \frac{1}{2} + \lambda_{22}(t_{k+1})][\beta(t_k)P_{11}(t_k) + \beta(t_k)Q_{vd}$$
$$+ \alpha(t_k)P_{12}(t_k)] + [-1 + \lambda_{22}(t_{k+1})]\phi(t_{k+1},t_k)P_{11}(t_k) \tag{5.22}$$

$$\frac{H(t_{k+1},t_k)}{\partial x_N(t_k)} + \frac{H(t_k,t_{k-1})}{\partial x_N(t_k)} =$$

$$\left[(0.5 + \lambda_{11}(t_{k+1}))\left\{2\phi P_{11}(t_k)\frac{\partial \phi}{\partial x_N(t_k)} + 0.5Q_\omega \frac{\left(2A(t_k)\phi\frac{\partial \phi}{\partial x_N(t_k)} - (\phi^2 - 1)\frac{\partial A(t_k)}{\partial x_N(t_k)}\right)}{A^2(t_k)}\right\}\right.$$
$$\left. + (-1 + \lambda_{12}(t_{k+1}))(\alpha(t_k)P_{12}(t_k) + \beta(t_k)P_{11}(t_k))\frac{\partial \phi}{\partial x_N(t_k)}\right]_{(t_{k+1},t_k)}$$
$$+ \left[(0.5 + \lambda_{11}(t_k))\left\{2\phi P_{11}(t_{k-1})\frac{\partial \phi}{\partial x_N(t_k)} + 0.5Q_\omega \frac{\left(2A(t_{k-1})\phi\frac{\partial \phi}{\partial x_N(t_k)} - (\phi^2 - 1)\frac{\partial A(t_{k-1})}{\partial x_N(t_k)}\right)}{A^2(t_{k-1})}\right\}\right.$$
$$\left. + (-1 + \lambda_{12}(t_k))(\alpha(t_{k-1})P_{12}(t_{k-1}) + \beta(t_{k-1})P_{11}(t_{k-1}))\frac{\partial \phi}{\partial x_N(t_k)}\right]_{(t_k,t_{k-1})} \tag{5.23}$$

The adjoint difference equations now may be written as

$$\lambda_{11}(t_k) = \frac{\partial H^*}{\partial P_{11}(t_k)} = [\frac{1}{2} + \lambda_{11}(t_{k+1})]\phi^2 + [\frac{1}{2} + \lambda_{22}(t_{k+1})]\beta^2(t_k)$$
$$+ [-1 + \lambda_{12}(t_{k+1})]\phi\beta(t_k)$$
$$\lambda_{12}(t_k) = \frac{\partial H^*}{\partial P_{12}(t_k)} = [\frac{1}{2} + \lambda_{22}(t_{k+1})]2\alpha(t_k)\beta(t_k) \qquad (5.24)$$
$$+ [-1 + \lambda_{12}(t_{k+1})]\phi\alpha(t_k)$$
$$\lambda_{22}(t_k) = \frac{\partial H^*}{\partial P_{22}(t_k)} = [\frac{1}{2} + \lambda_{22}(t_{k+1})]\alpha^2(t_k)$$

The trajectory optimization results using the ensemble-averaging of 100 Monte Carlo runs were compared with the Euler Method and the optimal discrete representation results using the deterministic optimal trajectory. The results are plotted in Figures 32 and 33 for T = 0.1. Clearly, a considerable improvement is achieved by using the trajectory optimization method as compared to the other two methods for the cost functional given by (2.13). It was assumed that A(t) given by (5.16) was constant over the sampling period T in (5.19). An average value of x_N was selected over the interval (t_k, t_{k+1}) to obtain a better approximation of A(t). This required the differentiation of $H(t_{k+1}, t_k)$ in (5.18) with respect to $x_N(t_k)$ evaluated at (t_{k+1}, t_k) and (t_k, t_{k-1}) in (5.23) (15). Thus, it can be concluded from the results obtained that the trajectory optimization yields a considerable improvement over the other two methods compared. The results in Figure 33 correspond to the cost functional in (2.12). As shown in Figure 30 for small step sizes, the Euler Method shows a lower error covariance, while for higher step sizes (Figure 31), the other two methods show lower error covariances. Similarly, for the highly nonlinear system considered in this section,

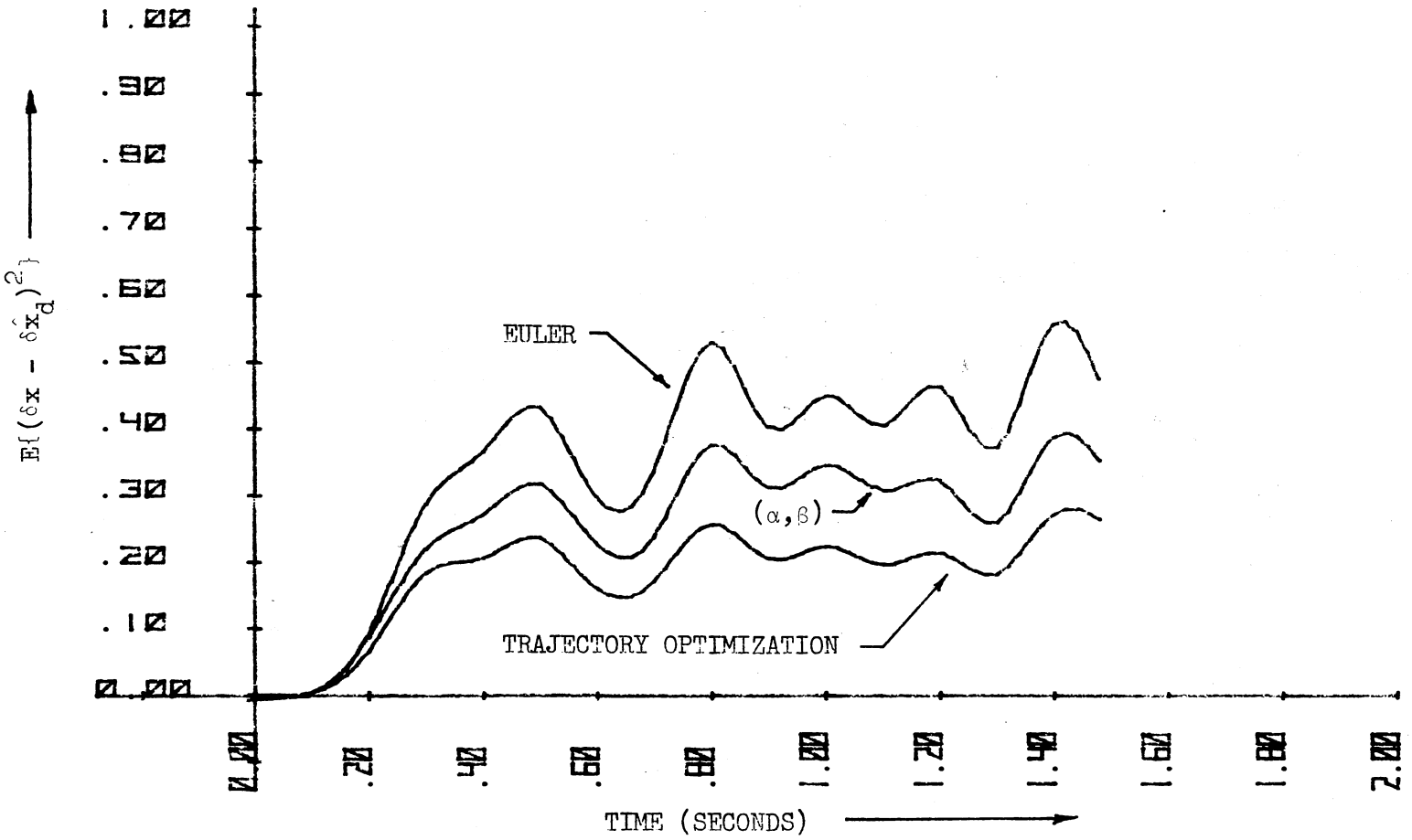

Figure 32. Comparisons of Error Covariance $E\{(\delta x - \delta \hat{x}_d)^2\}$ Obtained from Trajectory Optimization, Optimal Discrete Representation and Euler Methods for the First-Order Nonlinear System for T = 0.1

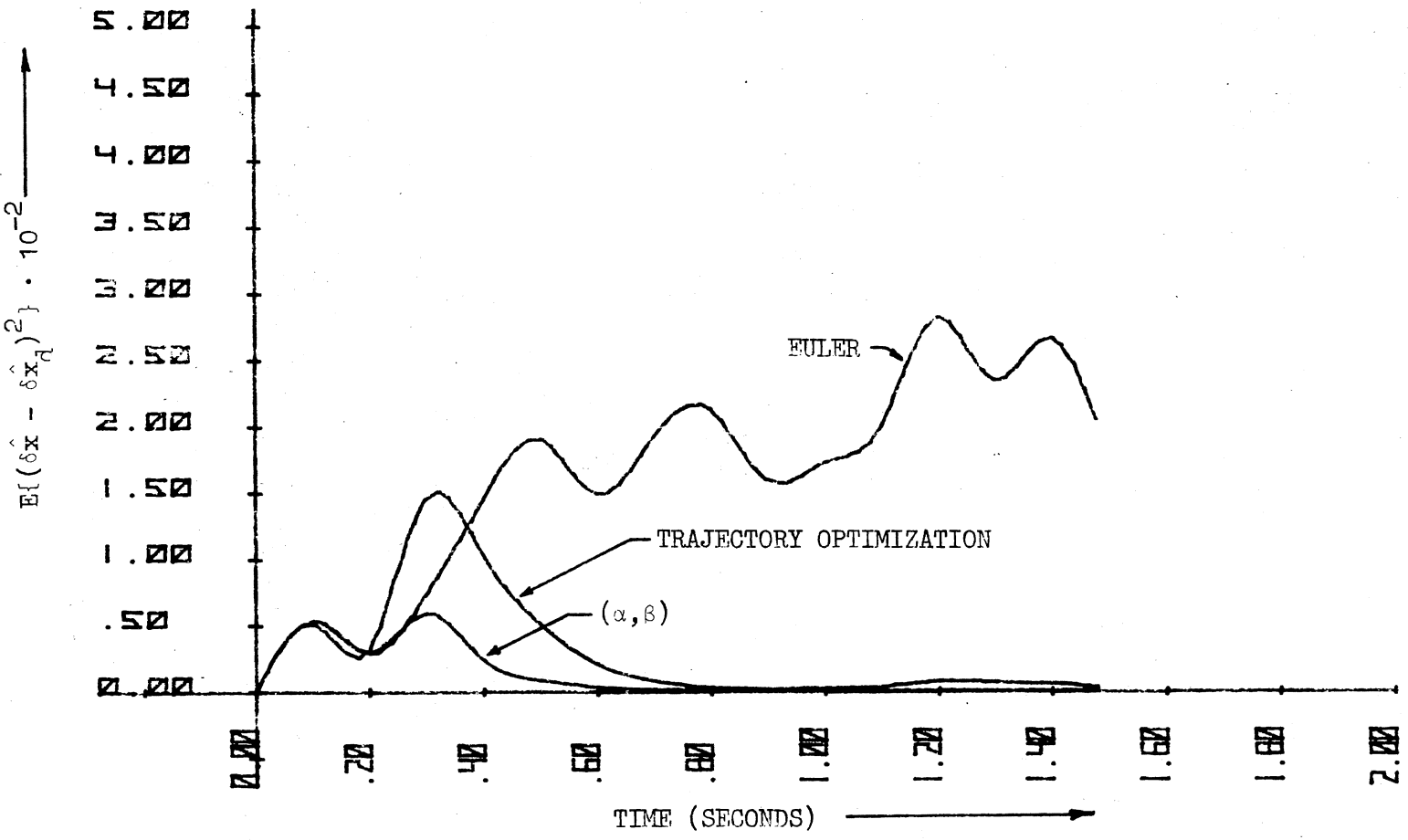

Figure 33. Comparisons of Error Covariance $E\{(\delta\hat{x} - \delta\hat{x}_d)^2\}$ Obtained from Trajectory Optimization, Optimal Discrete Representation and Euler Methods for the First-Order Nonlinear System for T = 0.1

T = 0.1 is a large step size and, thus, the results are consistent with those obtained earlier.

Summary

This chapter dealt with the development of the trajectory optimization procedure. Two nonlinear examples were used to illustrate the procedure. It was shown that a considerable improvement in the error covariance was obtained by using this procedure as compared to the Euler Method or the optimal discrete representation method.

CHAPTER VI

CONCLUSIONS AND RECOMMENDATIONS

Results and Conclusions

The basic contribution of this thesis research is the development of an optimal discrete representation for the continuous filtering algorithms for nonlinear stochastic systems. It was also shown that the trajectory optimization results showed considerable improvements over the existing methods. Two cost functionals were considered for comparing the results obtained by using the optimal discrete representations based on the state and its estimate using the variational Kalman filter. It was required for the two nonlinear systems considered that the nonlinearity be analytic in a neighborhood of the nominal trajectory. During the development of the complete optimization procedure, a first-order linear system and two nonlinear systems were considered.

In Chapter II steady-state optimizations were performed on the first-order linear example by using the Euler Method, the RK2 method, and the optimal discrete representation method based on the two cost functionals defined in that chapter. Since for linear systems the Kalman filter is the best filter, the optimal discrete representation results showed an improvement over the Euler Method but failed to show better results than the second-order RK2 method. For the second cost functional given by (2.12), the optimal discrete representation

demonstrated an improvement over both the Euler Method and the RK2 method. These results were reconfirmed in Chapter III, which dealt with the development of the optimization procedure based on a two-point boundary value problem. Consistent results were shown for the second-order nonlinear example, except for the cost functional given by (2.12). Since the variational filter is not the best filter for nonlinear systems, the results for this cost functional were only relative. In Chapter IV a procedure was developed for obtaining an acceptable accuracy and speed under constraint conditions. A major contribution was demonstrated in Chapter V by using trajectory optimizations. It was shown that a considerable improvement was achieved using trajectory optimization based on the optimal discrete representations.

Recommendations for Further Work

There are several possibilites for the extension of the research work performed in this thesis. The optimal discrete representation was developed based on the first-order integration method. It can be easily extended to include the higher order integration methods. The basic idea required would be the same as developed in this thesis research.

The basic concepts of this research can be further extended to the combined estimation and control problem. This extension will require the development of a joint procedure which gives the optimal discrete representation of the state estimate as well as the optimal variational Riccati controller. A new cost functional will be required to obtain the minimum J for the combined estimation and control problem.

A stochastic sensitivity analysis could be performed on the optimal

discrete representation method developed in this thesis. This analysis would be needed to determine system performance when the assumed parameters and/or input statistics vary from the design values. This extension will validate the optimal discrete representations for use in practical stochastic filtering and control applications.

If the input noise matrices Q_ω and Q_v in (2.9) and (2.10) are themselves white noise processes, then a knowledge of stochastic integration is needed to find $P_e(t)$ and $K(t)$, which will also be random. The relationship between stochastic integration and numerical integration formulas for deterministic systems should be investigated to obtain the solution of the stochastic integration problem.

SELECTED BIBLIOGRAPHY

(1) Wiener, N. Extrapolation, Interpolation, and Smoothing of Stationary Time Series with Engineering Applications. New York: John Wiley and Sons, Inc., 1949.

(2) Kolomogorov, A. N. "Interpolation and Extrapolation of Stationary Time Series." Bulletin of the Academy of Science, U.S.S.R. Math. Ser., Vol. 5 (1941), 3-14.

(3) Kalman, R. E., and R. S. Bucy. "New Results in Linear Filtering and Prediction Theory." ASME Transactions: Journal of Basic Engineering, Vol. 83D (March, 1961), 95-108.

(4) Kushner, Harold J. "Approximations to Optimal Nonlinear Filters." IEEE Transactions on Automatic Control, Vol. AC-12, No. 5 (October, 1967), 546-556.

(5) Ho, Y. C., and R. C. K. Lee. "A Bayesian Approach to Problems in Stochastic Estimation and Control." IEEE Transactions on Automatic Control, Vol. AC-9 (1964), 333-339.

(6) Bucy, R. S. "Nonlinear Filtering Theory." IEEE Transactions on Automatic Control, Vol. AC-10, No. 2 (April, 1965), 198.

(7) Mortensen, R. E. Optimal Control of Continuous-Time Stochastic Systems. Berkeley: Electronics Research Laboratory, University of California, Report No. ERL-66-1, August 19, 1966.

(8) Kuo, Te-Son, and James R. Rowland. "Adaptive Non-Linear Estimation for Bounded-Noise Systems." International Journal of Control, Vol. 19, No. 1 (January, 1974), 203-211.

(9) Kuo, Te-Son, and James R. Rowland. "A Moment Technique for Suboptimal Adaptive Nonlinear Filtering." 1970 SWIEEECO Conference Record, (April 22-24, 1970), 105-109.

(10) Bucy, R. S., and Kenneth D. Senne. "Realization of Optimum Discrete-Time Nonlinear Estimators." Proceedings of the First Symposium on Nonlinear Estimation Theory and Its Applications, San Diego, California, (September 21-23, 1970), 6-17.

(11) Alspach, Daniel L., and Harold W. Sorenson. "Approximation of Density Functions by a Sum of Gaussians for Nonlinear Bayesian Estimation." Proceedings of the First Symposium on Nonlinear Estimation Theory and Its Applications, San Diego, California, (September 21-23, 1970), 19-31.

(12) Lo, James Ting-Ho. Finite Dimensional Sensor Orbits and Optimal Nonlinear Filtering. Los Angeles: Department of Aerospace Engineering, University of Southern California, Technical Report USCAE 114, August, 1969.

(13) Jan, Y. G., and R. J. P. de Figueiredo. "Approximations to Optimal Nonlinear Filters Via Spline Functions." Proceedings of the Second Symposium on Nonlinear Estimation Theory and Its Applications, San Diego, California, (September 13-15, 1971), 127-131.

(14) Jazwinski, A. H. Stochastic Processes and Filtering Theory. New York: Academic Press, 1970.

(15) Sage, A. P., and J. L. Melsa. Estimation Theory With Applications to Communications and Control. New York: McGraw-Hill Book Company, 1971.

(16) Jazwinski, A. H. "Filtering for Nonlinear Dynamical Systems." IEEE Transactions on Automatic Control, Vol. AC-11 (1966) 765-766.

(17) Bass, R. W., V. D. Norum, and L. Schwartz. "Optimal Multichannel Nonlinear Filtering." Journal of Math. Anal. and Appl., Vol. 16 (1966), 152-164.

(18) Fisher, J. R. "Optimal Nonlinear Filtering." Advances in Control Systems, Vol. 5 (1967), 197-300.

(19) Jazwinski, A. H. Stochastic Processes with Application to Filtering Theory. Seabrook, Maryland: Analytical Mechanics Associates, Report No. 66-6, 1966.

(20) Schwartz, L., and Edwin B. Stear. "A Computational Comparison of Several Nonlinear Filters." IEEE Transactions on Automatic Control, Vol. AC-13, No. 1 (February, 1968), 83-86.

(21) Wishner, R. P., J. A. Tabaczynski, and M. Athans. "A Comparison of Three Nonlinear Filters." Automatica, Vol. 5 (1969), 487-496.

(22) Kaminski, P. G., A. E. Bryson, and S. F. Schmidt. "Discrete Square-Root Filtering: A Survey of Current Techniques." IEEE Transactions on Automatic Control, Vol. AC-16, No. 6 (December, 1971), 727-736.

(23) Bierman, G. J. "A Comparison of Discrete Filtering Algorithms." IEEE Transactions on Aerospace and Electronic Systems, Vol. AES-9, No. 1 (January, 1973), 28-37.

(24) Mendel, Jerry M. "Computational Requirements for a Discrete Kalman Filter." IEEE Transactions on Automatic Control, Vol. AC-16, No. 6 (December, 1971), 748-758.

(25) Gaston, Jerry A., and James R. Rowland. "Realtime Digital Integration for Continuous Kalman Filtering in Nonlinear Systems." Computers and Electrical Engineering, Vol. 2, No. 2 (June, 1975), 131-140.

(26) Bucy, R. S., M. J. Merritt, and D. S. Miller. "Hybrid Computer Synthesis of Optimal Discrete Nonlinear Filters." Proceedings of the Second Symposium on Nonlinear Estimation Theory and Its Applications, San Diego, California, (September 13-15, 1971), 59-87.

(27) Holmes, Willard M., and James R. Rowland. "Realtime Continuous Kalman Filtering for Hybrid Computer Applications." Proceedings of Eighth Annual Princeton Conference on Information Science and Systems, Princeton, New Jersey, Paper C-4.5 (March 28-29, 1974).

(28) Holmes, Willard M., and James R. Rowland. "Optimal Hybrid Computer Partitioning for Kalman Filter Mechanizations." Proceedings of the Fifth Symposium on Nonlinear Estimation Theory and Its Applications, San Diego, California, (September 23-25, 1974), 110-118.

(29) Benyon, Peter R. "A Review of Numerical Methods for Digital Simulation." Simulation, Vol. 11 (November, 1968), 219-238.

(30) Rowland, James R., and Willard M. Holmes. "A Variational Approach to Digital Integration." IEEE Transactions on Computers, Vol. C-20, No. 8 (August, 1971), 894-900.

(31) Nigro, Bart J., Richard A. Woodward, and C. Russell Brucks. A Digital Computer Program for Deriving Optimum Integration Techniques for Real-Time Flight Simulation. Buffalo, N. Y.: Bell Aerosystems Company, Report No. AMRL-TR-68-4, May, 1968.

(32) Rowland, James R., and Willard M. Holmes. "Dynamic Programming for the Partitioning of Numerical Simulations with Hybrid Computer Applications." IEEE Transactions on Computers, Vol. C-22, No. 5 (May, 1973), 516-523.

(33) Rowland, James R., and V. M. Gupta. "Digital Simulations for Monte Carlo Analysis." Proceedings of the Fifteenth Midwest Symposium on Circuit Theory, University of Missouri, Rolla, Missouri, Vol. 1, Paper V. 3 (May 4-5, 1972).

(34) Rowland, James R. "Optimal Digital Simulations for Random Linear Systems with Integration Constraints." Computers and Electrical Engineering, Vol. 1, No. 1 (June, 1973), 111-118.

(35) Brown, R. J., and J. R. Rowland. "Trajectory Optimization for Closed-Loop Nonlinear Stochastic Systems." IEEE Transactions on Automatic Control, Vol. AC-17, No.1 (February, 1972), 116-118.

(36) Brown, R. J., Jr. and J. R. Rowland. "Trajectory Optimization for the Nonlinear Combined Estimation and Control Problem." Preprints of the IFAC Fifth World Congress, Paris, France, Paper 32.6 (June 12-17, 1972).

(37) Fletcher, R., and M. J. D. Powell. "A Rapidly Convergent Descent Method for Minimization." Computer J., 6 (1963), 1963-1968.

(38) Kuester, James L., and Joe H. Mize. Optimization Techniques with Fortran. New York: McGraw-Hill Book Company, 1973, 355-366.

(39) Sims, C. S., and J. L. Melsa. "A Survey of Specific Optimal Techniques in Control and Estimation." International Journal of Control, Vol. 14, No. 2 (August, 1971), 299-308.

(40) Sims, C. S., and J. L. Melsa. "Specific Optimal Estimation." IEEE Transactions on Automatic Control, Vol. AC-14 (April, 1969), 183-186.

(41) Rowland, J. R., and V. M. Gupta. "Optimal Constrained Discrete Representations of Continuous Filtering Algorithms." Proceedings of the Sixth Symposium on Nonlinear Estimation Theory and Its Applications, San Diego, California, (September 15-17, 1975), 219-222.

(42) Bryson, Arthur E., Jr. and Yu-Chi Ho. Applied Optimal Control. Mass.: Blaisdell Publishing Company, 1969, 432-437.

(43) Denham, W. H. Choosing the Nominal Path for a Dynamic System with Random Forcing Functions to Optimize Statistical Performance. Harvard: Division of Eng. and App. Physics, Harvard University, Tr 449, 1964.

VITA γ

Vijayendra Mohan Gupta

Candidate for the Degree of

Doctor of Philosophy

Thesis: OPTIMAL DIGITAL MECHANIZATIONS OF STOCHASTIC FILTERING ALGORITHMS

Major Field: Electrical Engineering

Biographical:

Personal Data: Born in Chiswick, London, U.K., January 11, 1949, the son of Mr. and Mrs. M. C. Gupta.

Education: Graduated from Higher Secondary School, New Delhi, India, in May, 1966; received the Bachelor of Engineering (Honours) degree in Electrical Engineering from Birla Institute of Technology and Science, Pilani, Rajasthan, India in 1971; received Master of Science degree from Oklahoma State University, Stillwater, Oklahoma in May, 1973; completed requirements for the Doctor of Philosophy degree at Oklahoma State University in July, 1976.

Professional Experience: Graduate Research Assistant, School of Electrical Engineering, Oklahoma State University, from January, 1972 to May, 1975 and June, 1976 to present; Graduate Teaching Assistant, School of Electrical Engineering, Oklahoma State University, from August, 1975 to May, 1976.

Professional Societies: Member of Eta Kappa Nu and the Institute of Electrical and Electronics Engineers.